Republic of Iraq
Ministry of Higher Education and Scientific Research
University of Babylon
College of Education for Pure Sciences
Department of Physics

Effect of cold plasma on Optical and electrical properties of polymeric Blend Doped with Nano -Sliver

A Thesis

Submitted to the Council of the College of Education for Pure Sciences of University of Babylon in Partial Fulfillment of the Requirements for the Degree of Master in Education/ Physics

By

Zahraa Hassoun Obaid Farhan

B.Sc. in Physics

(University of Babylon 2006 A.D)

Supervised By

Prof. Dr. Bahaa Hussien Salih Rabee

2023A.D. 1445 A.H

بسم الله الرحمن الرحيم

((وَنُرِيدُ أَن نَّمُنَّ
عَلَى ٱلَّذِينَ
ٱسْتُضْعِفُواْ
فِي ٱلْأَرْضِ وَنَجْعَلَهُمْ
أَئِمَّة وَنَجْعَلَهُمُ
ٱلْوَٰرِثِين))

صدق الله العظيم

(سورة القصص : آية ٥)

Dedication

In front of me and on my back is the Commander of the Faithful, peace be upon him.

To that soul that always accompanied me, to the soul of my dear father.. to my mother and brothers..to my.husband and children And the people of determination and strength.. I dedicate this humble work to them.

Zahraa… 

Acknowledgments

Thanks be to **God**, either for a blessing.. or for a curse to be paid.. to Him be thanks always and forever...

To my virtuous teacher, **(Dr. Bahaa H Rabee)** who strived.. directed.. worked.. and watched.. and was keen.. and worked hard.. to teach me.. and to understand me..

In order to show my message in the best condition..

He has a thousand greetings and peace from me..

I would like to express my sincere gratitude to the chair of the Department of physics at the College of Education for pure sciences and to **Dr. Ahmed Hashim** for their kind assistance and valuable comments.

Zahraa…

Abstract

The (PVA/PAA/Ag) nanocomposites have been prepared by using casting method with variant content of (Ag) nanoparticles (2, 4, 6 and 8) wt.%. The structural, optical and AC electrical properties of (PVA/PAA/Ag) nanocomposites have been investigated. The structural properties include optical microscope (OM), Field-emission scanning electron microscope (FE-SEM) and Fourier transformation infrared ray (FT-IR) . The optical microscope images showed that Ag nanoparticles form a continuous network inside the polymers when the ratio of (8) wt.%. FESEM measurements reveal the surface morphology of the (PVA/PAA/Ag) nanocomposites films, which are homogeneous and coherent with aggregates or chunks scattered at random on the top surface. The variation in the morphology after exposed Ar plasma nanoparticles is the outcome of the impression progression encouraged by argon plasma species on the (PVA/PAA) surface. FTIR spectra showed a shift in some bands and change in the intensities of other bands comparing with pure (PVA/PAA/Ag) films, this indicates there is no interaction between the polymers and the added nanoparticle. The optical properties before and after exposed Ar plasma exhibited that the absorbance, absorption coefficient, refractive index, extinction coefficient, dielectric constant (real, imaginary) and optical conductivity of (PVA/PAA) blend increased with the increasing of the concentrations of the Ag. The transmittance and the energy gap for indirect transition (allowed, forbidden) decreased with the increasing of the concentrations of Ag nanoparticles. it is decreased from 4.76 eV to 2.91 eV for the allowed indirect energy gap and from 4.25 eV to 1.64 eV for the forbidden indirect energy gap before exposed to the argon plasm, while the indirect energy gap decreased from 3.52 eV to 1.64 eV for the allowed and from 2.98 eV to 0.15 eV for the forbidden

after exposed argon plasma. The optical properties after irradiation have high values compared before irradiation which attributed to increased free charge carriers and polarized. This give as good indicator these samples could be used as photodetector device. The dielectric properties explain that the dielectric constant and dielectric loss for (PVA/PAA) blend are increased with the increasing of Ag nanoparticles concentration and decreasing with the increase of frequency of the applied electric field while the A.C electrical conductivity increased with the increasing of nanoparticles concentration and frequency of the applied electric field before and after exposed Ar plasma. The dielectric constant, dielectric loss and A.C electrical conductivity after irradiation have high values compared before irradiation which attributed to the increased free charge carriers and polarized, these properties can be used for films in capacitors, transistor and electronic circuits. The (PVA/PAA/Ag) nanocomposites were tested as antibacterial for against gram-positive (Staphylococcus aureus) and gram-negative (Escherichia coli). The result obtained the inhibition zone diameter increases with the increase in Ag nanoparticles concentrations. It is increased to 20 mm for E. coli. at concentration 8% wt. Ag and 26 mm for S. aureus. at concentration 8% wt. Ag.

List of contents

List of figures:

List of Table:

List of abbreviations:

Abbreviation	Meaning
A	**Absorbance**
B	**Constant Depended on Type of Material**
I_A	**Absorbed light intensity**
I_o	**Incident intensity of light**
T	**Transmittance**
I_t	**Intensity of transmittance ray**
E_{ph}	**Phonon energy**
$\propto$	**Absorption Coeffiient**
d	**Thickness**
Eg^{opt}	**Energy gap between direct transition**
$\mathcal{E}'$	**Dielectric constant**
$\mathcal{E}''$	**Dielectric loss**
R_B	**Resistivity**
R	**Exponential Constant**
K_o	**Extinction coefficient**
R	**Reflectance**
N	**Refractive Index**
λ	**Wave length of light**
$\mathcal{E}_1$	**Real part of the dielectric constant**
$\mathcal{E}_2$	**Imaginary part of the dielectric constant**
σ	**Electrical conductivity**
P	**Total dipole moment**
N_o	**Number of molecules for a unit of volume**
$\in_\circ$	**Permittivity of free space**
E	**Electrical field intensity**
Eg	**Energy gap**
Re	**Electronic polarization**
P_i	**Ionic Polarization**
P_d	**Orientation Polarization**
P_o	**Inter facial Polarization**
w	**Angular frequency**
f	**Frequency**
I_p	**Conduction current**
I_q	**Capacitate current**
C_p	**The capacity**
C_o	**Vacuum capacitor**
h	**The planck's constant**
k	**Extinction coefficient**
D	**Dissipersion factor**

$\overrightarrow{E_l}$	**Internal field of a molecule**
$_{op}\sigma$	**Optical Conductivity**
V.B	**Valence Band**
C.B	**Conductive Band**
M_{oc}	**Ocular magnification**
M_{obj}	**Objective magnification**
C	**Velocity of light**
A_r	**the area**
V_m	**the maximum voltage**
a_o	**The polarixability**
ν	**Photon frequency**

Chapter One
Introduction and Literature Survey

1.1 Introduction

In the nineteenth century, contrary to what some believe, the composition of polymers was unknown until two centuries ago, when scientists sought to determine how these materials were formed, and to seek to establish a way to achieve their artificial manufacture. In ready composite these separate materials are connected by interface layer coupling two immiscible phases–matrix and reinforcement or filler. Properties of two phases, reinforcement or filler distribution in matrix and adhesion phenomena between filler and matrix determine final properties of composite. The idea of connecting two or more different constituents into one substance gives almost infinite possibilities to create new engineering materials characterized by variety of different properties. Because of these diverse properties, composite materials are successfully used in almost all areas of industry and science. Especially popular are composites in automotive, electrical and electronic, aerospace and machine building industries, sport and leisure industry, civil engineering, etc [1].

Nanotechnology can be defined as the ability to work near the molecular level, atom by atom, to create large structures with fundamentally new properties and functions. Nanotechnology can be described as the precision-creation and precision control of atomic-scale matter [2]. It offers new design, characterization, production, and application of systems, devices and materials at the nanometer scale. It is an interesting and vibrant field of research. Their roots can be traced back to feyn man's famous lecture in 1959, in which he suggested that for entities with nanoscopic dimensions new physical phenomena should arise [3].

1.2 Hot and cold plasma

Plasma is often described as the fourth state of matter, together with gases, liquids and solids, a definition which does little to illuminate their main

physical attributes. In fact, a plasma can exhibit behaviors characteristic of all three of the more familiar states, depending on its density and temperature, so obviously need to look for other distinguishing features. A simple textbook definition of a plasma [4] would be: a quasi-neutral gas of charged particles showing collective behavior. This may seem precise enough, but the rather fuzzy-sounding terms of 'quasi-neutrality' and 'collectivity' require further explanation. The first of these, 'quasi-neutrality', is actually just a mathematical way of saying that even though the particles making up a plasma consist of free electrons and ions, their overall charge densities cancel each other in equilibrium [5].

Now that have established what plasmas are, it is natural to ask where can find them. In fact, they are rather ubiquitous: in the cosmos, 99% of the visible universe—including stars, the interstellar medium and jets of material from various astrophysical objects—is in a plasma state. Closer to home, the ionosphere, extending from around 50 km (equivalent to 10 Earth radii) to 1000 km, provides vital protection from solar radiation to life on Earth. Terrestrial plasmas can be found in fusion devices (machines designed to confine, ignite and ultimately extract energy from deuterium–tritium fuel), street lighting, industrial plasma torches and etching processes, and lightning discharges [6]. Needless to say, plasmas play a central role in the topic of the present school, supplying the medium to support very large travelling-wave field structures for the purpose of accelerating particles to high energies. Hot and cold plasma physics two branches of plasma physics that with different types of plasma. Here are some basic concepts in each branch [7]:

1- Cold plasma: in cold plasma, the temperature of plasma is relatively low, usually around room temperature or lower. The plasma particle is not highly ionized and collisions between particles are relatively frequent. the Debye length, which is a measure of the screening distance between charged particles

in the plasma, is relatively short in cold plasma. cold plasma is often used in industrial applications, such as plasma cutting and surface treatment [8]

2- Hot plasma: In hot plasma, the temperature of plasma is high, often in the millions of degrees Celsius. the plasma particles are highly ionized and collisions between particles are infrequent. The Debye length in hot plasma is relatively long. Hot plasma is often found in natural phenomena, such as stars and the Earth's ionosphere, and in fusion experiment.

3-Plasma parameters: Plasma parameters are variables that describe the properties of a plasma, such as density, temperature Debye length,. These parameters can be used to understand and predict the behavior of the plasma [9].

4-Plasma waves: plasma waves are oscillations in the plasma that are caused by the collective motion of the plasma particles. These waves can be used to probe the properties of the plasma and to manipulate the plasma in various ways.

5-Plasma confinement: plasma confinement refers to the ability to confine a plasma within a certain region, such as a confinement is important in fusion experiments, where the plasma must be confined long enough for fusion reactions to occur.

1.3 Polymer Composite

Polymers are one of the most widely used materials, due to their versatile properties. Polymers contain properties which make them unique and virtually irreplaceable for some applications. For example, elastomers have the ability to deform by a thousand percent with an applied force and, after the force is removed, they can restore their initial shape. In general, polymers are known for their low density with intermediate stiffness and strength. Although polymers have ideal properties for a wide range of applications, they were unable to be used for applications requiring electrical conductivity. When

there was the addition of a conductive filler particle, it was discovered that a polymer would allow the flow of current through its system, this increased the number of industrial applications for polymers [10]. Materials that contain a polymer matrix with conductive filler are known as conductive polymer composites. These composites are known for having high dielectric constants and for being extremely conductive. This is achieved by the conductive filler forming a network throughout the composite which allows for the flow of current through the composite. The conductivity of these composites can increase by several orders of magnitude. Since the matrix consists of a polymer, these composites have the potential of increasing in flexibility, if the polymer used in the matrix is flexible. The composite can be brittle and weak due to the amount of filler that is needed to produce a highly conducting material. The main advantage of conductive polymer composites is that they unique characteristics that different of both a metal and of a polymer [11]. The system can either have a random microstructure or a segregated microstructure. A random microstructure consists of a polymer matrix with filler particles that are sporadically placed throughout the matrix. These composites have isotropic characteristics and the filler shows no bias to its location. A segregated microstructure consists of filler particles that show bias to their location. These composites have filler-rich regions along with polymer rich regions [11]. Figure (1.1) shows a representation of a segregated versus a random microstructure.

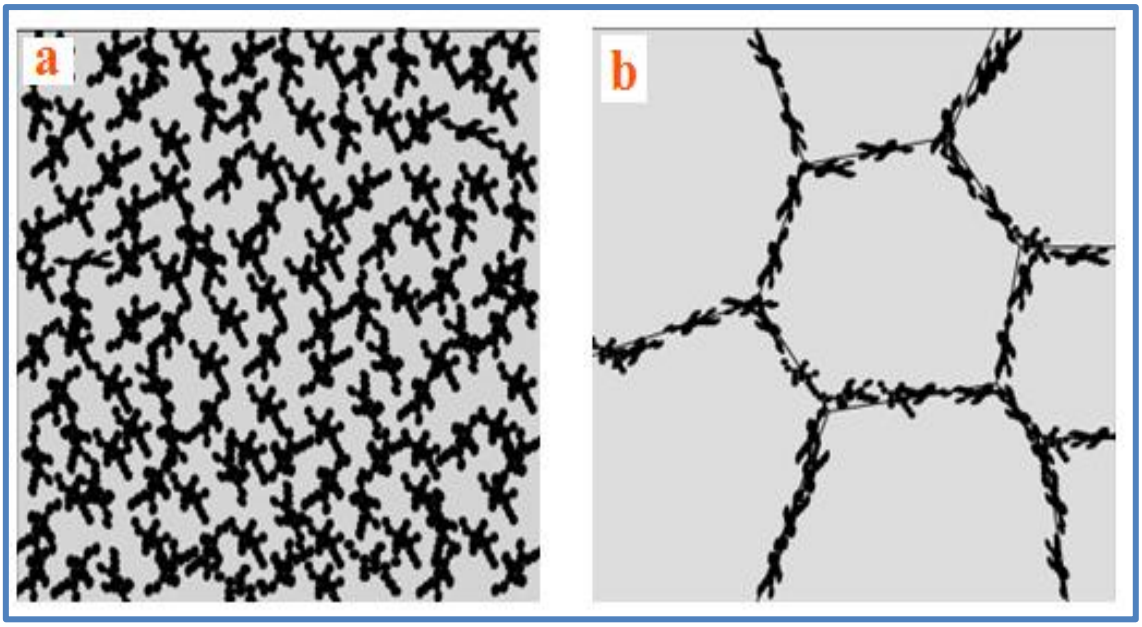

Figure (1.1): A representation of (a) Randomly Oriented Microstructure (b) Segregated Microstructure [11].

1.4 Classification of Polymers

Polymers can be classified in many different ways. The most obvious classification is based on the origin of the polymer, i.e., natural vs. synthetic. Other classifications are based on the polymer structure, polymerization mechanism, preparative techniques, or thermal behavior [12].

1.4.1 Thermal Classification of Polymers:

Polymers can be classified into two groups according to the effect of temperature [13].

1-Thermoplastic: These polymers soften when heated and harden when cooled. These materials are normally fabricated by the simultaneous application of heat and pressure. The properties of these polymers are changed by the effect of temperature. When the temperature increases, they become flexible and sticky; by lowering the temperature, these polymers return to their original solid state. This is because the molecules in a thermoplastic polymer are connected by relatively weak intermolecular forces (Van der Waals forces). Common thermoplastic is: acrylics, PVC, nylons, polypropylene, polystyrene, polymethyl methacrylate (plastic lenses or perspex), etc.

2-Thermoset Polymers: These polymers are chemically changed when heated. Thermosets are usually three-dimensional networked polymers in which there is a high degree of cross-linking between polymer chains. After being heated, these polymers become insoluble, non-conductive of heat and electricity, and hard because molecules of these polymers are connected by strong covalent chemical bonds. Phenol formaldehyde resin and urea-formaldehyde resin are examples of this type of polymers.

1.4.2 Classification Based on the Structure of Polymers.

A polymer is formed when a very large number of structural units (repeating units, monomers) are made to link up by covalent bonds under appropriate conditions. The functionality of a molecule is simply its interlinking capacity or the number of sites it has available for bonding with other molecules under the specific polymerization conditions [14]. Polymers are classified depending on the structural composition to [15-17]:

1. Linear: The chains of polymer hold it together by many Vander Waals bonds. Examples of linear polymers are polyethylene, fluorocarbons, polystyrene, nylon, and polyvinyl chloride are shown in Fig.(2.1 a).

2. Branched: Side-branch chains bond to the main ones during synthesis of the polymer. These reduce the packing efficiency, so lower density are shown in Fig.(2.1 b).

3. Cross linked: Cross-linked polymers consist of smaller polymer chains which are bonded together. Each chain is bonded to many chains. Many of the rubber materials consist of polybutadiene cross linked with(S)atoms are shown in Fig.(2.1 c).

4. Network: Mer units with three active covalent bonds are form 3D networks e.g. epoxies are shown in Fig. (2.1 d).

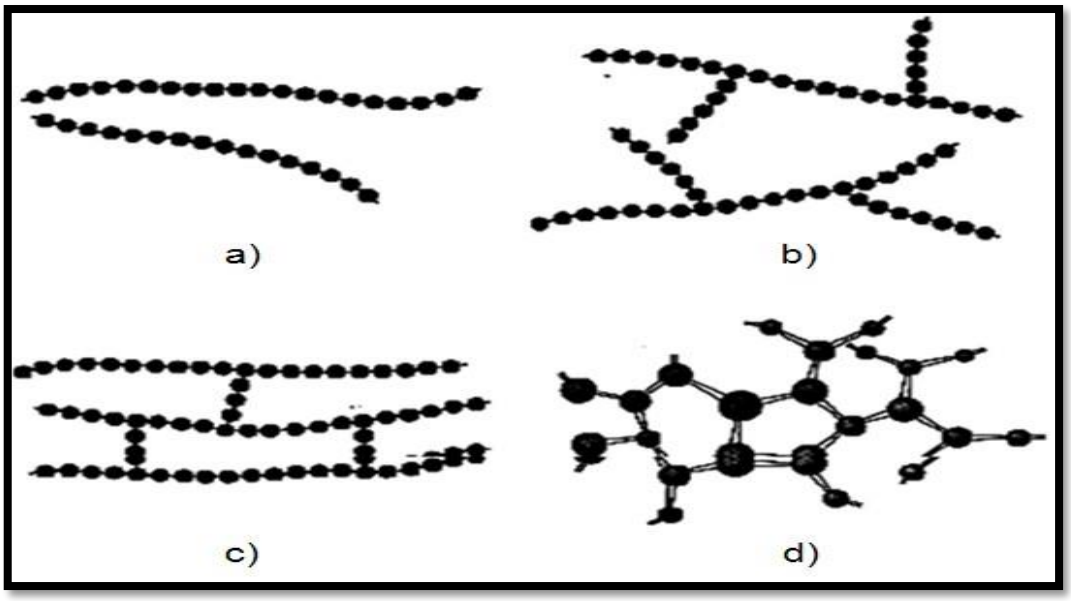

Figure (1.2): The type of polymers (a) Linear polymer, (b) Branched Polymer, (c) Cross-linked polymer, (d) Network polymer [16].

1.5 Nanocomposites

Nanocomposite is a class of materials with unique physical properties and wide application potential in diverse areas [18]. Distribution of nano scaled inorganic fillers into an organic polymer to form polymer nanocomposites has gained increasing interest in recent years. Controlling the nanostructure, composition and morphology of nanocomposites plays an essential role in their applications. Novel properties of nanocomposites can be obtained by successful imparting of the characteristics of parent constituents to a single material [19]. These materials differ from both pure polymers and inorganic fillers in some physical and nano scale inorganic fillers are opening pathways for engineering flexible composites that exhibit attractive mechanical, thermal, optical and electrical properties compared with conventional composites [20]. Although the terms nanomaterial and nanocomposite represent new and exciting fields in materials science, such materials have actually been used for centuries and have always existed in nature. However, it is only recently that the means to characterise and control

structure at the nanoscale have stimulated rational investigation and exploitation. A nanocomposite is defined as a composite material where at least one of the dimensions of one of its constituents is on the nanometre size scale [21]. The term usually also implies the combination of two (or more) distinct materials, such as a ceramic and a polymer, rather than spontaneously phase-segregated structures. The challenge and interest in developing nanocomposites is to find ways to create macroscopic components that benefit from the unique physical and mechanical properties of very small objects within them. The fracture toughness of such biocomposites, on the other hand, hinges on the ultimate tensile strength, σ_f, of the reinforcement. Crucially, the use of a nanomaterial allows access to the maximum theoretical strength of the material, since mechanical properties become increasingly insensitive to flaws at the nanoscale [22]. This observation is an extension of the classic approach to strong materials, namely to reduce the dimensions until critical flaws are excluded. At the nanoscale, highly crystalline reinforcements are used in which all but the smallest atomistic defects can be eliminated. It is clear that a high aspect ratio must be maintained in order to ensure suitable stress transfer. This general concept of exploiting the inherent properties of nanoscaled materials is not limited to the mechanical properties of a material, since a wide range of physical properties also depend on defect concentrations. In addition, the small size scale can generate inherently novel effects through, for example, quantum confinement, or through the dramatic increase in interfacial area.The concept of creating both structural and functional multi-phase nanocomposites with improved performance is currently under development in a wide variety of metallic, ceramic, and polymeric matrices, although the emphasis to date has been on polymeric systems. Similarly, the filler particles can be organic or inorganic with a wide range of material compositions and structures. The resulting composites generally exhibit a

number of enhanced properties, so that the material cannot easily be classified as a structural or functional composite. The term reinforcement, as opposed to plain filler, is equally frequently used for the nanoscale component, without a clear distinction [23].

1.6 Materials used in the Study

1.6.1. Polyvinyl Alcohol (PVA)

PVA (Poly-vinyl alcohol) is synthetic polymer employed since the early 1930s in a wide range of industrial, commercial, medical and food applications including resins, surgical threads, lacquers and food-contact applications [24]. Poly (vinyl alcohol) is a synthetic polymer that comes in the form of a granular powder that is odorless, transparent, tasteless, white, or cream-colored [25]. Polyvinyl alcohol, may be combined in water. that the benefit of being resistant to solvents and oils, as well as having outstanding characteristics [26]. It has been used in a wide range of applications and is also widely used in semiconductor applications. Figure (1.3) shows the chemical structure of PVA [27]. Table (1.1) explain some physical and chemical properties of PVA [28, 29].

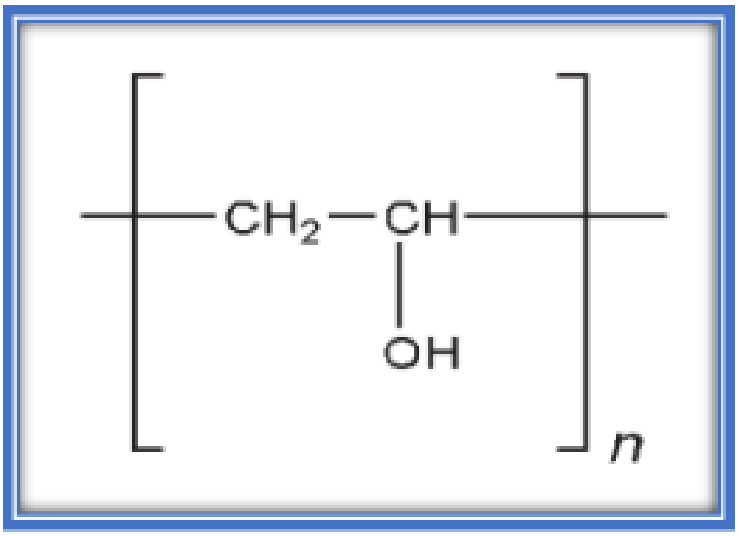

Figure (1.3) The Chemical Structure of PVA [28].

Table (1.1): Physical and Chemical Properties of Poly(vinyl Alcohol) (PVA) [29].

Property	Description
Energy gaps	6.27 eV
Appearance	White to an ivory white granular powder
Molecular formula	$(C_2H_4O)_n$
Density	1.3 g/cm^3
Refractive index	1.55
Glass transition temperature T_g	75-85 ºC
Melting temperature T_m	230 ºC
Molecular Weight	30000 (g/mol)

1.6.2. Polyacrylic Acid (PAA)

Polyacrylic acid (PAA) is a non-toxic, biocompatible, and biodegradable polymer that gained lots of interest in recent years. PAA nano-derivatives can be obtained by chemical modification of carboxyl groups with superior chemical properties in comparison to unmodified PAA. For example,

nano-particles produced from PAA derivatives can be used to deliver drugs due to their stability and biocompatibility. PAA and its nanoconjugates could also be regarded as stimuli-responsive platforms that make them ideal for drug delivery and antimicrobial applications. These properties make PAA a good candidate for conventional and novel drug carrier systems. Here, we started with synthesis approaches, structure characteristics, and other architectures of PAA nanostructure [30]. Then, different conjugations of PAA/ nanostructures and their potential in various fields of nanomedicine such as antimicrobial, anticancer, imaging, biosensor, and tissue engineering were discussed. Finally, biocompatibility and challenges of PAA nanoplatforms were highlighted. Polyacrylic acid acts as an anionic polymer in water [31]. Radiation, allyl ethers of hydrocarbons, and other chemical substances can crosslink poly (acrylic acid). At temperatures above 200 °C, PAA can also be cross-linked [32]. Polyacrylic acid may release water and form an insoluble cross-linked network at high temperatures. The cross-linked PAA may create a gel-like structure. The case of poly (acrylic acid)-graft chitosan is an example of chemical cross-linking [33]. Figure (1.4) shows the chemical structure of PAA [34]. Table (1.2) explain the some physical and chemical properties of PAA [35].

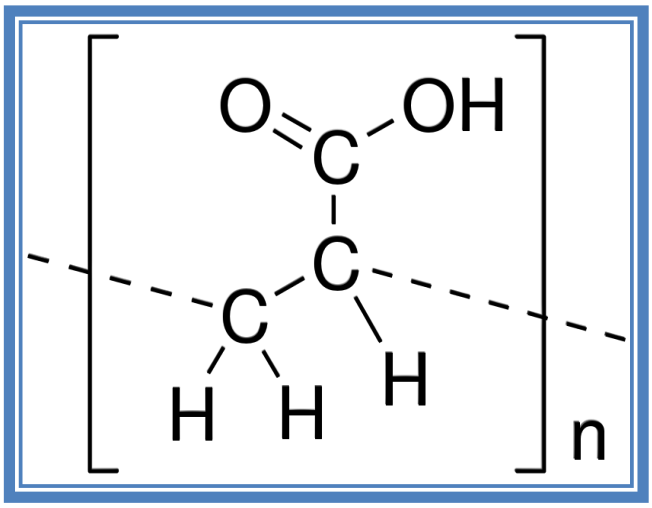

Figure (1.4) The Chemical Structure of PAA [34].

Table (1.2): Physical and Chemical Properties of Polyacrylic Acid (PAA) [35].

Property	Description
Energy gaps	3.93 eV
Appearance	White powder
Chemical formula	$(C_3H_4O_2)_n$
Density	1.22 g/cm^3
Refractive index	1.52 at wavelength 450 nm
Glass transition temperature (T_g)	100 ºC
Melting temperature (T_m)	280 ºC
Molecular Weight	100000 (g/mol)

1.6.3. Silver nanoparticle (Ag NPs)

Noble metal nanoparticles have lately become the subject of investigation because to their unique characteristics, which differ from those of bulk materials. The size, shape, and changes in the surroundings of nanoparticles all influence these qualities [36]. Silver nanoparticles have unique properties (optical, electrical, and magnetic qualities that are affected by size and form) that can be utilized as an antibacterial agent, biosensor materials, composite fibers, superconducting materials that can be used at a cryogenic temperature, cosmetics, and electronic components, which have piqued the interest of researchers. Ag NPs have been produced and stabilized using a variety of physical and chemical processes. Physical and chemical characteristics of silver nanoparticles are described in Table (2.3) [37].

Table (1-3): The Physical and Chemical Properties of Silver Nanoparticles [37].

Properties	Silver (Ag)
Energy gaps	**2.28 eV**
Atomic number	**47**
Mass number	**107.86**
Structure	**FCC**
Lattice constant	**0.409 (nm)**
Density	**10.5 ($g.cm^{-3}$)**
Melting temperature	**961.8 ºC**
Boiling temperature	**2212 ºC**
Electrical conductivity	**6.30×10^5 $(\Omega.cm)^{-1}$**

1.7 Literature Survey

In (2014), C. Mandolfino, *et. al.* [38]

the effect of cold plasma treatment on polyethylene and polypropylene substrates, a large number of samples were exposed to radio frequency (RF) low pressure plasma, using mainly air as working gas. In particular, the optimization of three plasma process parameters, exposure time, voltage and working gas, were studied performing roughness measurement, contact angle evaluation and lap-shear tests. The experimental results show that the optimized plasma process may remarkably change the surface morphology, increasing wettability properties of the surfaces and shear strength of the bonded joints. These good properties remain almost unchanged even after some days of storage in the laboratory.

In (2015), A. M. El Sayed and S. El-Gamal [39] studied the synthesis and investigation of the electrical and dielectric properties of Co_3O_4/(CMC+PVA) nanocomposite films. Scanning electron microscopy images revealed a good dispersion of Co_3O_4 NPs on the surface of the

CMC/PVA films. The current–voltage characteristics are of non-ohmic behavior. The dielectric permittivity (ε') was studied in the frequency and temperature range of 5.0 kHz–5.0 MHz and 308–408 K and was found to depend on the Co_3O_4 content. The dielectricm loss (ε") also increases and shows wave-like behavior with increasing Co_3O_4 ratio. Increasing Co_3O_4 NPs content leads to the formation of more number of three-dimensional semiconducting connected networks inside CMC/PVA matrix, leading to increasing both DC and AC conductivities. The correlated barrier hoppingm(CBH) is the most suitable mechanism to explain the AC conduction behavior in the Co_3O_4/ Na-CMC/ PVA nanocomposite films.

In (2016), Z. A. Al-Ramadhan *et al.* [40] studied the optical and morphological properties of (PVA-PVP-Ag) nanocomposites, which prepared by casting method, UV-Vis spectroscopy at a wavelength of (200-900) nm was used to evaluate the optical characteristics, by increasing Ag nanoparticle concentration, the energy gap of indirect transition (allowed and forbidden) decreased from (4.8-3.9 allowed) to (4.7-3.8 forbidden). The AFM and OM data revealed a homogeneous distribution, a very smooth surface, and minimal roughness.

In (2017), N. A. Awang *et al.* [41], studied the effects of surface treated boron nitride (BN) nanoparticles in Low Density Polyethylene (LDPE) on the partial discharges (PD) characteristics by following CIGRE Method II at 7 kV rms applied voltage. The phase resolved PD characteristics were performed. The results revealed that by treating the nanofillers with cold plasma, the PD resistance of LDPE were highly achieved compared with the untreated BN nanofillers.

In (2017), A. G. El-Shamy *et al.* [42] studied the influence of gamma irradiation on the electrical and dielectric properties of silver/polymer composite (Ag/PVA) films with thickness 0.18 mm. The films were prepared

by the in-situ chemical reduction and later irradiated with gamma (γ) radiation doses (25, 50, 75, 100, 125 KGy). The content of Ag (0.4 wt %) in the PVA films were determined by the atomic absorption spectroscopy (AA). The films were characterized by the dielectric spectroscopy and Current-Voltage (I–V) measurements. The dielectric constant (ε') value decreased with the increasing gamma irradiation doses. The conductivity films and dielectric loss increased with the increasing gamma irradiation doses: $\sigma = 4.9 \times 10^{-8}$ S m^{-1} was found at gamma radiation dose of 125 KGy. The Poole-Frenkel emission is the prevailing transport mechanism for all the samples.

In (2017), H. T. Salloom *et al.* [43], studied Silver- Poly vinyl alcohol Ag/ PVA nanocomposite films were prepared by casting method at room temperature with different amount of $AgNO_3$ solution (0.001, 0.0015, and 0.002ml). The prepared nanocomposites were characterized using UV–VIS spectrophotometer and the optical properties were investigated in the wavelength range 300-800 nm. The absorption peaks showed a shift towards higher wavelength with increasing $AgNO_3$ concentration while the energy band gap and absorption edges shifted towards lower energies with the increase of AgNO3 concentration.

In (2018), A. M. Ismail, *et al*. [44], studied the Lithium ions-doped polyvinyl alcohol/polyvinyl pyrrolidone (PVA/PVP) films. The results indicated that absorbance A and absorption index (α) are increased. The optical band gap E_{opt} of the composites showed significant decrease from 2.98 to 2.196 eV by adding Li_2SO_4 . The dependence of read dielectric constant ε_1, imaginary dielectric constant ε_2 and optical conductivity (σ_{op}) opt on photon energy hυ were also studied. The indirect optical gap of the doped blend refers to the existence of charge transfers complexes in the host polymer by the addition of small amounts of Li ions.

In (2019), F. M. Ali *et al*. [45] explored the Structural and optical characterization of PVA-PVP -Cu^{2+} composite films containing high quality semiconducting polymers of copper ions doped poly(vinyl alcohol) (PVA): poly(vinyl pyrrolidone (PVP). poly(vinyl pyrrolidone) with a weight ratio of 50:50 PVA-PVP with x wt% copper . The standard method of solution casting was used, and it was successful in producing composite films with x values of 0, 3, 5, 15, and 20 wt% .

In (2020), H. S. Rasheed *et al.* [46] utilized the casting method to investigated the effect of adding ZrC nanoparticles on obtical a (PVP-PVA) blend and how it affected the optical characteristics of the mixture for a humidity sensor application. The optical properties showed a decrease in absorbance with increasing concentration of ZrC nanoparticles, The energy gap gets larger as the amount of ZrC nanoparticles in the sample's weight increases. The coefficient of extinction (k), as well as both the real and imaginary constants, were found to be increased with increasing in the concentration of ZrC nanoparticles.

In (2020), M. R. Atta, *et al.* [47], studied PVA and AgNPs were incorporated in BNC to develop AgNP/PVA/BNC films through reduction and UV methods. The mechanical properties of the film were enhanced due to the addition of PVA. The BNC fibers were broken and physically reconnected by the PVA solution, and the film made more flexible by the PVA. The oxygen barrier capacity was improved because of the dense 3D network structure of BNC which restricted the flow of oxygen and reduced the oxidation rate. The films were able to inhibit the growth of E .coli O157:H7 in broth medium and on raw beef, and effectively control the number of natural bacteria on raw beef, providing a potential method to prolong beef shelf-life. The UV films exhibited stronger antimicrobial properties than the R films in all antimicrobial experiments.

In (2021), M. R. Atta *et al.* [48] studied various amounts of AuNPs were added to polyvinyl alcohol/carboxymethylcellulose (PVA/CMC, 40/60) via the casting method. FTIR spectra showed the interaction between PVA/CMC and AuNPs. The ultra-violet and visible (UV/VIS.) spectra showed emerge new peak of surface plasmon resonance (SPR) of AuNPs for the filled samples. SEM images showed bright spots on the sample's surface, which was attributed to AuNPs. AC conductivity exhibited enhancement after the addition of gold nanoparticles. The ε′ and ε″ were reduced with increasing the frequency.

In (2021), Zainab S. J. and Majeed A. H. [49], studied the (CMC-PAA-ZrC) nanocomposites using the casting process and various percentages of nano Zirconium carbide (0, 1.5, 3, 4.5, and 6) wt%. The dielectric properties of nanocomposites showed that the dielectric constant, dielectric loss and A.C electrical conductivity of (CMC-PAA) blend increase with the increase in ZrC nanoparticles concentrations. Also, the dielectric constant and dielectric loss of (CMC-PAA-ZrC) nanocomposites decrease while the A.C electrical conductivity increases with the increase in frequency. Scanning electron microscopy shows the surfaces of the films (CMC-PAA-ZrC) several randomly distributed aggregates or fragments on the top surface, consistent and coherent. Results of applications showed the nan composites high linear attenuation coefficients have gamma ray sources Co-60 and Cs-137.

In (2022), T. A. Hameed, *et al.* [50] studied developing sustainable cellulose/polyvinyl pyrrolidone (carboxymethyl cellulose (CMC)/PVP) films for optoelectronic applications, Al-doped ZnO nanoparticles were incorporated into CMC/PVP films to create a synergistic effect arising from the excellent electrical properties of Al and the outstanding optical features of ZnO. The infrared spectra showed an overlap between functional groups that proves the interaction between the CMC/PVP blend and the particles. The

scanning electron microscopy images of the films revealed a change in the film surface in response to the filler concentration. The optical bandgap was gradually red-shifted with increasing the ZAL concentration, whereas the Urbach energy showed an opposite trend.

In (2022), Hussien H. M. and Al-Timimi, M. H [51] studied of polymeric films (CMC/PAA) prepared by solution casting method and reinforced with magnesium oxide particles (MgO NPs) by Precipitation method with different weight ratios (0, 3, 5, and 7) wt%.The results of scanning electron microscopy (SEM) reveal that the polymeric film (CMC/PAA) appears to be homogeneous and interconnected and, when applied (CMC/PAA:MgO 7%) forms well-dispersed aggregates in the nanocomposites films. (FTIR) the spectrum revealed that (MgO NPs) does not have a destructive effect on the polymer structure as there are no covalent bonds between (CMC, PAA, and MgO NPs). The optical properties of the nanocomposites were measured. The optical results showed that by increasing the nanomaterial concentration، the (reflectance, absorption coefficient, reflection index, extinction coefficient, and the real and imaginary dielectric constant) increased while the transmittance and energy gap decreased.

1.8 Aim of the Research

The aim of this study is;

1- Preparation of the (PVA/PAA/Ag) nanocomposites using casting method.
2- Effect of the cold plasma on the electrical and optical properties of (PVA/PAA/Ag) nanocomposites.
3- The (PVA/PAA/Ag) nanocomposites will applay for antibacterial applications.

Chapter Two
Theoretical Part

2.1 Introduction

This chapter includes a general description of the study's theoretical part, including physical concepts, relationships, scientific clarifications, and laws applied to explain the study's findings.

2.2 Morphological and Structural

2.2.1 Optical Microscope (OM)

A compound optical microscope is an optical tool that magnifies an object (or specimen) and projects it onto the retina of the eye or onto an imaging device using visible light [52,53]. The term "compound" refers to how two lenses, the objective lens and the eyepiece (or ocular), work together to generate the image's final magnification [54].

$$M_{final} = M_{obj} \times M_{oc} \quad \text{..... (2.1)}$$

Where: M_{obj} is objective magnification, M_{oc} is ocular magnification.

Both diffracted (rays that interact with the specimen) and non-diffracted (rays that pass through the specimen without deviating) rays are gathered by the objective lens in most kinds of transmitted light microscopy and contribute to picture generation [55].

2.2.2 Field-emission Scanning Electron Microscope (FESEM)

The scanning electron microscope is undoubtedly one of the most important electron beam technology inventions of the twentieth century. Ever since the first commercial instrument appeared in the early 1960s, the design of the scanning electron microscope has been constantly evolving and improving [56]. Recognition that the FE-SEM is much more than a powerful microscope came early. In addition to providing high-resolution topographical

images of the surface of a specimen, it was realized that the FESEM could also provide a variety of different contrast modes, where information relating to things like the surface voltage is embedded in its output signals [57]. FESEM has a magnification range of 5 to 300, 000 times, and an acceleration voltage parameter for a coating analysis range between 10 and 20kV , at higher magnifications, much more surface detail is visible in biological samples when using an acceleration voltage between 2 kV and 300 V [58]. Scanning electron microscopy is commonly used in metallurgy, geology, biology, and medicine, where the user can obtain a strong depth of view with high magnification images and analyze individual crystals or other features [58]. When using in combination with the closely related technique of a high-resolution FESEM image will display information down to 25 Angstroms, or better. One may decide the composition of individual crystals or features [59].

2.2.3 Fourier Transforms Infrared (FT-IR) Spectroscopy

Fourier Transforms Infrared (FT-IR) is chemical investigative spectroscopy. This measures the infrared intensity with light wavenumber. The wavenumbers consist of infrared light that is divided into three regions, far-infrared, mid-infrared and near-infrared, which are between (4 ~ 400 cm^{-1}), between (400 ~ 4,000cm^{-1}) and finally, between (4,000 ~ 14,000 cm^{-1}), respectively [60].

The permissible of this technology depends on detects the chemical functional group's vibration in a sample. Where, the chemical bonds will stretch when the interaction happened between the infrared light and the matter [61]. Here, the infrared radiation is absorbed by the chemical functional group at a specific range of wavenumber irrespective of the rest of the molecule structure [62].

2.3 The Optical Properties

The variations electronic characteristics with size resulting in major variations in the optical characteristics of nanoscale materials [63]. When particles are reduced to an enough small size, quantum effects limiting the energies where the holes and electrons can be existed in the particles, due to the fact that energy is proportional to wavelength, the optical properties of the particles can be finely tuned depending on its size. Thus, by changing the size of particles, it is possible to cause them to absorb or emit light at specific wavelengths [64].

The study of polymer optical characteristics advances our understanding of the internal structure of the polymer, the type of the bonds, and the application possibilities of polymers. Knowing the transmittance and absorption spectra of a polymer enables the identification of numerous optical properties over a wide range of wavelengths. By examining the ultra - violet spectra, we can determine the type of bonds, energy beams and orbitals [65].

The visible light spectrum gives adequate information about a material's behavior for solar applications. The infrared spectrum is necessary in order to determine the overall structure of a polymers and the elements that consisting its chemical structures [65].

2.3.1 Absorbance (A)

Absorbance can be defined as the ratio between the absorbed intensity (I_A) by material and the incident intensity of light (I_O) [66].

$$A = I_A/I_O \quad \text{..... (2.2)}$$

2.3.2 Transmittance (T)

The transmittance (T) of a film is defined as the ratio for the intensity of rays that pass through it (I_T) to the intensity of incident rays (I_O) [67].

$T = I_T / I_O$ …….…….…..…....…….…..... (2.3)

2.3.3 Fundamental Edge of Absorption

The fundamental edge of absorption is defined as a rapid increase in absorption when the amount of energy absorbed is nearly equalize to the energy gap between the bands. As a result, the fundamental absorption edge denotes the region where there is the least amount of energy differential between the top points in the valence bands and bottom points in the conduction bands [68]. The regions of absorption can be divided into three distinct regions [69]:

A. High absorption region

This region is represented in figure (2.1) portion (A), in the region of high absorption, where ($\alpha \geq 10^4$) cm^{-1}. In this region, the absorption coefficient correlates to transitions between stretched states in the valence and conduction band. .

B. Exponential region

This region can be seen in the figure (2.1) portion (B). The absorption coefficient for this region is between ($1 \leq \alpha \leq 10^4$) cm^{-1} . The absorption in this region is caused by transitions between extended states and localized states in the band tail. This is referred to it as the Urbach edge.

C. Low absorption region

There is an extremely low absorption coefficient (α) in this region, which is about ($\alpha < 1cm^{-1}$). The transition occurs in this region as a result of state density within space motion caused by structural defects. As showed in figure (2.1), the portion (C).

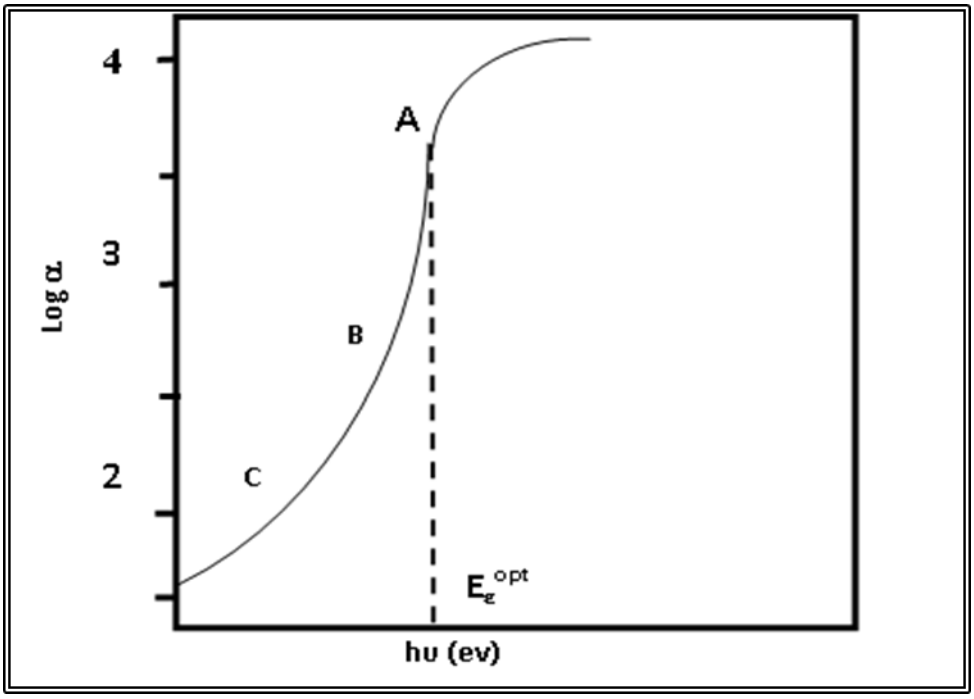

Figure (2.1): The Relationship between the Absorption Edge and the Absorption Regions [61].

2.3.4 The Electronic Transitions

There are two main types of electronic transitions [70].

1. Direct transition

This transition occurs in semiconductors if the bottom for (C.B) is directly above the top for (V.B.). This indicates that their wave vectors are equal, i.e. ($\Delta K = 0$). Absorption happens at this stage when ($h\upsilon = E_g^{opt}$).

This type of transition requires the conservation laws of momentum and energy. There are two types of direct transitions [71].

a- Direct Allowed Transition:

This transition occurs between the highest points in $(V.B)$ and the bottom points in $(C.B)$, as observe in the Fig (2.2-a)

b- Direct Forbidden Transition:

These transitions occur between points adjacent to the lowest point in the conduction band $(C.B)$ and the highest point in the valence band $(V.B)$ [72], as showed in the Fig (2.2.b). Absorption coefficient of this type of transition is calculated as follows:

$$\alpha h\upsilon = B(h\upsilon - E_g^{opt})^r \quad \ldots\ldots\ldots\ldots\ldots\ldots\ldots\ldots\ldots\ldots\ldots\ldots\ldots (2.4)$$

Where E_g^{opt} : The energy gap between direct transitions, B: Constant varies with different materials, r: is exponential constant, and its amount depends on the nature of the transition, $r = 1/2$ for allowed direct transition, $r = 3/2$ for forbidden direct transition , α: is the absorption coefficient, h: is the Planck's constant, υ: is the photon frequency.

2. Indirect transitions

In this form of transition, the bottom for $(C.B.)$ doesn't over the peak for $(V.B.)$, as shown in the curve (E-K),and the electron moves from the $(V.B.)$ to the $(C.B.)$ in a way that isn't perpendicular where the values of the waves vectors of the electrons before and after this transition are not the same $(\Delta K \neq 0)$. This type of transition occurs with the assistance of a particle termed a "Phonon," which is necessary for conservation of the momentum and energy law. Indirect transitions are classified into two types [72]:

c- Allowed indirect transitions:

These transitions occur between the lowest point in $(C.B.)$ and the highest point in $(V.B.)$, which are located in the (K-space's) difference region, as showed in the Figure (2.2.c).

d-Indirect forbidden transitions:

These transitions occur between points adjacent the top for $(V.B.)$ and points adjacent the bottom for $(C.B.)$ [73], as shown in Fig (2.2.d). Absorption coefficient of a transition involving phonon absorption calculated by:

$$\alpha h\upsilon = B(h\upsilon - E_g^{opt} \pm E_{ph})^r \quad \text{..... (2.5)}$$

When: E_{ph}: Phonon energy, is (+) phonon emission, and (-) phonon absorption, r=2 for allowed indirect transition, r=3 for forbidden indirect transition.

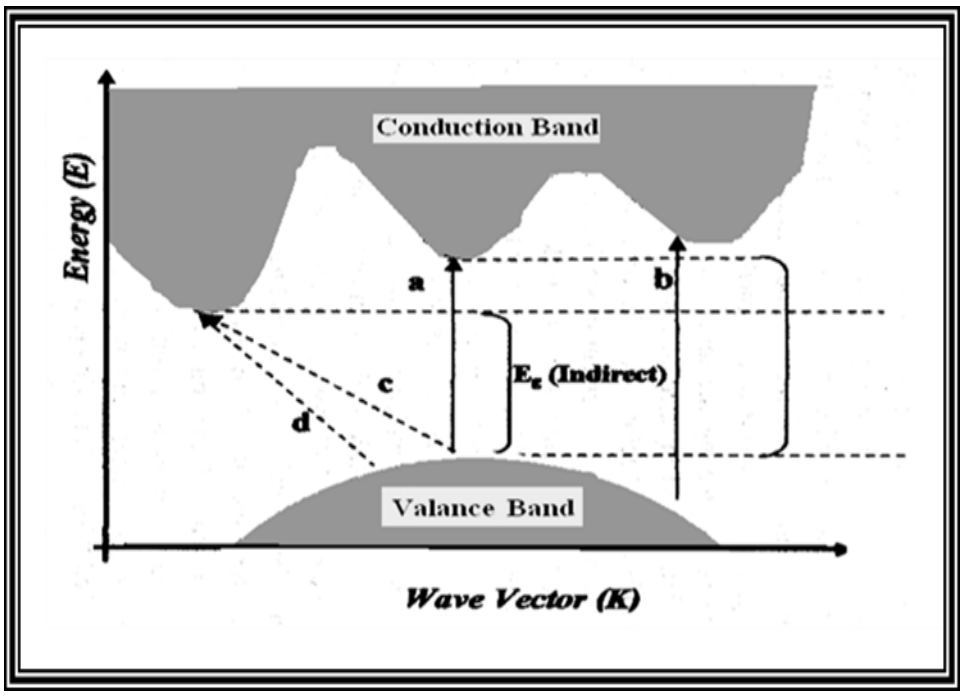

Figure (2.2): Types of Transition [59]
a- allowed direct transition. c- allowed indirect transition
b- forbidden direct transition. d- forbidden indirect transition

2.3.5 The Optical Constants

There are many important reasons for studying the optical constants of materials. Firstly, the usage of materials at optical applications like interference filters, reflective coatings, and optical fiber necessitates an accurate understanding of their optical constants over a broad wavelength range. Secondly, all materials' optical properties can be connected to their electronic band structure, atomic structure, and electrical properties [74].

2.3.5.1 Absorption Coefficient (α)

The absorption coefficient is defined as the decrease in the ratio of incident wave relative to unit length in the direction of a wave propagation within the medium [75]. The absorption coefficient (α) is proportional to the energy of the incident photon ($h\upsilon$).

Photon energy calculated by Planck's law [76] :

$$E = h\upsilon = hc / \lambda \quad \text{……...……..…..(2.6)}$$

Where: c: is the light's velocity and λ: is the light's wavelength. The transmittance of an absorbent medium with a thickness of (d) is calculated by this equation [77]:

$$T = (1 - R)^2 exp(-\alpha\, d) \quad \text{……..…….. (2.7)}$$

Where: T: transmittance, R: is the reflectance. If a light of intensity (I_O) is incident on a film of thickness (d), the transmitted intensity (I_T) can be calculated as follows [78]:

$$I_T = I_O\, exp\,(-\alpha\, d) \quad \text{……...…....(2.8)}$$

$$I_T / I_O = exp\,(-\alpha\, d) \text{……. (2.9)}$$

where : $T = I_T \ / \ I_O$

$T = \ exp\ (-\alpha d)$ ……....(2.10)

$1/T \ = \ exp\ (\alpha\ d)$…….... (2.11)

Then:

$\alpha\ d \ = \ 2.303\ logs\ (I_O \ / \ I_T)$…….. (2.12)

But $A = \ log\ (I_O \ / \ I_T)$

$\alpha\ d \ = \ 2.303 \ \times \ A$ ……..…….(2.13)

Then:

$\alpha \ = \ (2.303 \ \times \ A) \ / \ d$ ……..…....(2.14)

Where: (d) is the thickness of the sample in centimeters, (A) is the absorbance of the material.

2.3.5.2 Refractive Index (n)

The refractive index is the ratio of the velocity of light in a vacuum (C) to its velocity through a material. The refractive index (n) was determined using equation (2.16) depending on the extinction coefficient (k) and reflectance as described in the following equation [79]:

$n = (1 + R^{\frac{1}{2}})/(1 - R^{\frac{1}{2}}$ ……..……(2.15)

where (R) is the reflectance. Additionally, the following equation can be used to calculate the transmittance (T) and absorbance (A):

$R \ + \ A \ + \ T \ = \ 1$ ……..…… (2 .16)

The following equation can be used to calculated the refractive index(n) [80]:

$$n = (1 + R^{\frac{1}{2}})/(1 - R^{\frac{1}{2}}) \quad \text{……..……..…(2.17)}$$

Where (R) is the reflectance

2.3.5.3 Extinction Coefficient (k_o)

The extinction coefficient (k_o) denotes the amount of attenuation of an electromagnetic wave passing through a material, with its values dependent on the structure of free electrodes and the material density [81]. It denotes the imaginary value of the refractive index that is complex (N) [82]:

$$N = n - i\mathrm{k_o} \text{ ……..……..……..……..... (2 .18)}$$

when: n : is the real value for refractive index. The extinction coefficient (k_o) can be calculated by using equation [83]:

$$k_o = \alpha\, \lambda/4\pi \text{ ……. (2 .19)}$$

Where λ : is the wavelength of photon beams that are incident.

2.3.5.4 Dielectric Constant (ε)

The dielectric constant demonstrates matter's possibility to polarize, it can respond very difficultly with multiple frequencies. At optical frequencies, which are expressed by waves of light, electronic polarity is more dominates than other types of polarization. real and Imaginary dielectric constants can be computed using the equation [84]:

$$\varepsilon = \varepsilon_1 - i\varepsilon_2 \text{ ……..…..…… (2.20)}$$

where: ε is the complex dielectric constant and (ε_1, ε_2) are the real and the imaginary parts of the dielectric constant, respectively. The imaginary and real parts of the dielectric constant are related to (n) and (k) values [84].

$\varepsilon = N^2$ …….. (2.21)

$(n - ik)^2 = \varepsilon_1 - i\varepsilon_2$ ……..…. (2.22)

From equation (2.20) real and the imaginary complex dielectric coefficient can be written as following [85]:

$\varepsilon_1 = (n^2 - k^2)$ ……..……..…… (2.23)

$\varepsilon_2 = (2nk)$ ……..……..……. (2.24)

2.3.5.5 Optical Conductivity (σ_{op})

Optical conductivity (σ_{op}) is directly related to absorption coefficient (α) and refractive index (n) by the following relation [86]:

$\sigma_{op} = \alpha\, n\, c/4\pi$ …….. (2.25)

2.4 Electrical Properties

Is it possible to classify matter into conductors, semiconductors, and insulators depending on its electrical conductivity. Conductivities of some polymers (10^{-12} ohm^{-1} cm^{-1}) for polyamides and (~10^{-17}ohm^{-1}cm^{-1}) (10^{-16} ohm^{-1} cm-^{1}) for polystyrene [87]. The electrical conductivity of materials and their range is depicted Fig (2.3).

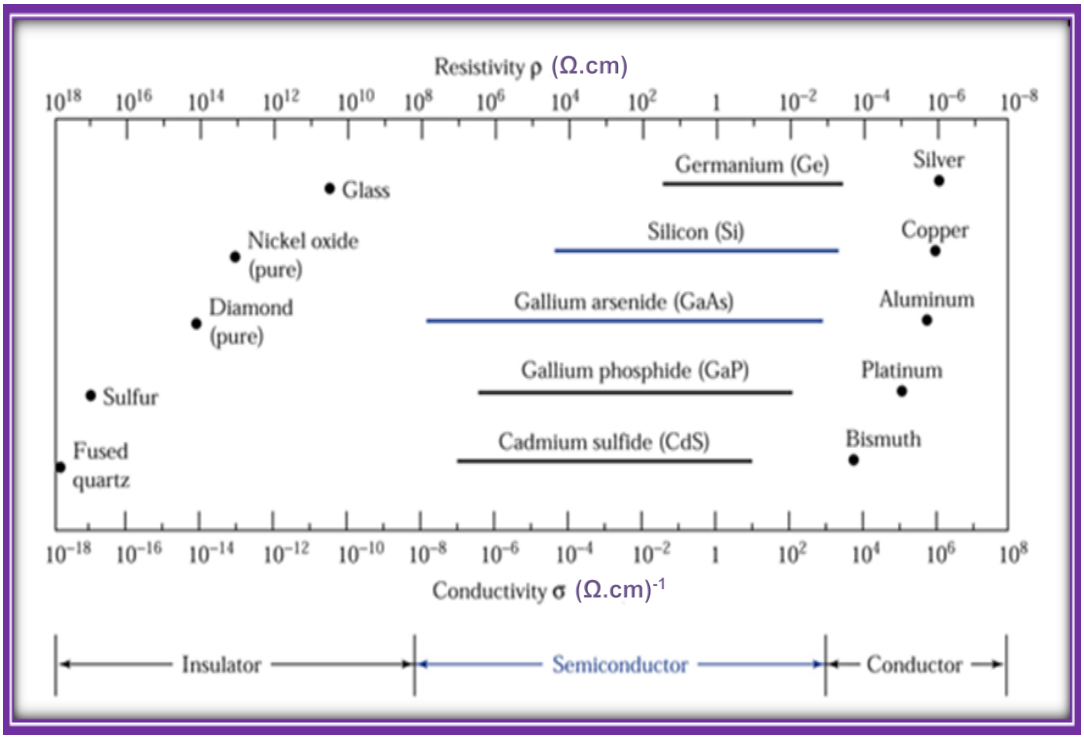

Figure (2.3): The Electrical Conductivity for Materials [87].

The electrical properties of a material are determined by its chemical composition, its atomic arrangement, and the presence for energy gap flaws. This flaw can be decreased in a many of ways, like annealing. The electrical properties are also significantly reliant on the technique used for preparation and the deposition conditions [88].

2.5 The Electrical Polarization

Electric polarization is a phenomenon that occurs when the centers of negative and positive charges don't coincide. When an electric field is applied to a dielectric material, this phenomenon usually appears. Because an electric field is applied during electrical resistivity measurements, polarization in a material can happen during electrical resistivity measurements [89]. It's worth noting that this polarized surface charge density (formerly represented by (P) and also referred to as simply polarization or induced polarization) is perfectly equal to the value of the dipole moment for each unit volume [90]:

$P = N_m \mu$ …….. … ……. (2.26)

Where: N_m is the number of molecules. We can make the following assumption about the dipole moment being proportionate to the electrical field [91]:

$\mu = a_o E$ …… ..(2.27)

where: a_o: is a constant called the polarizability.

E: is an electrical field intensity.

The relation between the electrical displacement (flux density) (D) and (E) is shown by [92]:

$D_o = \varepsilon_o E$ ……(2.28)

where: $\varepsilon_o = 8.854 \times 10^{-12} F/m$ is the permittivity of a vacuum.

The electric flux density in the dielectric part is proportional to that in vacuum by [93]:

$D = \varepsilon_o E + P$ …… (2.29)

As:

$D = \varepsilon' \varepsilon_o E$ …… (2.30)

But, $\varepsilon' = D / \varepsilon_o E$

Then:

$\varepsilon' = 1 + P/(\varepsilon_o E)$ ……..…….. (2.31)

The polarizability and dielectric constant are related by the Clausius-Mossotti equation [91]:

$(N_m\ a_o)/(3\varepsilon_o) = (\varepsilon' - 1)/(\varepsilon' + 2)$ .....(2.32)

Polarization of material can be detected by the components of this polarization so that the total polarization can be calculated, figure (2.4) depicts the several types of polarization [94]:

$P = P_e + P_i + P_d + P_o$ ..... (2.33)

A- Electronic Polarization (P_e) :

Electronic polarization arises as a result of a distortion in the charge distribution caused by an external electric field. A separation arises between the positive charge of the nucleus and the center of the negative charge, resulting in the generation of induced dipoles [95]. Electronic polarization occurs in a relatively short period of time (10^{-15} seconds) and is not affected by temperature [96], as shown in Figure 1. (2.4-a).

B- Ionic Polarization (P_i):

It was generated as an ionic compound with ionic properties. It occurred when matter was subjected to an electric field, which altered the lengths of the ionic bonds, resulting in the formation of a net dipole moment in the molecule that did not exist previously [95]. It only lasts for about 10^{-11}–10^{-13} seconds [96]. The temperature has no effect on this type of polarization, as showed in the Figure (2.4-b).

C- Rotational or Orientation Polarization (P_d) :

It's also called as molecular polarization [94]. This occurs in molecules with a perpetual dipole moment [97]. When the electric field is applied, the dipoles revolve around of the axis, also arrange themselves in direction of the

field. This type of polarization is dependent on temperature and takes a long time to occur [95], as showed in the Figure (2.4-c).

D- Space Charge or Interfacial Polarization (P_o):

It occurs when a matter contains impurities, a vacuum, or a structural fault, which results in a concentration of opposing charges on the impurities terminals, this refers to the formation of dipoles within a molecule, atom, or zone of material. This type of polarization is dependent on homogeneity of matter and the rate of being free from impurities. It occurs mostly in radios frequency and can be expand to frequencies beneath audio and depending on flaws that produces the polarization [95], as illustrated in Figure (2.4-d).

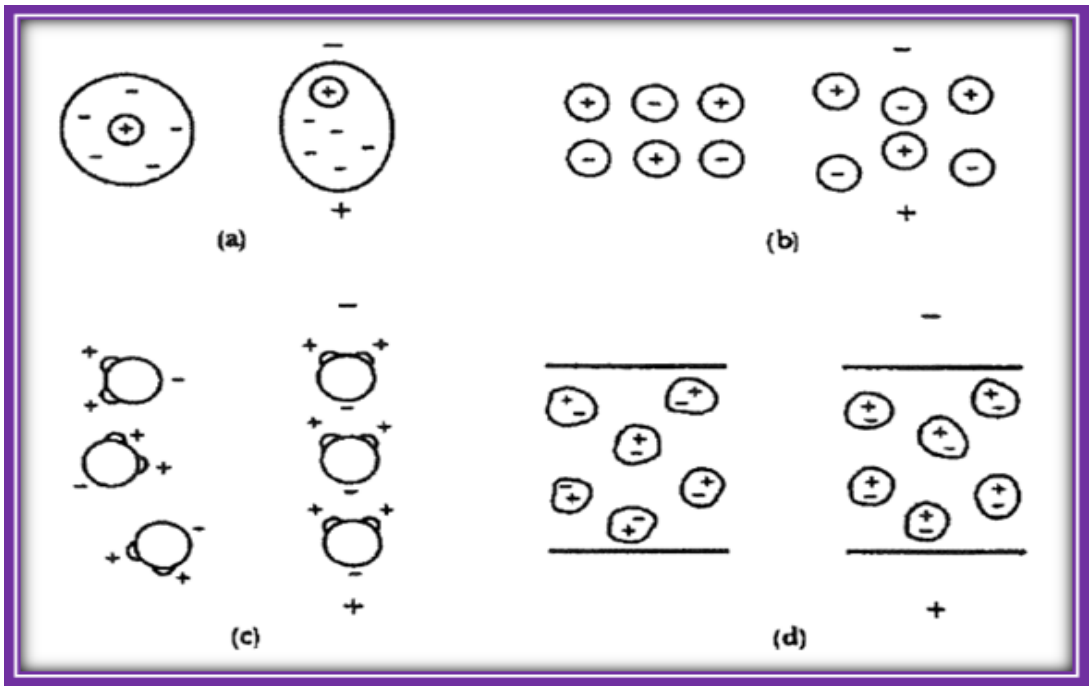

Figure (2.4): Four different Types of Polarization [94]

a: Electronic Polarization c: Orientation Polarization d: Space Charge b: Ionic Polarization

2.6 The (A.C) Electrical Conductivity

The (A.C) conductivity isn't the same as (D.C) conductivity, which is when the frequency of an electric field doesn't change during (D.C) conductivity, while the frequency of the electric field will change through (A.C) conductivity [98]. It is very common to use dielectric spectroscopy to study at the dielectric characteristics of polymers like (ε', tanδ,...), it is based on measuring the voltage and current (phase and amplitude of the A.C. system) [99].

The dielectric constant represents the ratio of the capacitance of the capacitor in the presence of the insulation between its plates to its capacitance in the presence of the vacuum, its amount varies from material to another depending on the amount of polarization in the material [100].

When the voltage is alternating $V = V_m\, e^{i\omega t}$ [100], is applied through a capacitor (C) contains insulator, therefore, the currents moving through the capacitor (C) precedes the voltage by the phase ($\pi/2$) [101]:

$$I = i\,\omega CV \qquad \ldots\ldots\ldots\ldots\ldots\ldots\ldots\ldots\ldots\ldots\ldots\ldots\ldots\ldots\ldots\ldots\ldots\ldots \quad (2.34)$$

where (i) is an imaginary number ($i = \sqrt{-1}$), (ω) represent the angular frequency of the applied electric field ($\omega = 2\pi f$), (V_m) is the maximum voltage and (f) is the frequency.

This demonstrates that an electronic current (I) is the total of a conduction current (I_p), which is a same phase with (V), and the capacitance current (I_q), which has a phase changes of ($\pi/2$) ,as follows [102]:

$$I = I_p + iI_q \qquad \ldots\ldots\ldots\ldots\ldots\ldots\ldots\ldots\ldots\ldots\ldots\ldots\ldots\ldots\ldots\ldots\ldots\ldots\ldots\ldots \quad (2.35)$$

The capacitance of a capacitor made up of two parallel surfaces is determined by the following equation:

$$C = \varepsilon \, \varepsilon_o \, A_r/d \qquad \text{(2.36)}$$

Where : (d) is the thickness and (A_r) is the area.

Substituting equation (2.36) into equation (2.34), obtain:

$$I = i \, \omega \, \varepsilon \, \varepsilon_o V \, A_r/d \qquad \text{(2.37)}$$

After then, the dielectric constant is considered as a complex quantity (ε). The difference of the complex dielectric constant's real and imaginary portions is described by equation [103]:

$$\varepsilon = \varepsilon' - i \, \varepsilon'' \qquad \text{(2.38)}$$

where: ε'' is the dielectric loss.

Therefore, obtain

$$I = i \, \omega \, \varepsilon_o \, (\varepsilon' - i \, \varepsilon'') \, V \, A_r/d \qquad \text{(2.39)}$$

When equation (2.34) is compared to equation (2.38),then:

$$I_p = \omega \, \varepsilon_o \, \varepsilon'' \; V \, A_r/d \qquad \text{(2.40)}$$

$$I_q = \omega \, \varepsilon_o \, \varepsilon' \; V \, A_r/d \qquad \text{(2.41)}$$

Figure (2.5) shows that the loss factor (tanδ) is determined by the equation [101]:

$$tan \, \delta = I_p / I_q = \varepsilon''/ \varepsilon' \qquad \text{(2.42)}$$

At low frequencies, the capacitor can be expressed by an ideal capacitor and resistance R_p linked in parallel, so [102]:

$$I = I_p + iI_q = V/R_p + i\,\omega C_p\,V \quad \text{……..(2.43)}$$

As a result, the impedance (Z) is then equal to [100]:

$$1/Z = 1/R_p + i\,\omega\,C_p \quad \text{……..… (2.44)}$$

Using the equations (2.40), (2.41) and (2.43), one can get the following [100]:

$$R_p = d\,/\,\omega A_r \varepsilon_o\,\varepsilon'' \quad \text{…….(2.45)}$$

$$\varepsilon'' = 1\,/\,\omega\,R_p\,C_o \quad \text{……..……..…. (2.46)}$$

$$C_p = \varepsilon_o\,\varepsilon'\,A_r\,/d \quad \text{…….... (2.47)}$$

$$\varepsilon' = C_p\,/\,C_o \quad \text{..…….(2.48)}$$

$$\varepsilon'' = D\varepsilon' \quad \text{..…….(2.49)}$$

The dissipated power at an insulator is expressed by the existence of an alternating voltage as a function with alternating conductivity, as shown in equation (2.50):

$$\sigma_{A.C} = \omega\,\varepsilon_o\,\varepsilon'' \quad \text{…… (2.50)}$$

$\sigma_{A.C}$ is a temperature measurement in an insulating material caused by the dipoles rotating in their places (or the charges vibrating) as a result of the field alternating [104].

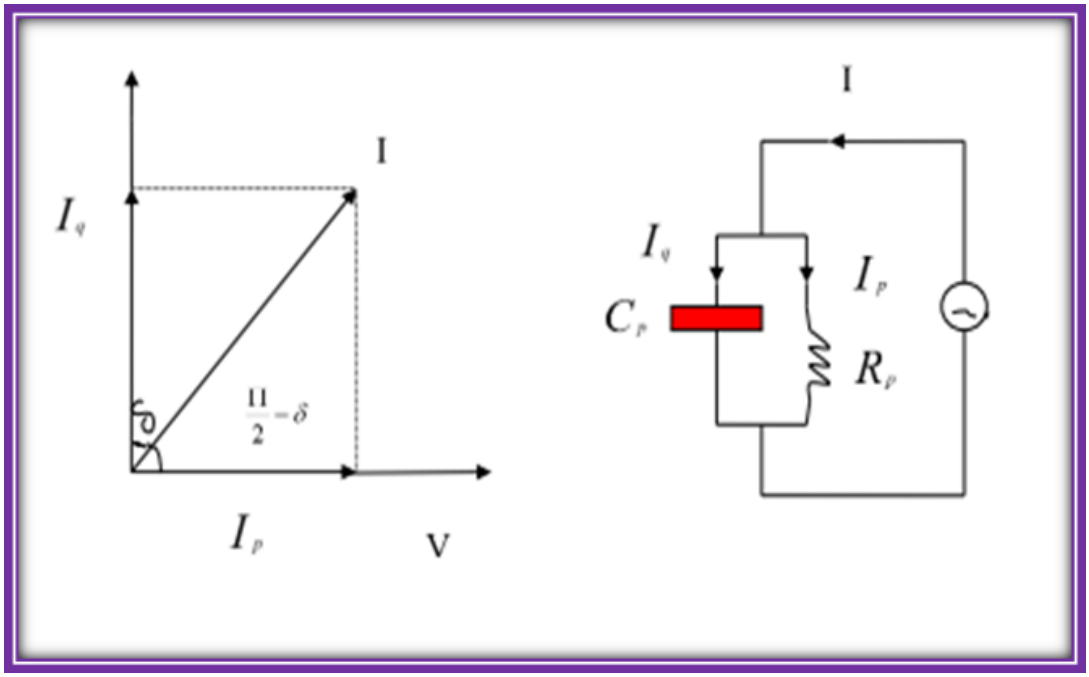

Figure (2.5): The circuit equivalent of a non-ideal capacitor. [101].

2.7 Anti-Bacterial Activity

Infectious disease development in general poses a severe threat to public health worldwide, particularly with the emergence of antibiotic-resistant bacterial species. As a result, there is an incentive to develop new bactericidal [105].In general, both gram-negative and gram-positive bacterial strains are considered to be a significant public health threat. Antibiotics are used to control infections caused by both community and hospital environments pathogens for many years [106,107].

Recent advancements in the domain of nano bio technology, especially the ability to prepare metal oxide nanoparticles with precise size and shape specifications, are anticipated to result in the development of new antibacterial agents. The size of nanoparticles has a major effect on their functional properties. As a result of their unique chemical, physical, and biological characteristics, nanoparticles have garnered considerable attention in various fields, including medicine [108,109].

Due to the wide spread use of the antibiotics in prevention and treatment of bacterial infections, resistant microorganisms have developed, necessitating the creation of new active molecules against bacteria. The size of nanoparticles is approximately the same as that of biological molecules and less than that of human cells. Nanotreatment strategies could be used to improve medical treatments [110].

2.8 Plasma Interaction with Matter

The interaction of plasmas and materials is one of the most interesting and critical subjects in the field of plasma technology. In fact, plasma processing has been the hallmark of plasma technology and its impact on the semiconductor industry. Plasmas are ubiquitous in nature and are responsible for some of the most fundamental interactions known to man. For example, in astrobiology, the early formation of the stars from interstellar media (ISM) dust and the presence of hydrogen molecules in interstellar space are conjectured to be governed by carbonaceous dust grain surface interactions with plasma energetic particles (hydrogen, helium) forming more complex organic molecules [111]. Ion-induced etching in modern high-density plasma-processing tools is driven by the complex energetic multi-particle interaction with material surfaces, and fluorescent lamps operate by a balance of the plasma-material interaction (PMI) under high gas pressure containers. When a plasma interacts with matter, several processes can occur, including [112]:

- Ionization: Plasma can ionize matter by stripping off electrons from atoms or molecules , creating positively charged ions and free electrons.

- Heating: When a plasma comes into contact with matter , it can transfer energy to the material , heating it up

- Surface modification: Plasma can modify the surface properties of materials by retching , deposition , or surface activation.

- Chemical reactions: Plasma can induce chemical reactions in matter by providing energy and creating reactive species , such as redicals.

- Erosion: High-energy plasma can erode or ablate material by physically sputtering atoms or molecules from the surface

These processes can have practical applications in a wide range of fields, including material processing, surface modification, plasma medicine and energy production.

Chapter Three
Experimental Part

3.1 Introduction

This chapter includes the steps of samples preparation for (PVA/PAA/Ag) nanocomposites, samples tests and measurements steps: optical Microscopic, FTIR, Field-emission Scanning Electron Microscope (FESEM), optical measurements A.C electrical measurements and antibacterial activity application.

3.2 The Materials Used in This Work

3.2.1 Polymers

Three polymers are used in this work:

A) **Polyvinyl Alcohol (PVA):** used as powder form and could be obtained from local markets with high purity (99.8%).

B) **polyacrylic Acid (PAA).:** it was obtained as powder form and could be obtained from local markets with high purity (99.8%).

3.2.2 Metals Nanoparticles

1. **Silver nanoparticles (Ag):** used as powder with particle diameter (20-40) nm from EPRUI. company and high purity (99.9%).

3.3 Preparation of (PVA/PAA/Ag) Nanocomposites

Casting method was fabricated of polyvinyl alcohol (PVA)/Polyacrylic acid (PAA) doped with silver nanoparticle (Ag) NPs. The blend film (70%PVA/30%PAA) was fabricated by dissolving of 1 gm in distilled water (30 ml). the fabricated of nanocomposite by adding of the Ag NPs to solution (PVA/PAA) with content 2, 4, 6 and 8 wt. %. The samples were prepared with thickness 110 μm. Figure (3.1) illustration the schematic of experimental work.

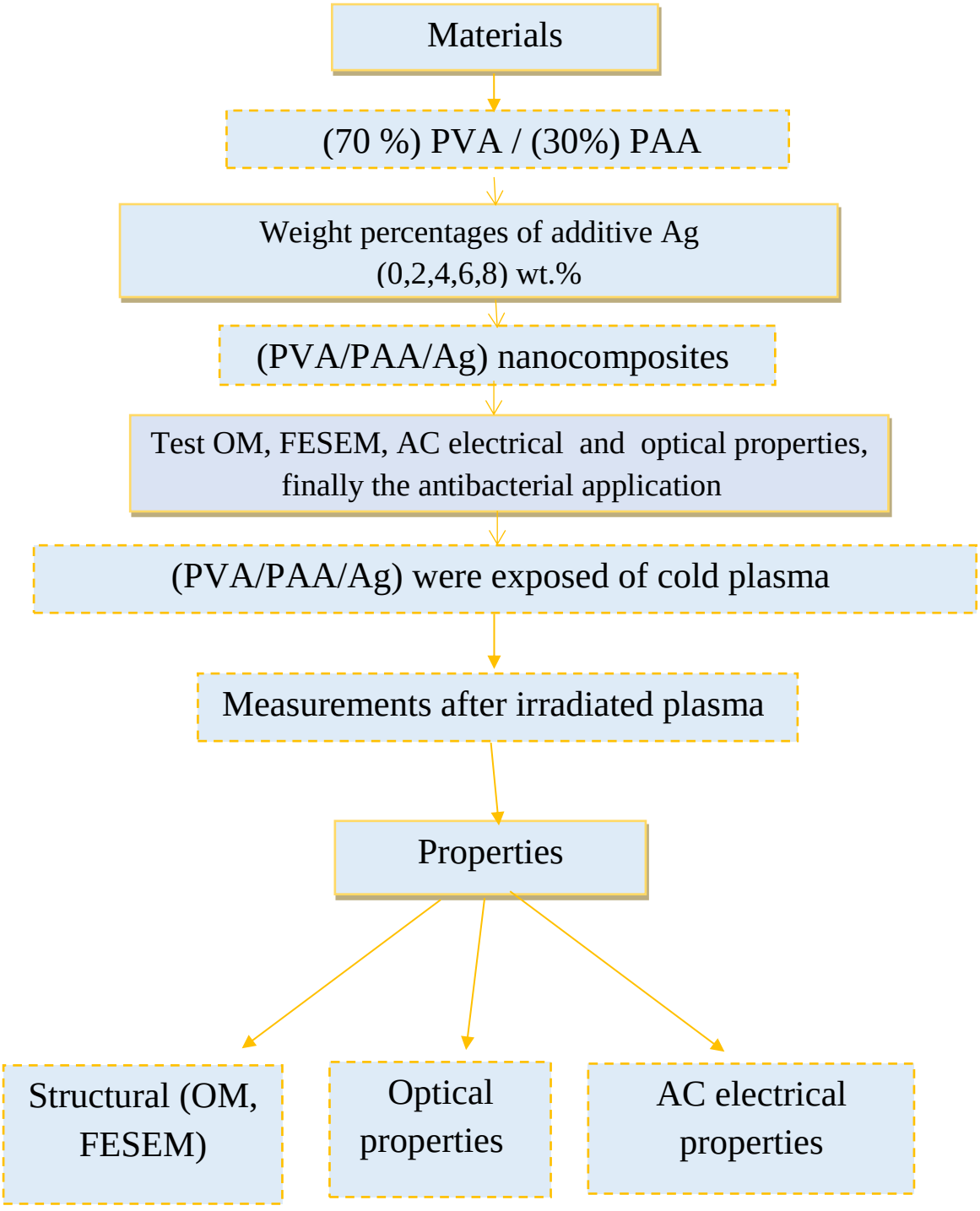

Figure (3.1): The Schematic of Experimental Work

3.4 Irradiation plasma

After prepared of (PVA/PAA/Ag) nanocomposite, the cold plasma (Ar gas) irradiated with voltage 5.6 KV , current 0.2 A, pressure 5 mbar and the diameter of the tube for generating the plasma is 5 mm are shown in figure (3.2), which consists of the following specifications:

-Tube end 3 mm

-Between the electrodes 1,5 cm

-Electrode thickness 1 mm

-Electrodes width 1 cm

-Frequency 5.6KHZ

-Voltage 5.16KV

-Inner tube diameter 3mm

-Outer tube diameter 5mm

-Plasma exposure time 40 s

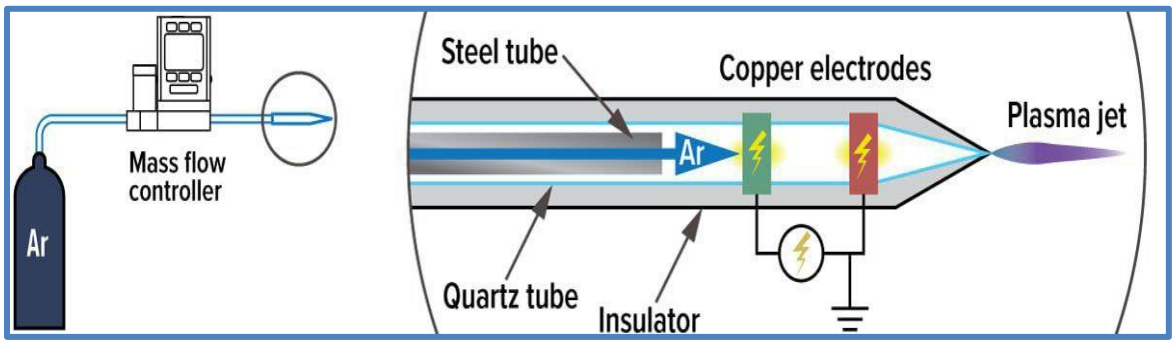

Figure (3.2): Cold plasma irradiation

3.5 Measurements of Structural Properties

3.5.1 Optical Microscope

The optical microscope supplied by Olympus name (Toup View) model (Nikon-73346) as shown in figure (3.3) and fitted with a light intensity automatic operated camera is used to analyze the sample of (PVA/PAA/Ag) Nano composites. This calculation was carried out Department of Physics,

University of Babylon/College of Education for Pure Sciences, under magnification(10x).

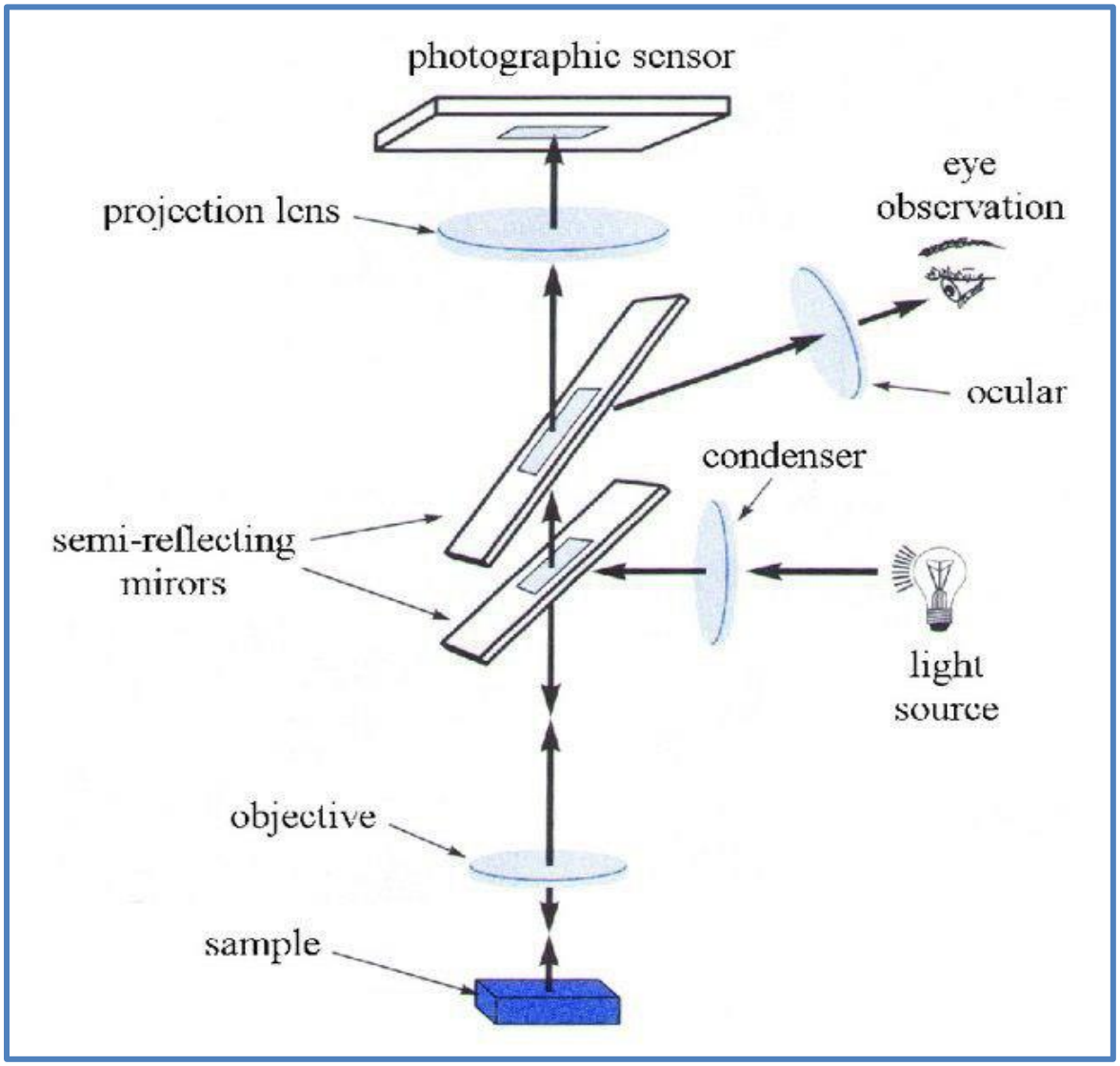

Figure (3.3): Optical Microscope

3.5.2 FTIR Spectral Characterization

FTIR spectra were recorded by FTIR (Bruker company, German origin, type vertex -70). FTIR was implemented in the University of Babylon /College of Education for Pure Sciences/Department of Physics. In this study, the considered wave number range is (500-4000) cm^{-1}, as shown in Figure (3.4).

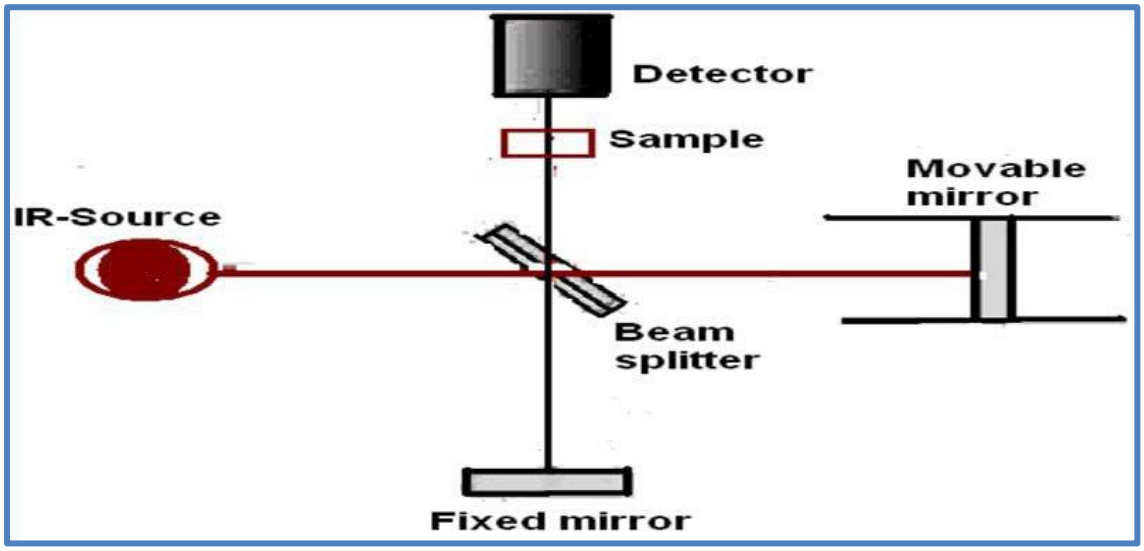

Figure (3.4): Fourier Transform Infrared (FTIR) Spectroscopy Device .

3.5.3Field-emission Scanning Electron Microscope

The Field-emission scanning electron microscope (FESEM) is an electron microscope that images the sample surface by scanning it with a high-energy beam of electrons in a raster scan pattern. The specimens for an FESEM testing must be electrically conductive, at least at the surface, and electrically grounded to prevent the accumulation of electrostatic charge at the surface. Small part of ($1cm^2$) was taken from the sample to examine it by FESEM. In this work low vacuum scanning electron microscope was used. The surface morphology of (PVA/PAA/Ag nanocomposites was observed using Tescan mira3 SEM microscope. is equipped with dual Bruker XFlash EDS detectors and Bruker Flash HD EBSD (Czech Tescan Instrument Co.) for analytical studies at the University of Tehran as shown in figure (3.5). The advantage was observed using this technique (Low vacuum SE detecto) is beam deceleration technology (BDT) for high resolution imaging and high surface sensitivity at very low kv and variable pressure operation, Fully integrated active anti-vibration system.

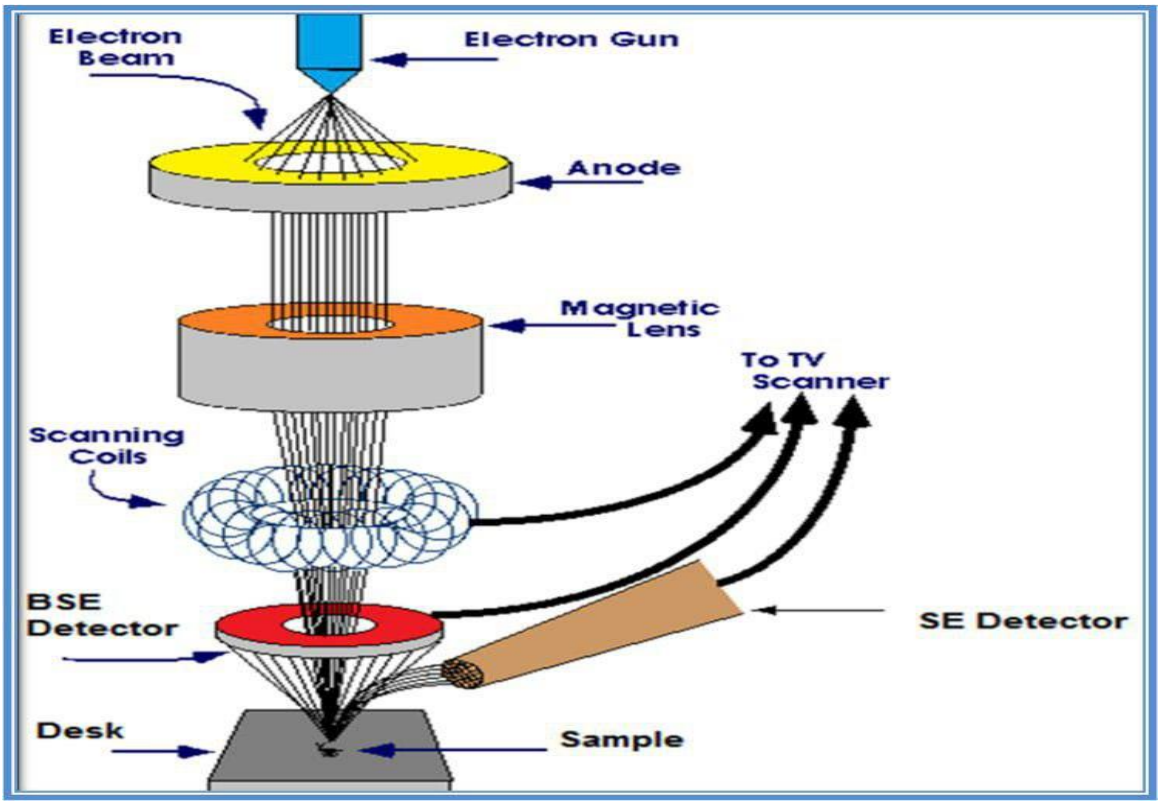

Figure (3.5): Image of System of FESEM Device.

3.6 Optical Properties Measurements

The absorption spectrum of (PVA/PAA/Ag) nanocomposites were recorded in the wavelength range (٢٠0-1100) nm using the double beam spectrophotometer (Shimadzu, UV-1800 Å) as shown in Figure (3.6). The absorption spectrum was recorded at room temperature. A computer program (UV Probe software) was used to get absorption. Implemented at Babylon university/college of education for Pure Sciences/department of physics.

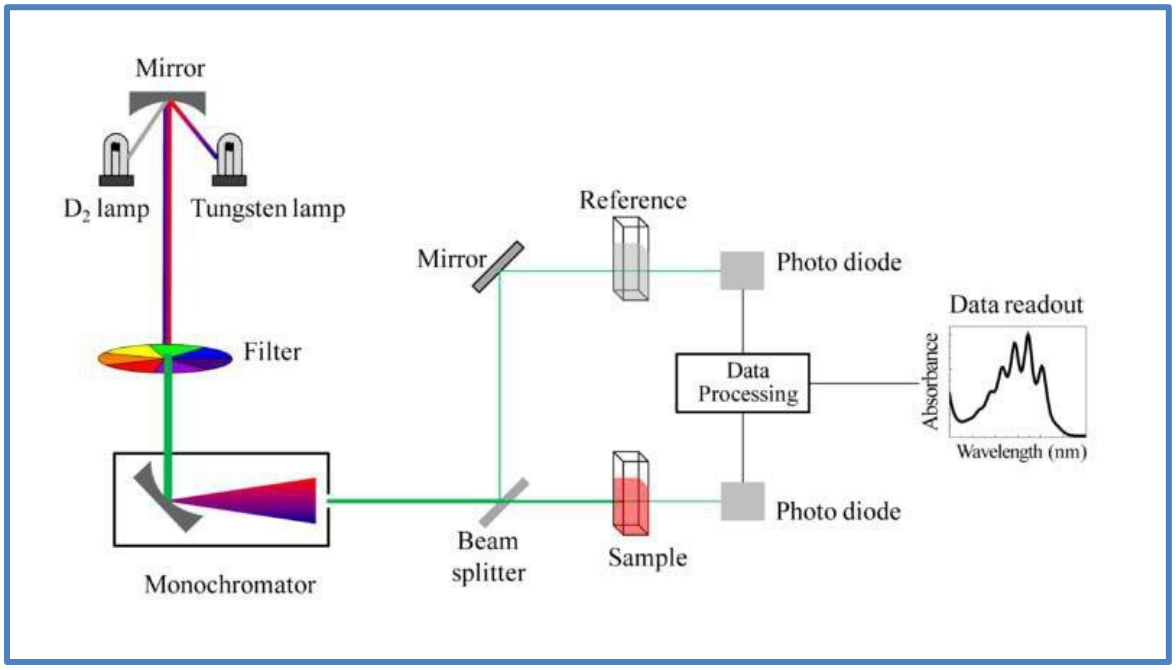

Figure (3.6): Image of UV Spectrophotometer (photometer).

3.7 A.C. Electrical Properties Measurement

The LCR meter style (HIOKI 3532-50 LCR Hi TESTER (Japan) is used to measure A.C. Electrical Conductivity at the University of Babylon/College of Education for Pure Sciences/Physics Department figure (3.7) shows a diagram for the A.C electrical measurement system. Only (1cm) from each one of the samples has been taken and put between two electrodes and by different frequencies from (100Hz-5MHz) at room temperature. The capacity and dissipated factor have been recorded for all 43 the samples. Dielectric constant, dielectric loss and conductivity have been calculated from this data.

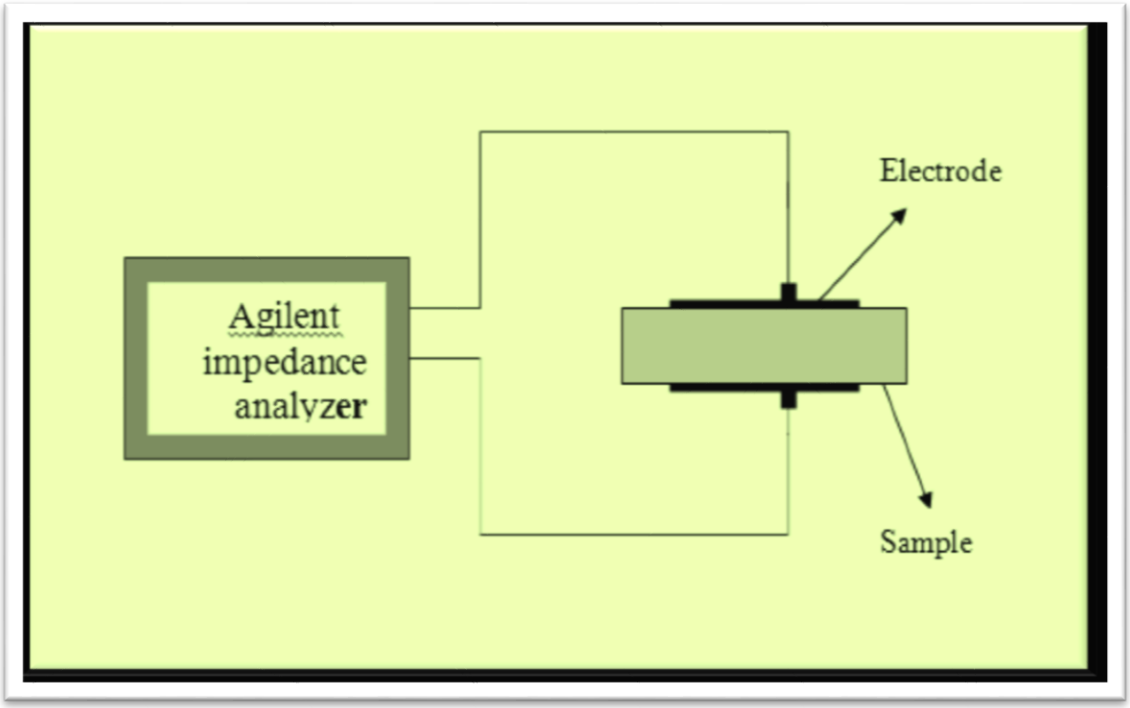

Figure (3.7): Diagram for system of A.C electrical measurement system

3.8 Application of (PVA/PAA/Ag) Nanocomposite Films

Antimicrobial activity of the (PVA/PAA/Ag) nanocomposites tested samples were determined using a disc diffusion method. The antibacterial activities were done by using gram positive (Staphylococcus aureus) and gram-negative (Escherichia coli). Bacteria (Staphylococcus aureus and Escherichia (coli) were cultured in Muller-Hinton agar. The disks of the (PVA/PAA/Ag) nanocomposites were placed over the media and incubated at 37°C for 24 hours. The inhibition zone diameter was measured.

Chapter Four

Results and Discussion

4.1 Introduction

This chapter included the results and its discussion of the structural, optical and (A.C) electrical measurements for (PVA/PAA/Ag) nanocomposites. It will also discuss the effect of different concentrations additive nanoparticles (Ag) in the optical microscope, fourier transform infrared rays (FTIR), Field-emission scanning electron microscope (FE-SEM) before and after exposed of argon plasma and antibacterial activity applications of (PVA/PAA/Ag) nanocomposites are also discussed.

4.2 The Structural Properties

4.2.1 The Optical Microscope

Figures (4.1), and (4.2) show the photomicrograph of the pure (PVA/PAA) composite and various content of silver nanoparticle (Ag NPs) before and after exposed of argon plasma respectively. From figure (4.1A), it can be note that at lower content, the Ag nanoparticles agglomerate as clusters. When the content of Ag nanoparticles is risen, the nanoparticles create a network within the (PVA/PAA) nanocomposites at 8 wt. percent, while in Figure (4.2A) after exposed of argon plasma, it can be obtained that surface become more roughness, while the content of Ag nanoparticles is increased in the figure (B, C, D and E), the nanoparticles create a network within the (PVA/PAA) nanocomposites at 8 wt. percent. On the other hand, it noted when the (PVA/PAA/Ag) nanocomposite is exposed to Ar plasma, the formation of pits and grooves, which indicates sufficient energy in the Ar plasma to extract this substance which noted of (PVA/PAA/Ag) nanocomposites at 8wt.% contents.

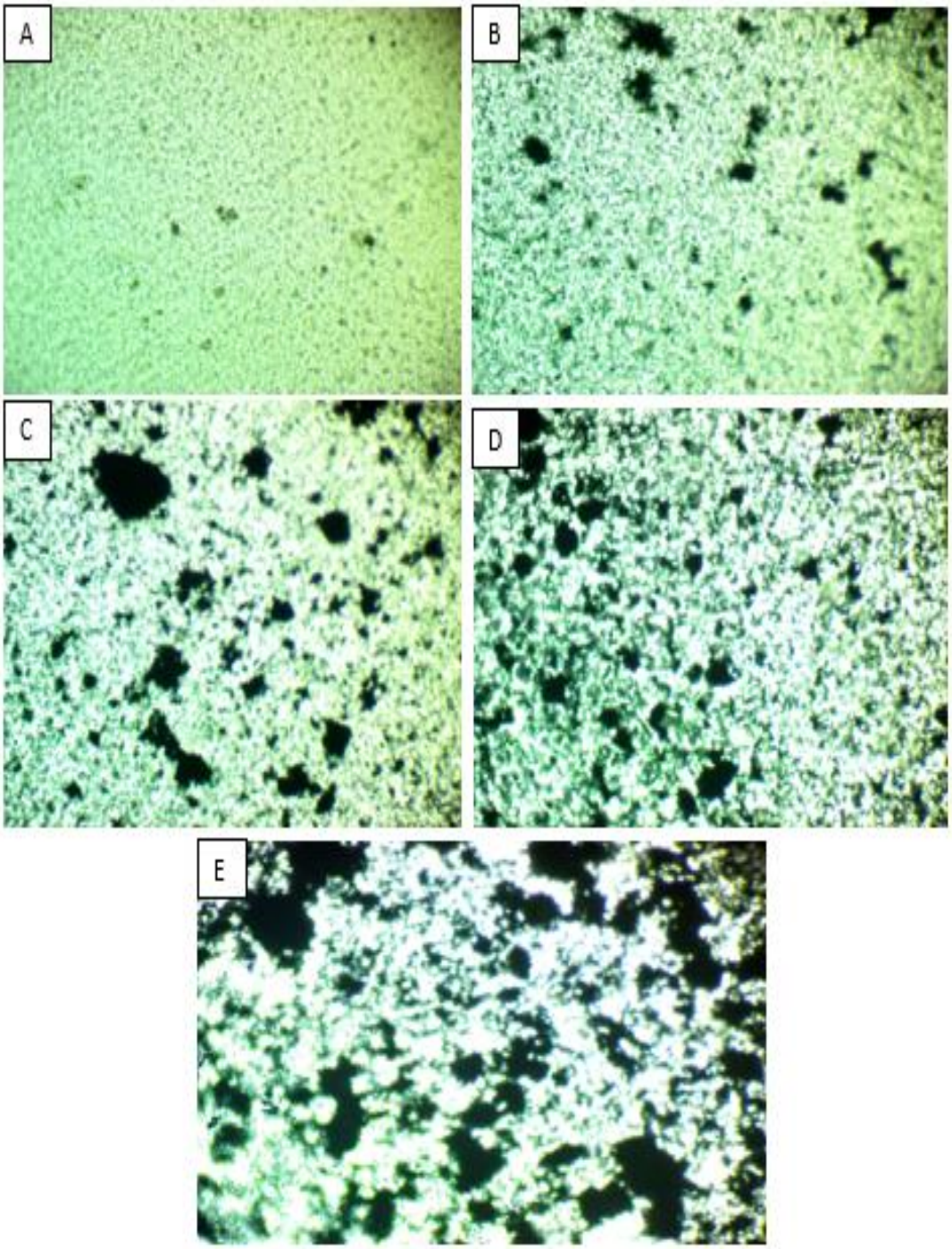

Figure (4.1) Images of OM (X10) for (PVA/PAA/Ag) Nanocomposites A. Pure Polymer, B. 2 wt.% of (Ag) NPs, C. 4 wt.% of (Ag) NPs, D. 6 wt.% of (Ag) NPs and E. 8 wt.% of (Ag) NPs.

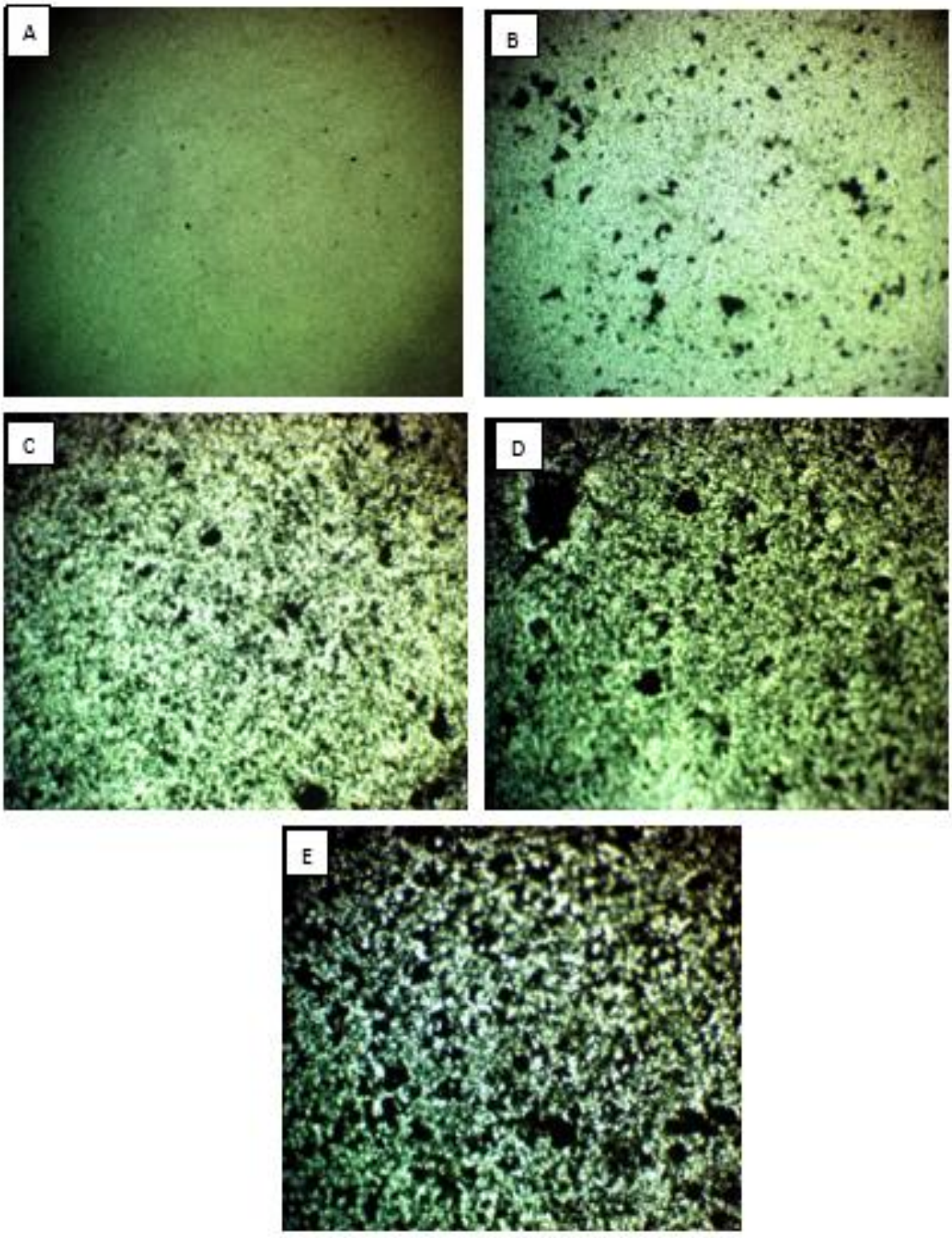

Figure (4.2) Images of OM (X10) for (PVA/PAA/Ag) nanocomposites after exposed Ar plasma: A. pure polymer, B. 2 wt.% of (Ag) NPs, C. 4 wt.% of (Ag) NPs, D. 6 wt.% of (Ag) NPs and E. 8 wt.% of (Ag) NPs.

4.2.2 Fourier Transform Infrared Rays (FTIR)

FTIR spectroscopy afford beneficial information about the connections between their functional groups. FTIR of pure (PVA/PAA) composite and its with variant content of (2, 4, 6 and 8) wt.% Ag NPs as reveal in Figure (4.3).

The functional groups of PVA/PAA seemed at 3228.28, 2461.02, 1647.23, and 1084.82 cm^{-1} matching to broad band to the stretching vibrations of "hydroxyl groups O–H (PVA and PAA), C=O stretching of the ester group carbonyl groups (PVA) , O-H ether group bending vibration , C-O stretching vibration" (PVA and PAA) [113] .

Because of the addition of variable ratios of Ag NPs. The transmittance reductions as the percentages of Ag NPs allocated to rise the density of NPs increase. This examination shows that there are no new absorption peaks, implying that there are no interactions between the (PVA/PAA) polymer matrix and the Ag NPs, which mean that the happened physical interaction between the nanoparticles and the polymer blend. This result agrees with researches [114,115].

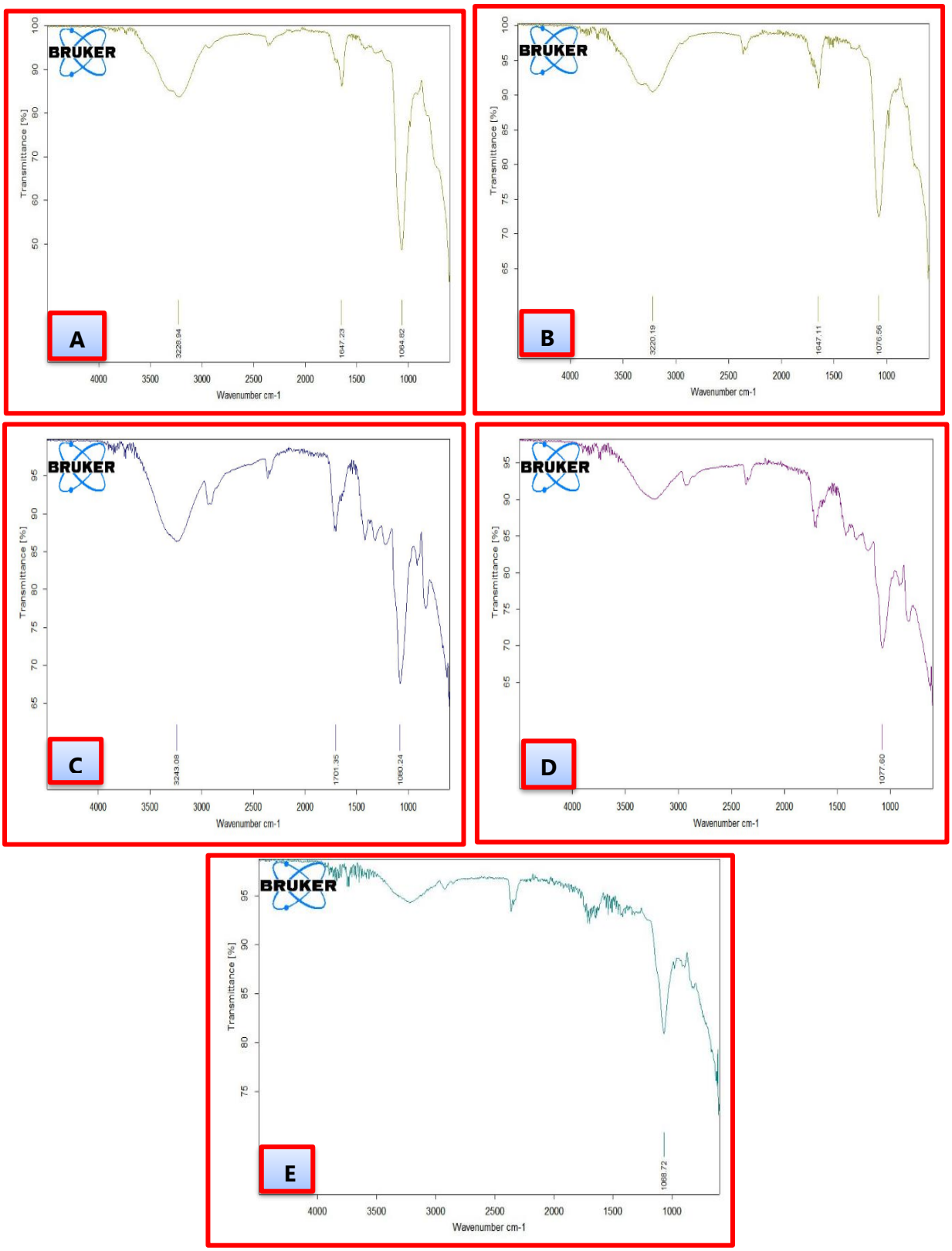

Figure (4.3): FTIR spectra of (PVA/PAA/Ag) Nanocomposites A. pure polymer, B. 2 wt.% of (Ag) NPs, C. 4 wt.% of (Ag) NPs, D. 6 wt.% of (Ag) NPs and E. 8 wt.% of (Ag) NPs.

4.2.3 Field-emission Scanning Electron Microscopy (FESEM)

FESEM is used to analyze the dispersion of nanocomposites particles in the polymer matrix and to thoroughly investigate the effect of silver nanoparticles material. Figure (4.4) and (4.5) demonstrations representative FESEM images of (PVA/PAA/Ag) nanocomposites films and with vary content of Ag NPs material with scale 10 µm before and after exposed Ar plasma respectively.

It was found to be smoother, more homogeneous, and more coherent in image (A) in figure (4.4). Though gradually growing the nanoparticles ratio in polymer (B, C, D and E), surface morphology shifts. The presence of a homogenous growth mechanism is shown by the formation of multiple spherical particle clusters on the surface of the nanocomposite's films. It gets softer as the content of both nanoparticles rises the Ag nanoparticles collective and are well distributed in (PVA/PAA/Ag) nanocomposites films in image (B, C, D and E).

When Ag nanoparticles are added to (PVA/PAA) composites at a concentration of 8 wt.%, they form a continuous within the network polymer, while in Figure (4.5). It is noted that the surface was changed after being exposed to argon plasma. The variation in the morphology is the result of the etching procedure promoted by argon plasma species on the (PVA/PAA) surface. Though gradually growing the nanoparticles ratio in polymer (B, C, D and E), distribution regular and homogenous spherical nanoparticle inside the polymer matrix and this nanoparticle increased with increasing concentration of Ag nanoparticle. This result agrees with [116,117].

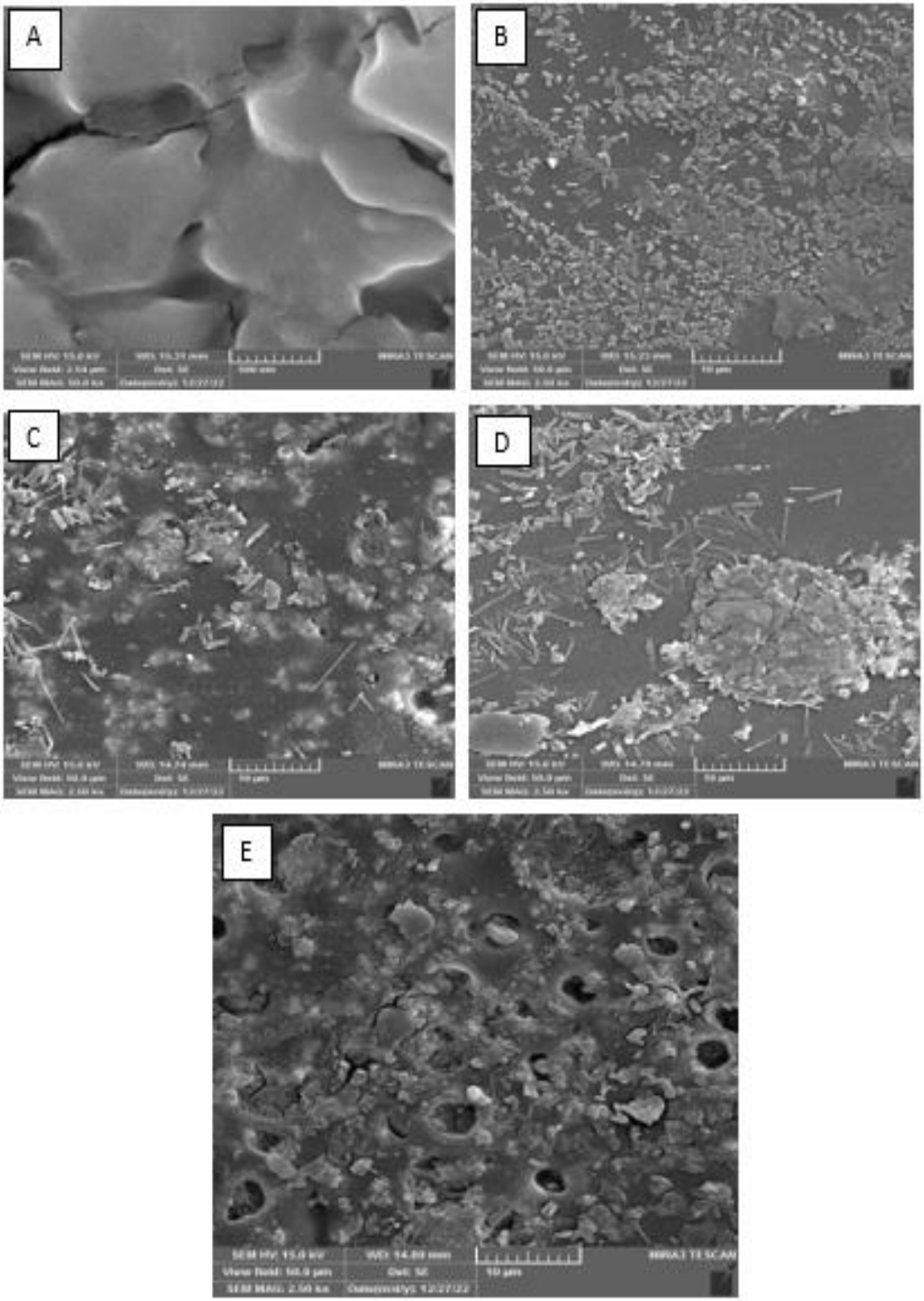

Figure (4.4): SEM images of (PVA/PAA/Ag) Nanocomposites, (A) for (PVA/PAA), (B) 2 wt.% Ag NPs, (C) 4 wt.% Ag NPs, (D) 6 wt.% Ag NPs, (E) 8 wt.% Ag NPs

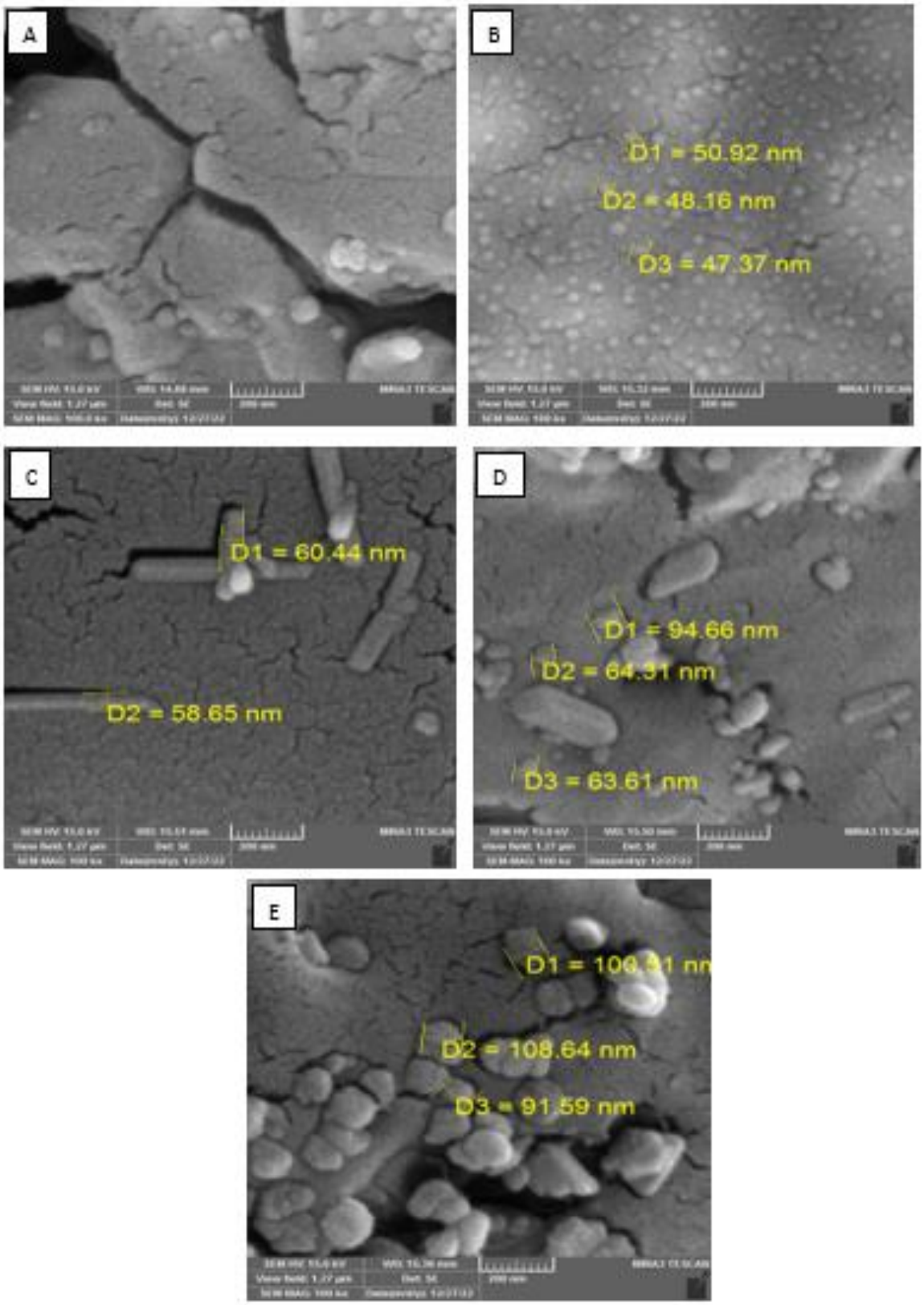

Figure (4.5): SEM images of (PVA/PAA/Ag) Nanocomposites after exposed Ar plasma :(A) for (PVA/PAA), (B) 2 wt.% Ag NPs, (C) 4 wt.% Ag NPs, (D) 6 wt.% Ag NPs, (E) 8 wt.% Ag NPs

4.3 Optical Properties

The main purpose of studying the optical properties of the (PVA/PAA/Ag) nanocomposites is to identify the effect of adding (Ag) nanoparticles on the optical properties of (PVA/PAA) films. The research covers the recording of the spectrum of absorbance for the (PVA/PAA/Ag) films at room temperature and calculating the absorption coefficient, extinction coefficient, and other optical constants, as well as identifying the types of electronic transitions and calculating energy gaps before and after exposed Ar plasma.

4.3.1 The Absorbance

The absorption (PVA/PAA/Ag) nanocomposite with various content of silver nanoparticle (Ag NPs) were recorded at wavelengths range (200-1100) nm at room temperature. The absorbance for (PVA/PAA/Ag) film with wavelength is revealed in figures (4.6) and (4.7) before and after exposed Ar plasma, respectively. As noted, the absorbance rises with rising content of Ag NPs, which attributed to donor level electrons being excited to the conduction band at high energies. Also, because photons provide enough energy to react with atoms, an electron can be excited from a lower to a higher energy level. Also, the absorbance exhibits a higher magnitude at shorter wavelengths, followed by a gradual decline as the wavelength increases. The observed phenomenon can be attributed to the density of the positional levels that arise from the presence of impurity atoms situated between the conduction and valence band. The absorption process takes place when electrons, which receive photons with an energy level lower than the optical energy gap of the incident photons, are transferred to auxiliary levels. The absorbance after irradiation has high values compared before irradiation which attributed to the

increased free charge carriers and polarized. This result agrees with [118,119,120].

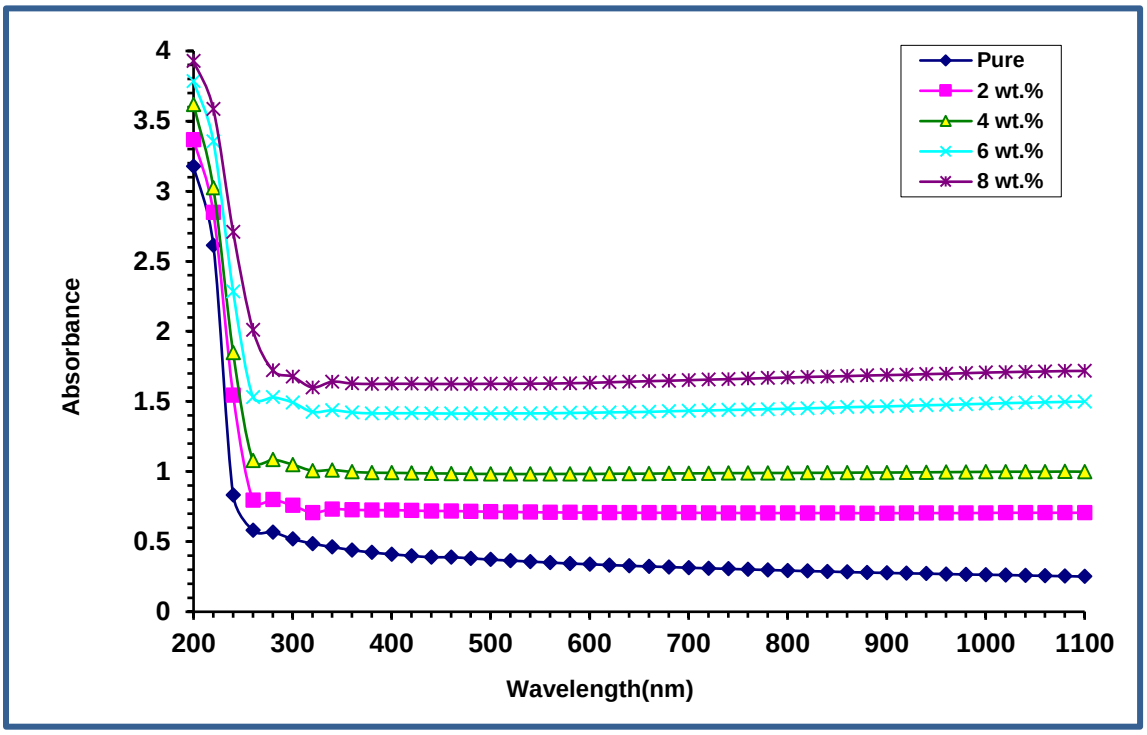

Figure (4.6): The absorbance as a function of wavelength of (PVA/PAA/Ag) nanocomposite with wavelength.

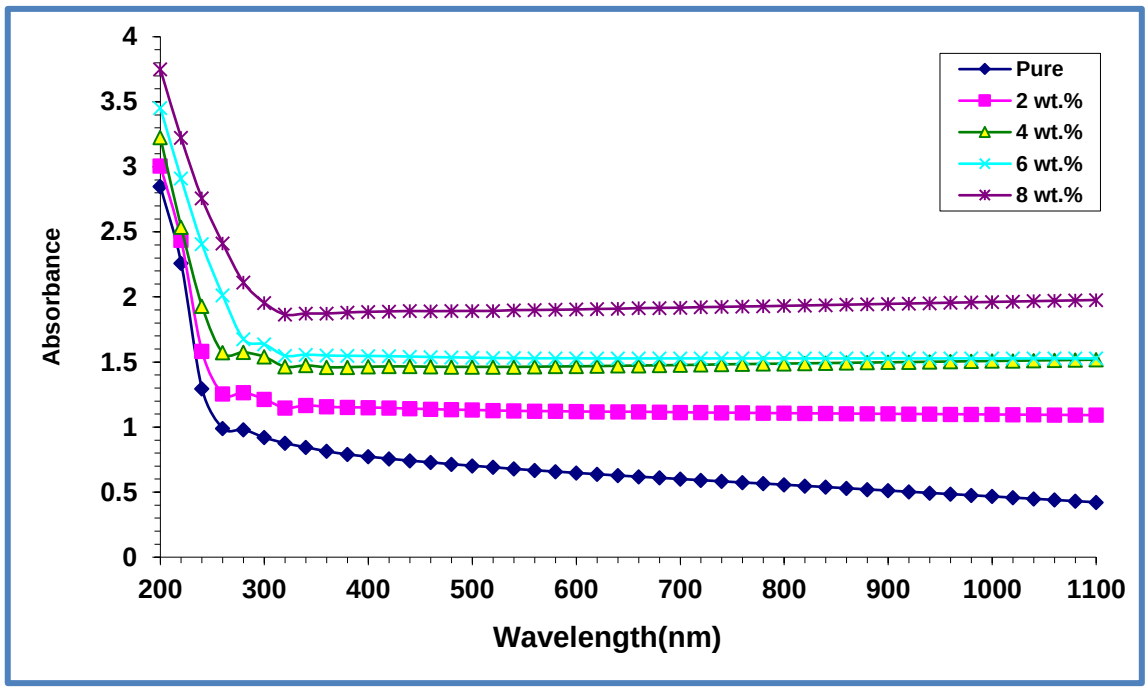

Figure (4.7): The absorbance as a function of wavelength of (PVA/PAA/Ag) nanocomposite with wavelength after exposed Ar plasma.

4.3.2 the Transmittance

The transmittance for (PVA/PAA/Ag) film with wavelength is revealed in figures (4.8) and (4.9) before and after exposed Ar plasma respectively. From this figure, it is observed that the transmittance reduces as the amount of Ag NPs nanoparticles rise which is due to the agglomeration of nanoparticles with rising content of Ag NPs. The transmittance after irradiation have reduce values compared before irradiation which attributed to the increased free charge carriers and polarized. This result agrees with [119,120].

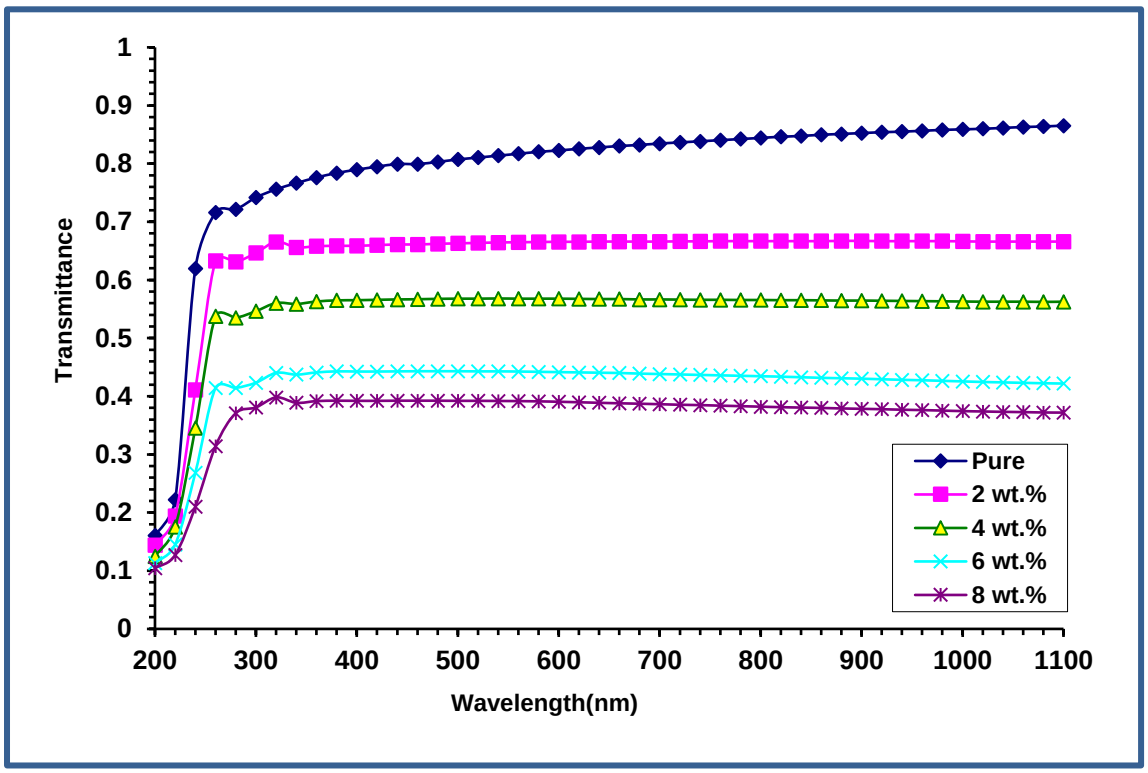

Figure (4.8): Variation transmittance of (PVA/PAA/Ag) nanocomposite with the wavelengths

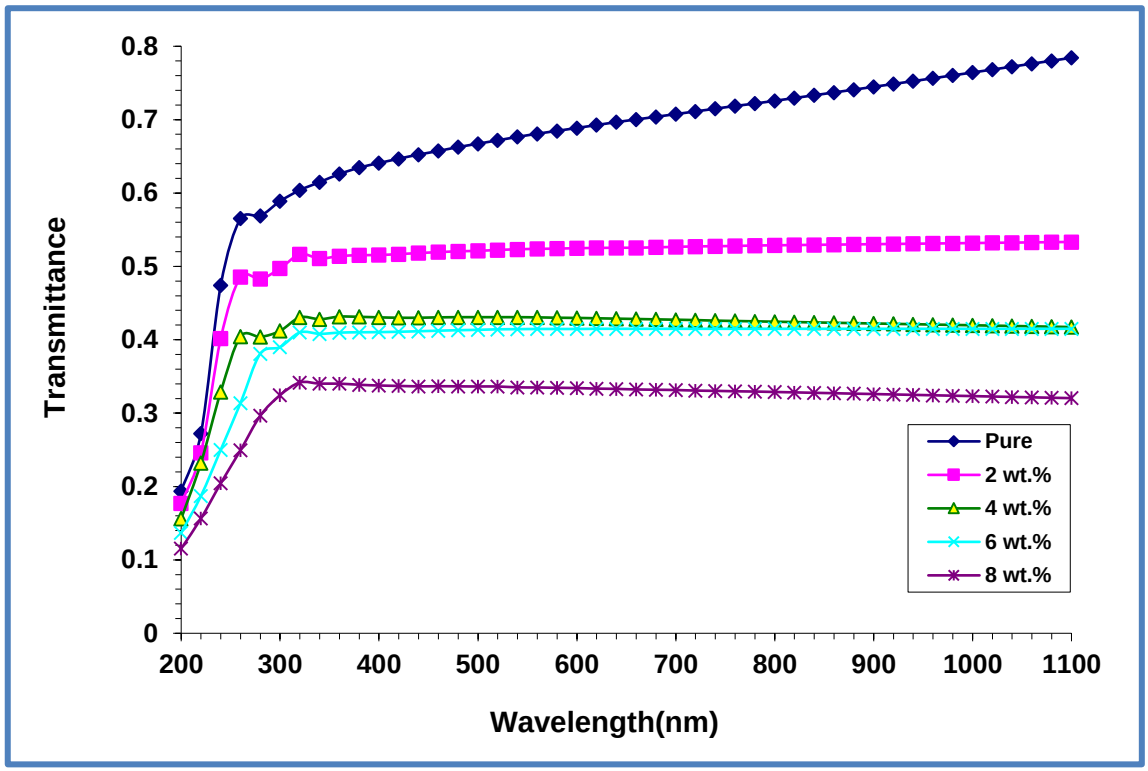

Figure (4.9): The transmittance as a function of wavelength of (PVA/PAA/Ag) nanocomposite with wavelength after exposed Ar plasma.

4.3.3 The Absorption coefficient

The absorption coefficient (α) of nanocomposites were calculated by equation (2-13). The α of (PVA/PAA/Ag) nanocomposite versus energy of photon is revealed in Figures (4.10) and (4.11) before and after exposed Ar plasma. The α might help you find out what kind of electron transition you're dealing with [19]. It is assumed that direct electron transitions occur when the material's absorption coefficient is large 10^4 cm^{-1}. When the α is low 10^4 cm^{-1}, an indirect transition of electrons is assumed. The values of α of (PVA/PAA/Ag) nanocomposite is less than 10^4 cm^{-1}, the transition of electron is indirect. The α of nanocomposites rises with the rises of the content of Ag NPs, this is due to the rise of various charge carriers and therefore rising the absorption and absorption coefficient for (PVA/PAA/Ag) nanocomposites. This result agrees with [119,120, 121].

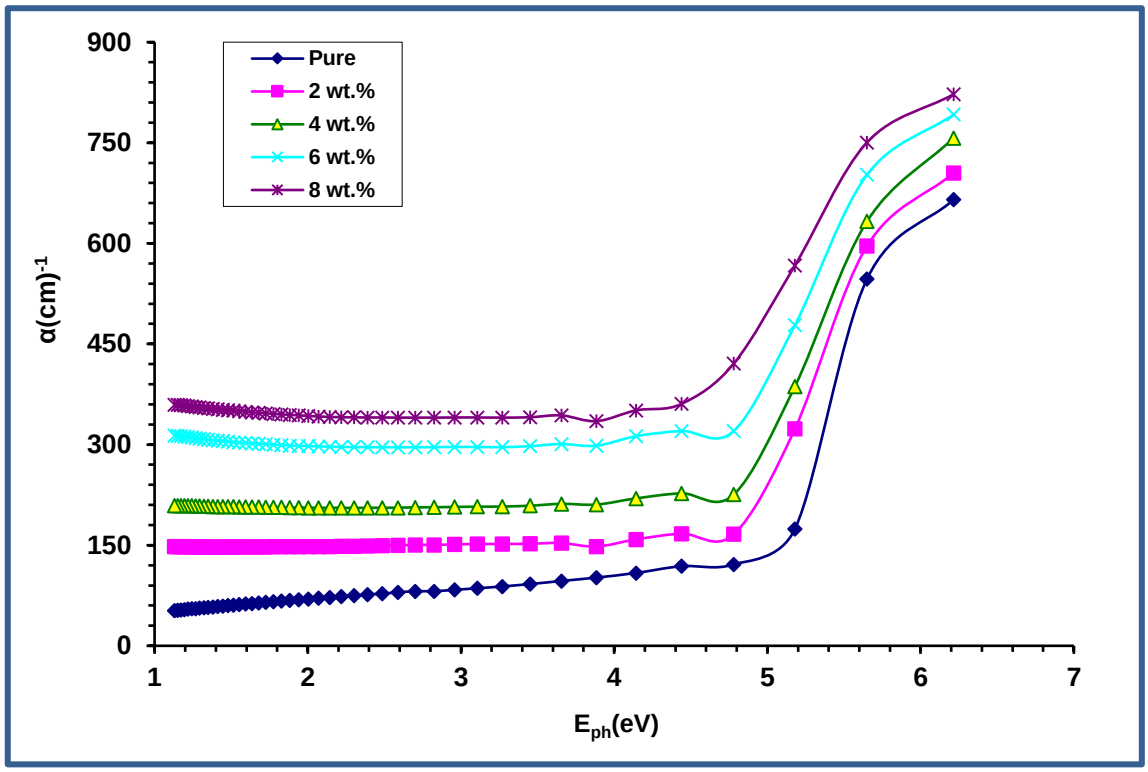

Figure (4.10): The variation absorption coefficient of (PVA/PAA/Ag) nanocomposite with the photon energies.

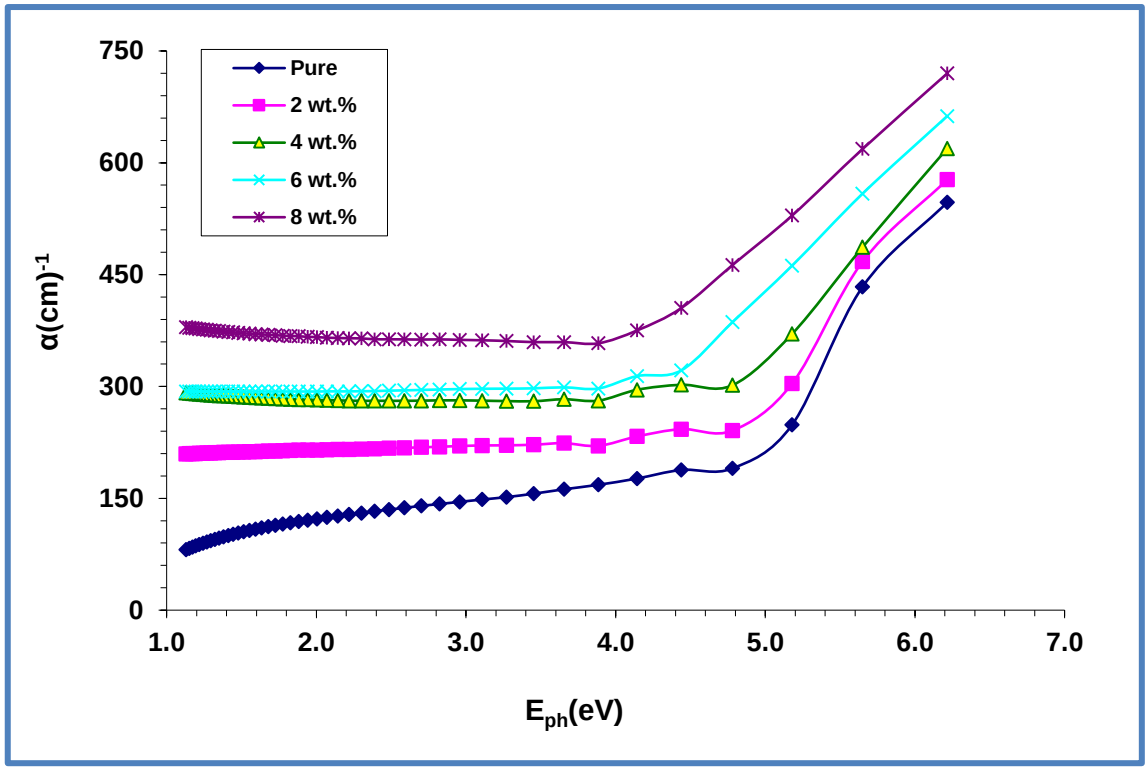

Figure (4.11): The Variation Absorption Coefficient of (PVA/PAA/Ag) Nanocomposite with the Photon Energies after exposed Ar plasma.

4.3.4 The indirect energy gap of (PVA/PAA/Ag) nanocomposite

The gap of energy of nanocomposites was planned by relation (2-5). The E_g for allowed and forbidden indirect transitions of (PVA/PAA/Ag) nanocomposites are explained in Figures (4.12), (4.13), (4.14), and (4.15) before and after exposed Ar plasma respectively. It can be finding the energy gap for the indirect transition by ploting the data or tang cut from the top of the curve to the (x axis) at (hv) [122]. From this figure, the E_g are reduce with the rises of the Ag NPs content. This action is due to the formation of levels in the E_g and therefore, these local levels reduce the energy gap with rise of the PVA/PAA/Ag nanocomposite. The allowed and forbidden indirect band gap after irradiation have reduce values compared before irradiation which attributed to the increased free charge carriers and polarized. Table (4-1) and (4-2) obtained the values of allowed and forbidden energy gap before and after exposed Ar plasma. This result agrees with [119.120,123].

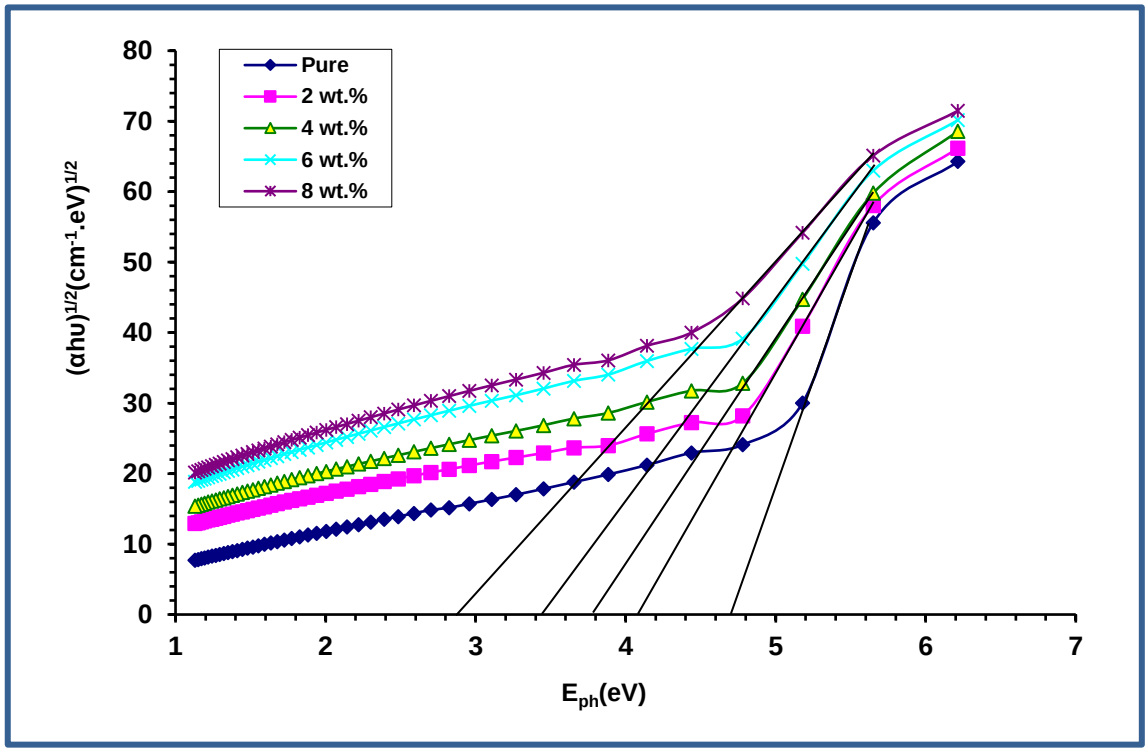

Figure (4.12): The E_g for the allowed indirect transition $(\alpha h\nu)^{1/2}$ $(cm^{-1}.eV)^{1/2}$ of (PVA/PAA/Ag) nanocomposite.

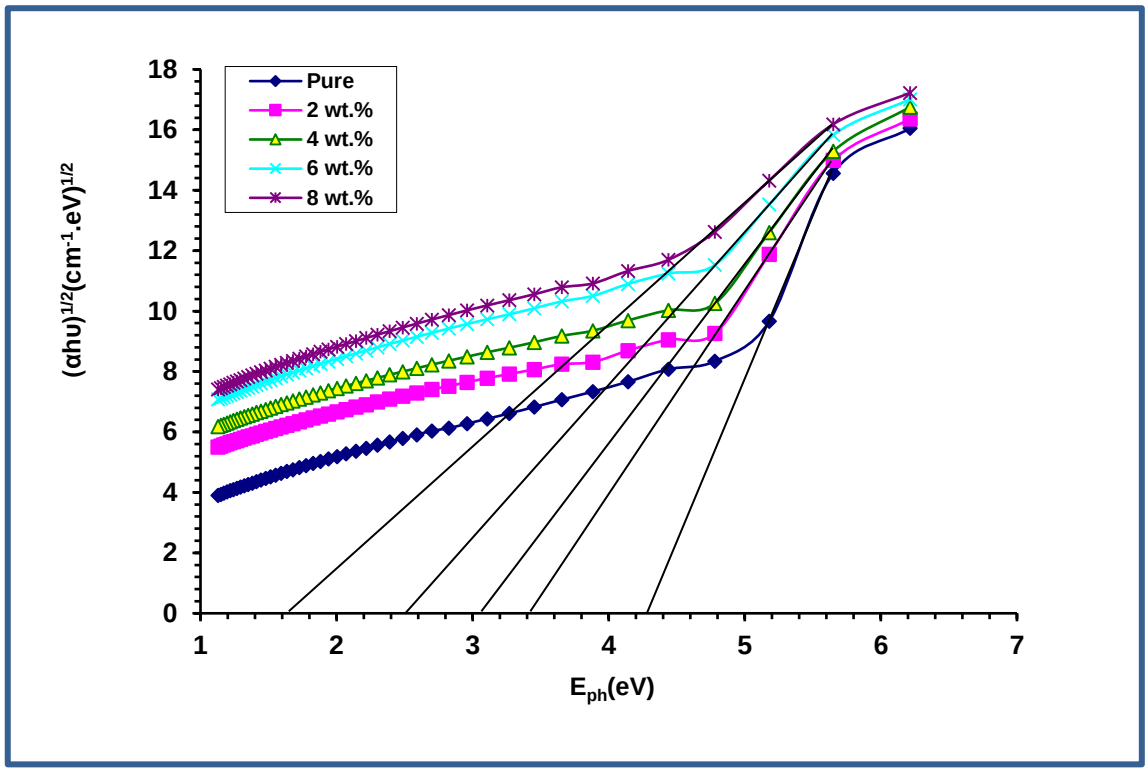

Figure (4.13): The E_g for the allowed indirect transition $(\alpha hv)^{1/2}$ $(cm^{-1}.eV)^{1/2}$ of (PVA/PAA/Ag) nanocomposite after exposed Ar plasma

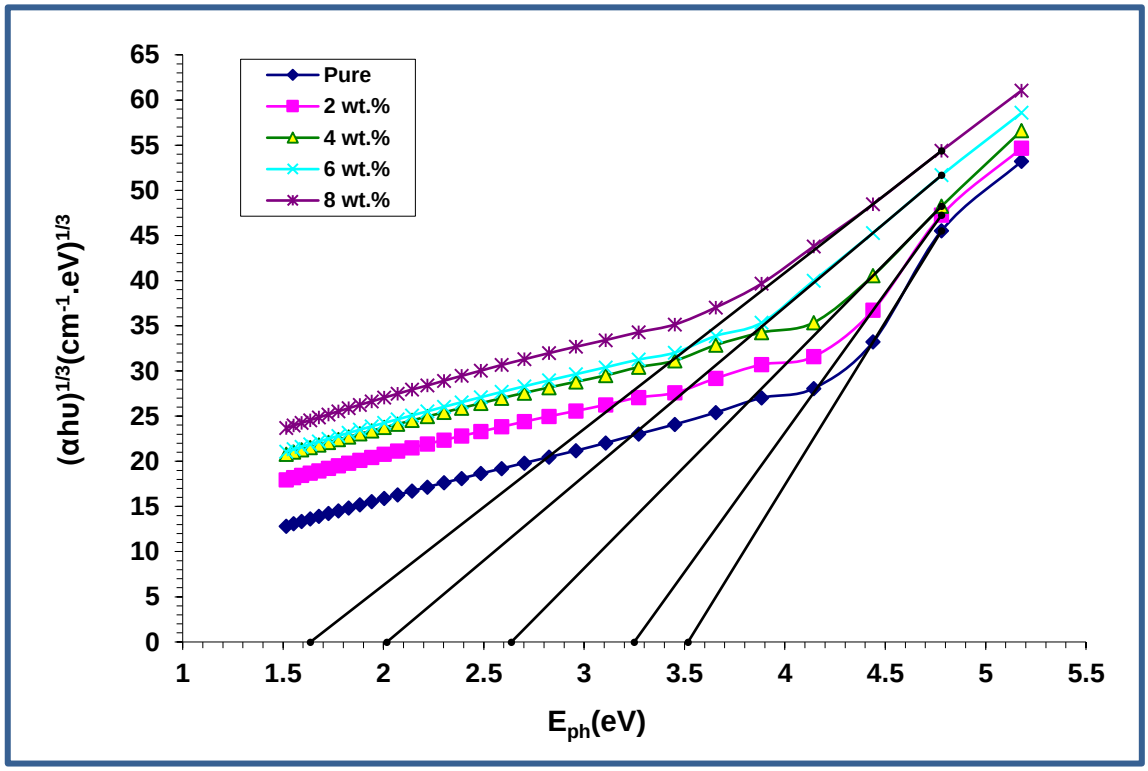

Figure (4.14): The E_g for the forbidden indirect transition $(\alpha hv)^{1/3}(cm^{-1}.eV)^{1/3}$ of (PVA/PAA/Ag) nanocomposite.

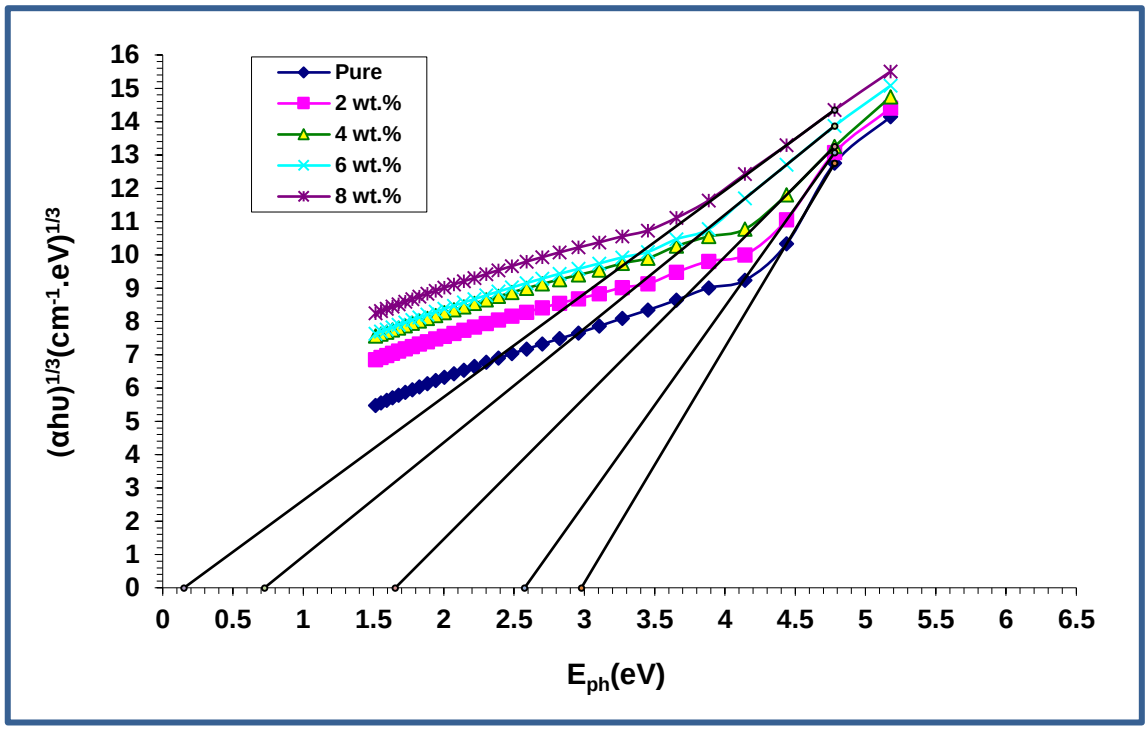

Figure (4.15): The E_g for the forbidden indirect transition $(\alpha h\nu)^{1/3}(cm^{-1}.eV)^{1/3}$ of (PVA/PAA/Ag) nanocomposite after exposed Ar plasma.

Table (4-1) The values allowed gap of energy of (PVA/PAA/Ag) nanocomposites

Content of Ag NPs wt.%	Allowed of indirect energy gap (eV)	Forbidden of indirect energy gap (eV)
0	4.76	4.25
2	4.15	3.42
4	3.82	3.08
6	3.44	2.53
8	2.91	1.64

Table (4-2) The values gap of energy of (PVA/PAA/Ag) nanocomposites after exposed Ar plasma

Content of Ag NPs wt.%	Allowed of indirect energy gap (eV)	Forbidden of indirect energy gap (eV)
0	3.52	2.98
2	3.25	2.57
4	2.64	1.66
6	2.02	0.72
8	1.64	0.15

4.3.5 The extinction coefficient

The extinction coefficient (k) was calculated by using the equation (2-19). Figures (4.16) and (4.17) explain the k of (PVA/PAA/Ag) nanocomposites versus of wavelength before and after exposed Ar plasma. It is observed that the extinction coefficient of nanocomposites rise with the rises of the Ag NPs content, this is due to the rise in optical absorption and photons distribution in the (PVA/PAA) polymer matrix. The extinction coefficient after irradiation have high values compared before irradiation which attributed to the increased free charge carriers and polarized This result agrees with [119,120,122].

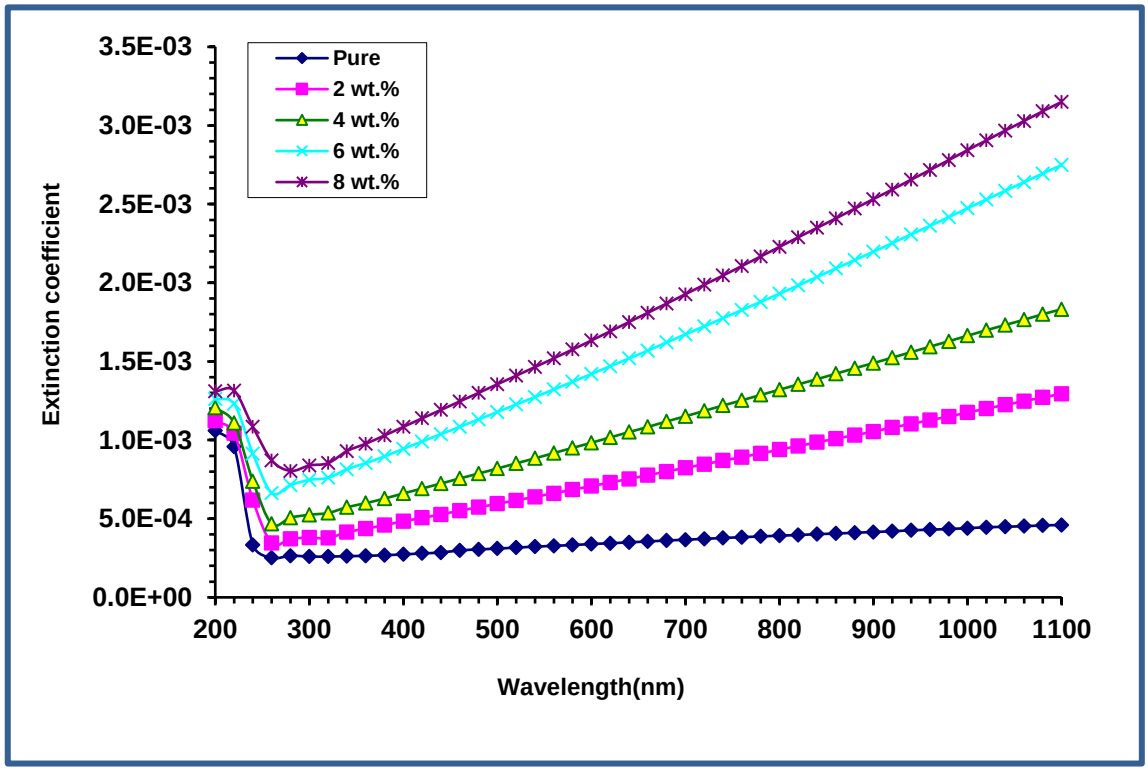

Figure (4.16): Variation of k for (PVA/PAA/Ag) nanocomposite with the wavelength.

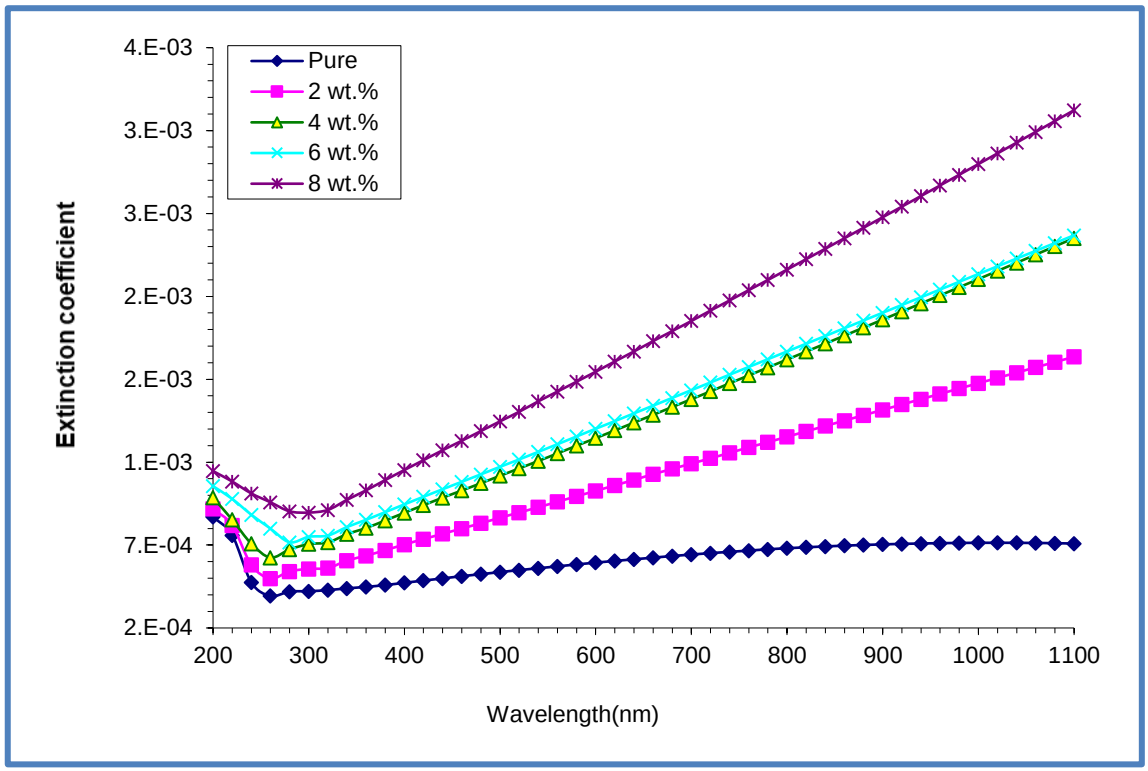

Figure (4.17): Variation of k for (PVA/PAA/Ag) nanocomposite with the wavelength after exposed Ar plasma.

4.3.6. The refractive index

The refractive index (n) is calculated by using equation (2-17). The n of (PVA/PAA/Ag) nanocomposites versus with wavelength are shown in figures (4.18) and (4.19) before and after exposed Ar plasma respectively. It is obtained that the refractive index rises with the rising of the content of Ag NPs. This action due to the rise of the density of nanocomposites. The refractive index after irradiation has high values compared before irradiation which attributed to the increased free charge carriers and polarized. This result agrees with researchers [119,120,124].

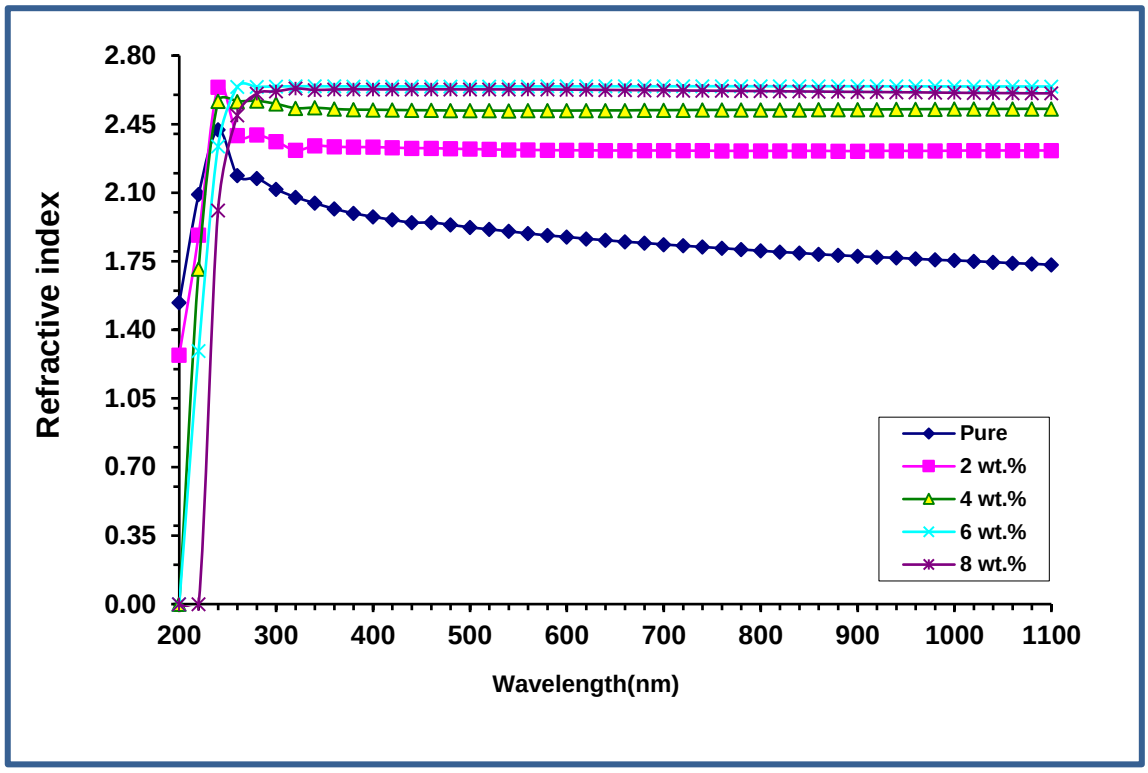

Figure (4.18): Variation of Refractive index for (PVA/PAA/Ag) Nanocomposite with Wavelength

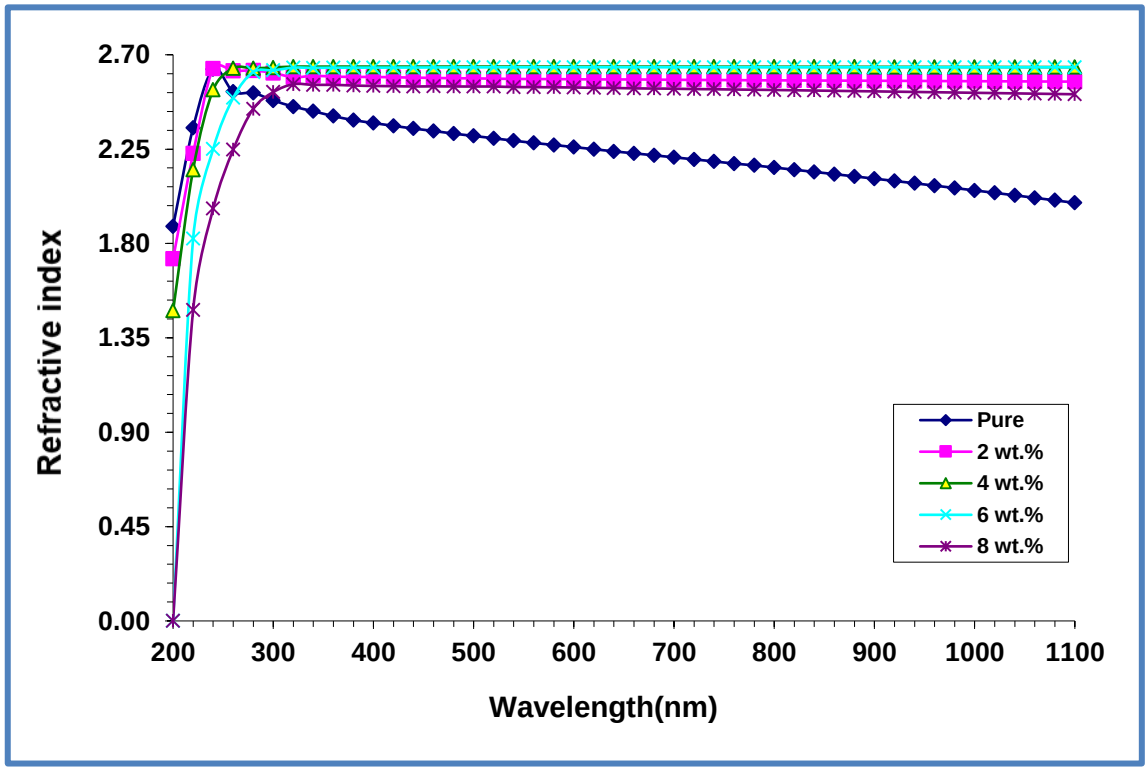

Figure (4.19): Variation of Refractive index for (PVA/PAA/Ag) Nanocomposite with wavelength after exposed Ar plasma

4.3.7 The Real and Imaginary Dielectric Constant

The equations (2-23) and (2-24) were used to calculated the real (ε_1) and imaginary (ε_2) parts of dielectric constant. The variation of ε_1 and ε_2 of (PVA/PAA/Ag) nanocomposites with wavelength are explain in figures (4.20), (4.21), (4.22), and (4.23) before and after exposed Ar plasma. From this figure, the ε_1, ε_2 of the nanocomposite are rise with the rises of Ag NPs content. The rise in electrical polarization related to the influence of nanoparticles content in the sample caused this finding [125]. The ε_1, ε_2 of nanocomposite change with wavelength. This is due to the ε_1 depends on refractive index since the outcome of extinction coefficient is minor, whereas the ε_2 depends on extinction coefficient. The real and imaginary parts of dielectric constant after irradiation have high values compared before irradiation which attributed to the increased free charge carriers and polarized. These results agree with researchers [119,120].

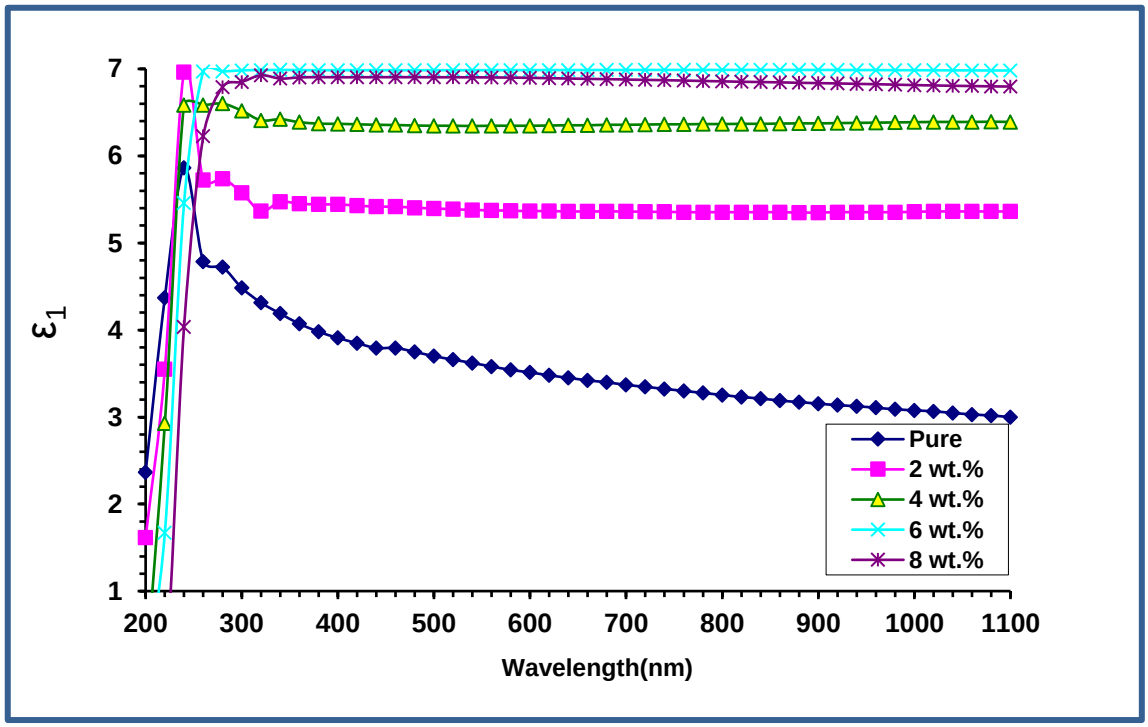

Figure (4.20): Variation of ε_1 of (PVA/PAA/Ag) Nanocomposites with the wavelength.

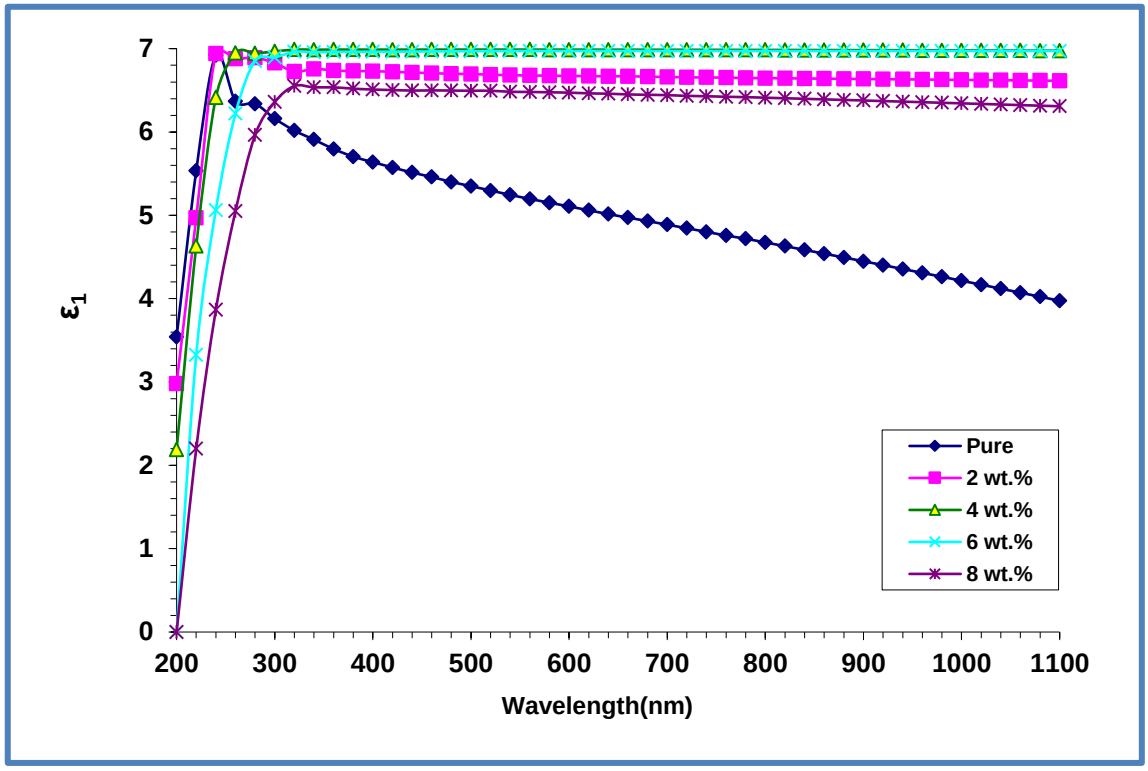

Figure (4.21): Variation of ε_1 of (PVA/PAA/Ag) nanocomposites with the wavelength after exposed Ar plasma.

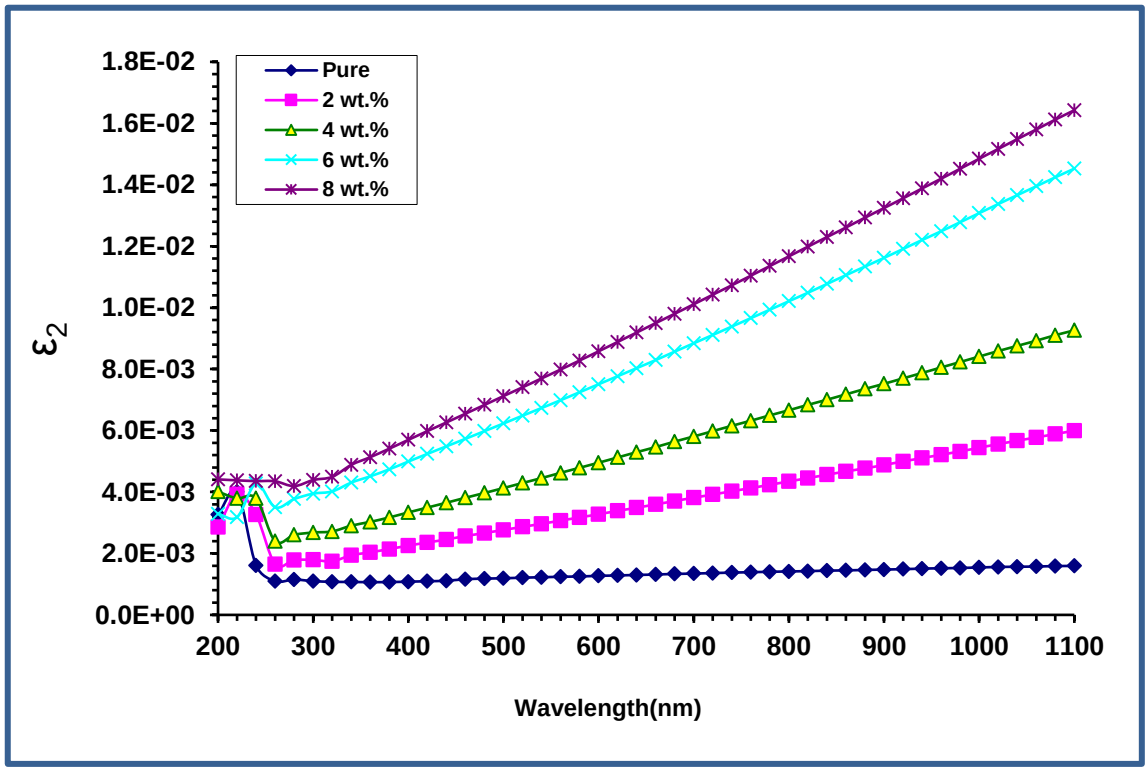

Figure (4.22): Variation ε_2 of (PVA/PAA/Ag) nanocomposites with the wavelength

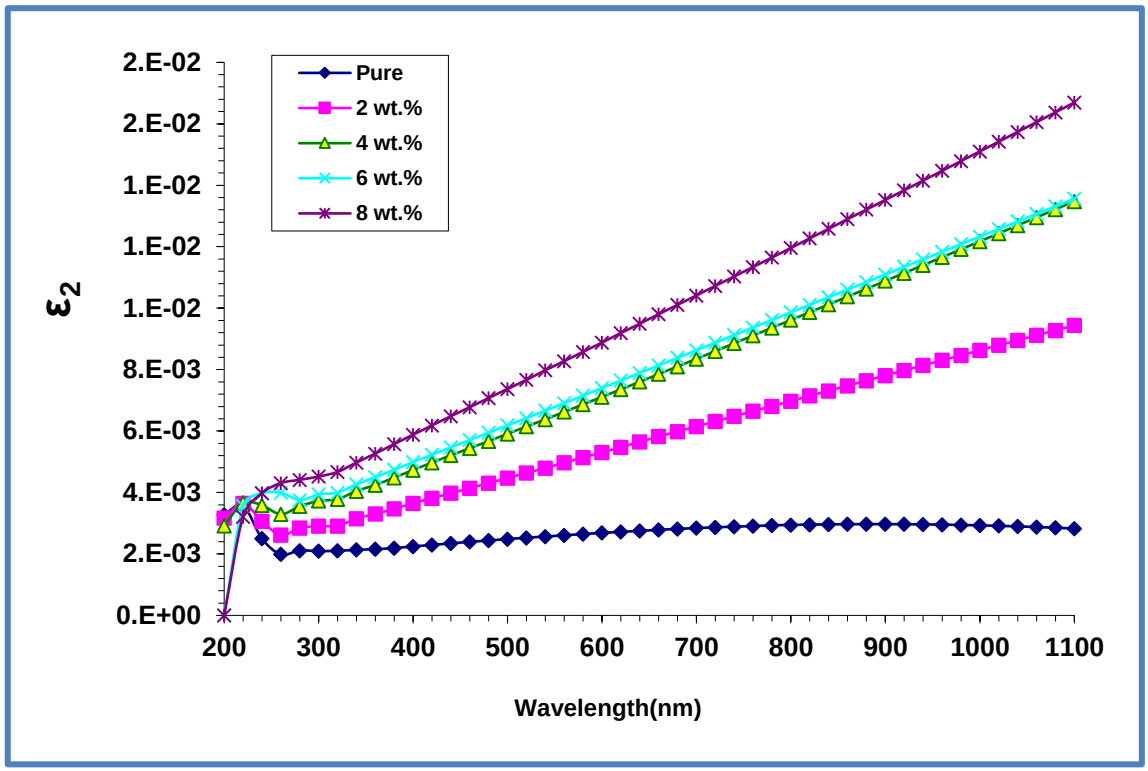

Figure (4.23): Variation ε_2 of (PVA/PAA/Ag) Nanocomposites with the wavelength after exposed Ar plasma

4.3.8. The Optical Conductivity

The optical conductivity was calculated from the equation (2-25). The σ_{op} of (PVA/PAA/Ag) nanocomposites with a wavelength are explain in figures (4.24) and (4.25). From this figure, the σ_{op} rise with rises of content of Ag NPs which is connected to the formation of localized levels in the energy gap, rising nanoparticle content induced a rise in the density of local phases in the band structure therefore, a rise in the absorption coefficient suggests an increase in σ_{op} of the nanocomposites and interaction phonon in network band. The optical conductivity after irradiation has high values compared before irradiation which attributed to the increased free charge carriers and polarized. This result agrees with [119,120,126].

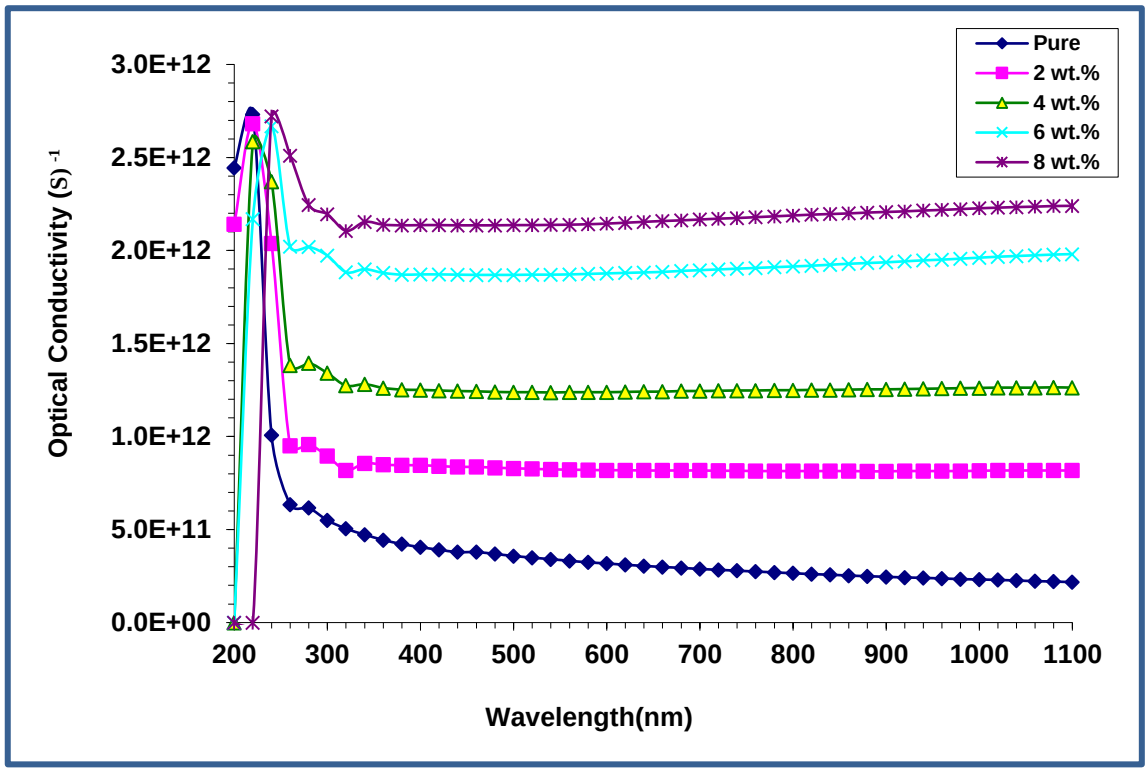

Figure (4.24): Variation σ_{op} of (PVA/PAA/Ag) Nanocomposites with the wavelength.

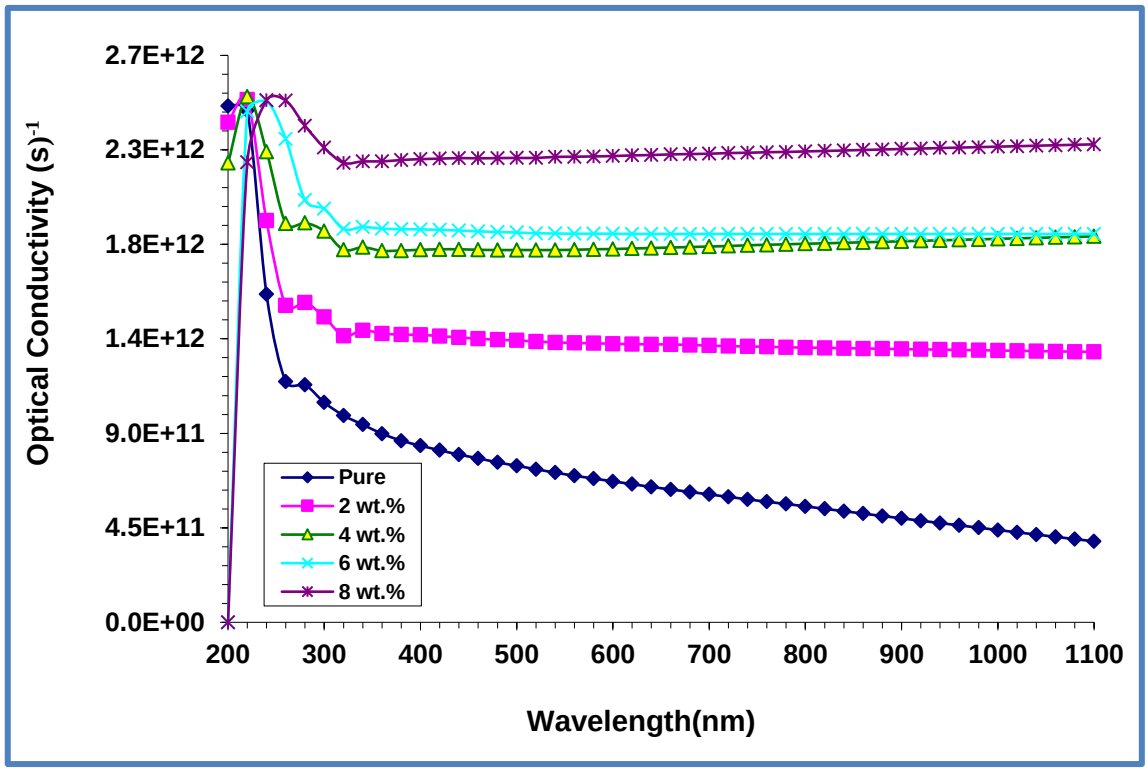

Figure (4.25): Variation σ_{op} of (PVA/PAA/Ag) Nanocomposites with the wavelength after exposed Ar plasma.

4.4 The A.C Electrical Properties of (PVA/PAA/Ag) nanocomposites

The (PVA/PAA/Ag) nanocomposites were investigated for their alternating current (A.C) electrical properties between 100 Hz and 5 MHz at room temperature. In order to identify the dielectric constant, that is the most essential of A.C characteristic, used the equation (2-48). The dielectric loss can be calculated by the dielectric constant and (tanδ), using the equation (2-49), while A.C electrical conductivity (σ_{AC}) can be calculated by equation (2-50) by substituting the values of (ε'').

4.4.1 The Dielectric constant for (PVA/PAA/Ag) Nanocomposites

The difference of dielectric constant of (PVA/PAA/Ag) nanocomposite with frequency is shown in figures (4.26) and (4.27) after and before irradiation plasma respectively. From this graph, it is clear that the dropped as the frequency increased. This is attributed to dipoles' slow rotation, which causes a lag between the frequency of the oscillating dipole and the applied field. The interfacial polarization, which is always current in materials with additional than one phase, is what causes the large values of 'at low frequencies [127], while in figures (4.28) and (4.29), the rise in the content of Ag NPs led to an enhancement in the consequences of the insulator constant before and after irradiation plasma respectively that cluster formation is responsible for. Because to the increased space charge polarization that resulted from this, the dielectric constant was increased the most [128].

Also, it is observed that the insulator constant after irradiation have high value compared with dielectric constant before irradiation which attributed to increased free charge carriers and polarized.

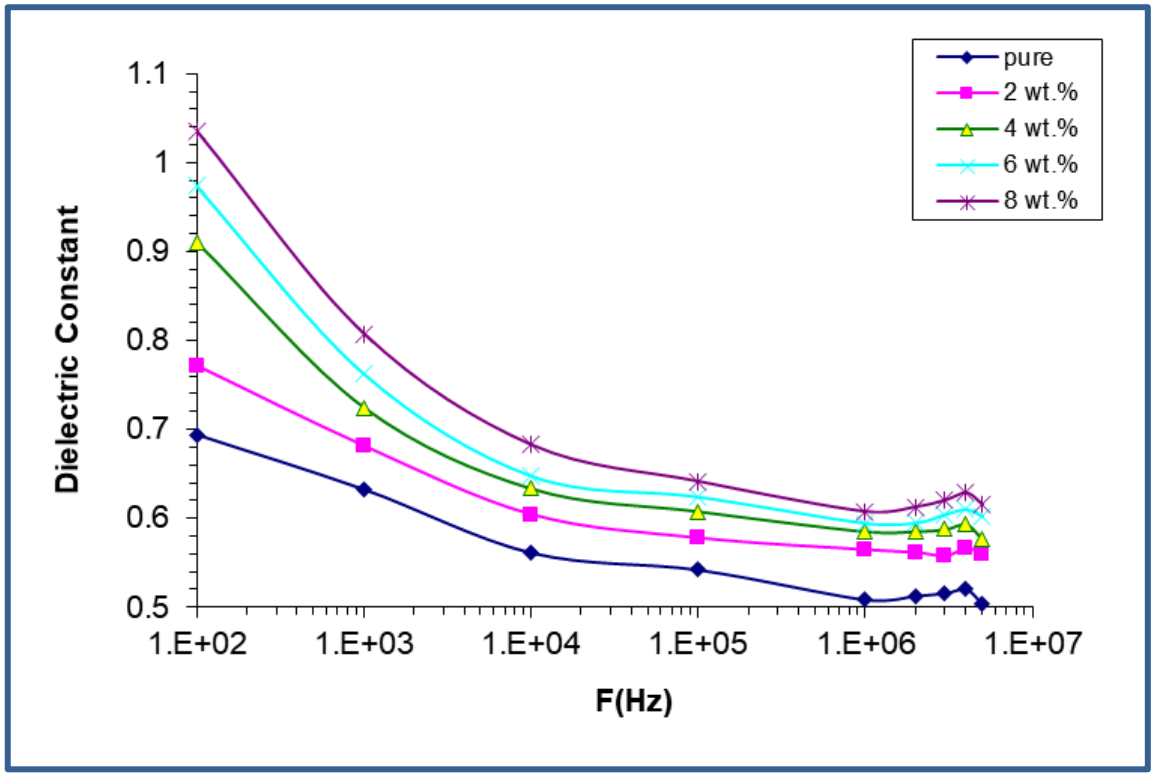

Figure (4.26): Variation of dielectric constant with frequencu of (PVA/PAA/Ag) nanocomposite.

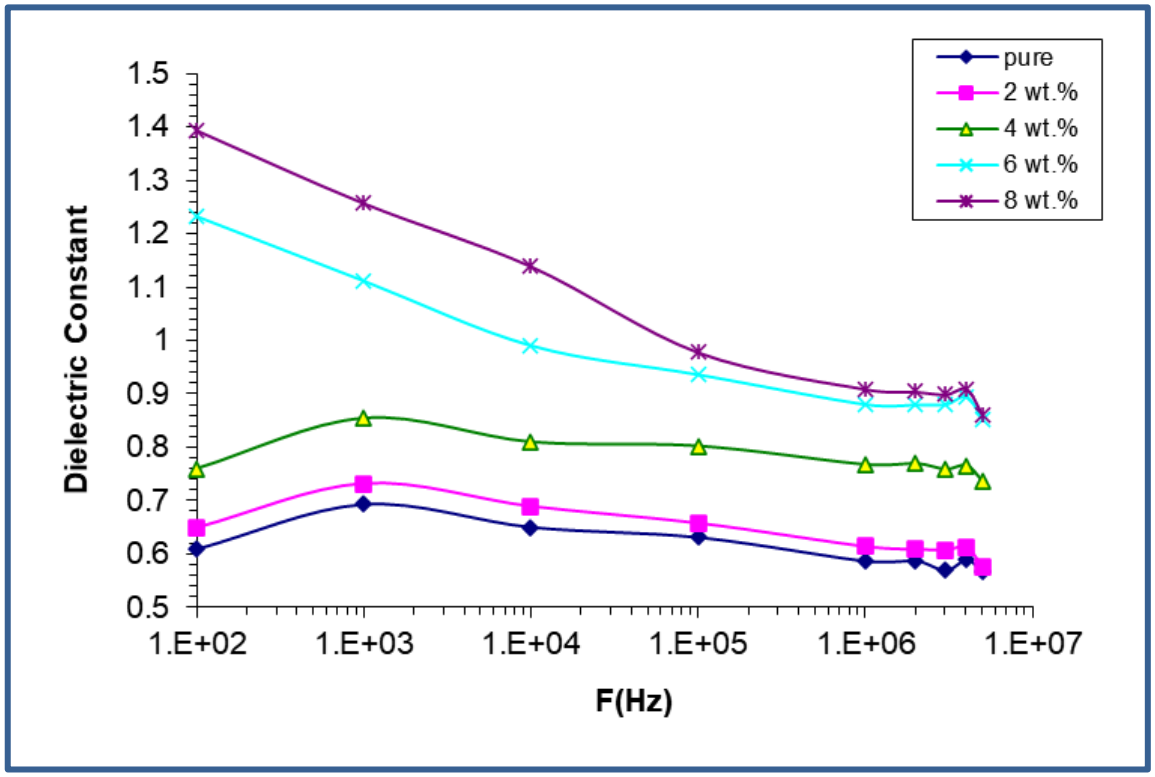

Figure (4.27): Variation of dielectric constant with frequencu of (PVA/PAA/Ag) nanocomposite after exposed Ar plasma.

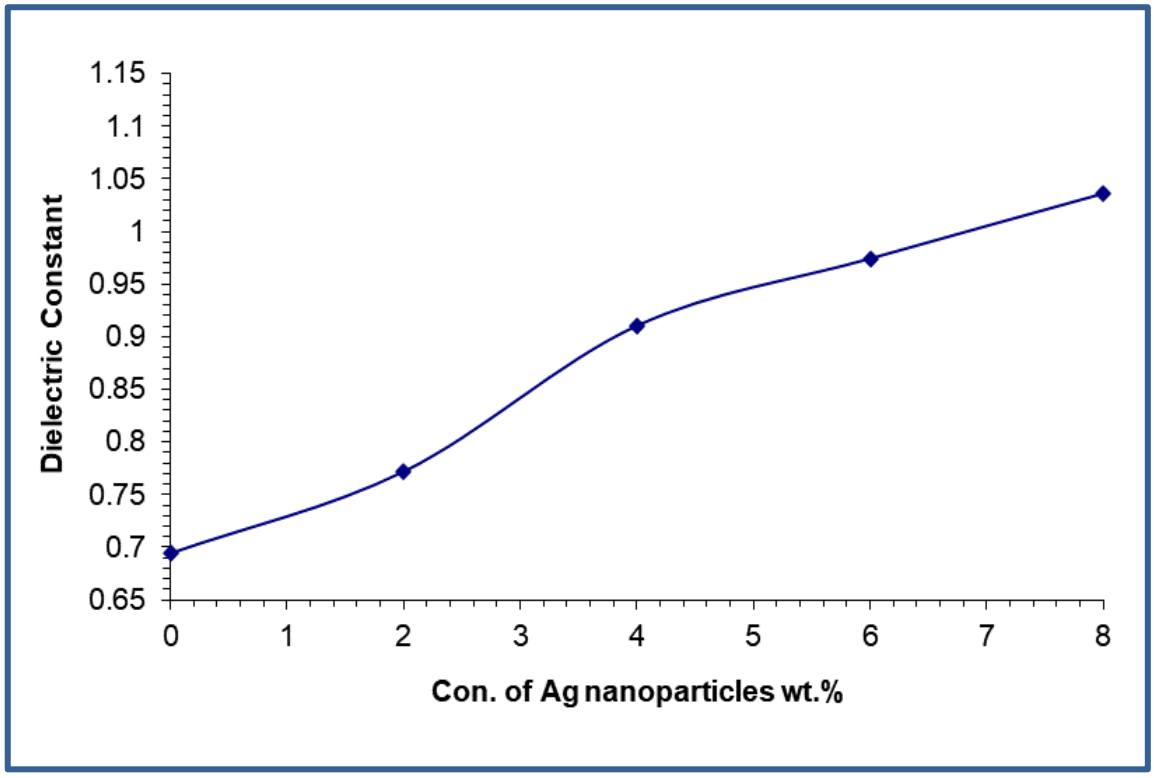

Figure (4.28): Effect of Ag NPs concentration on the Dielectric constant of (PVA/PAA/Ag) Nanocomposite

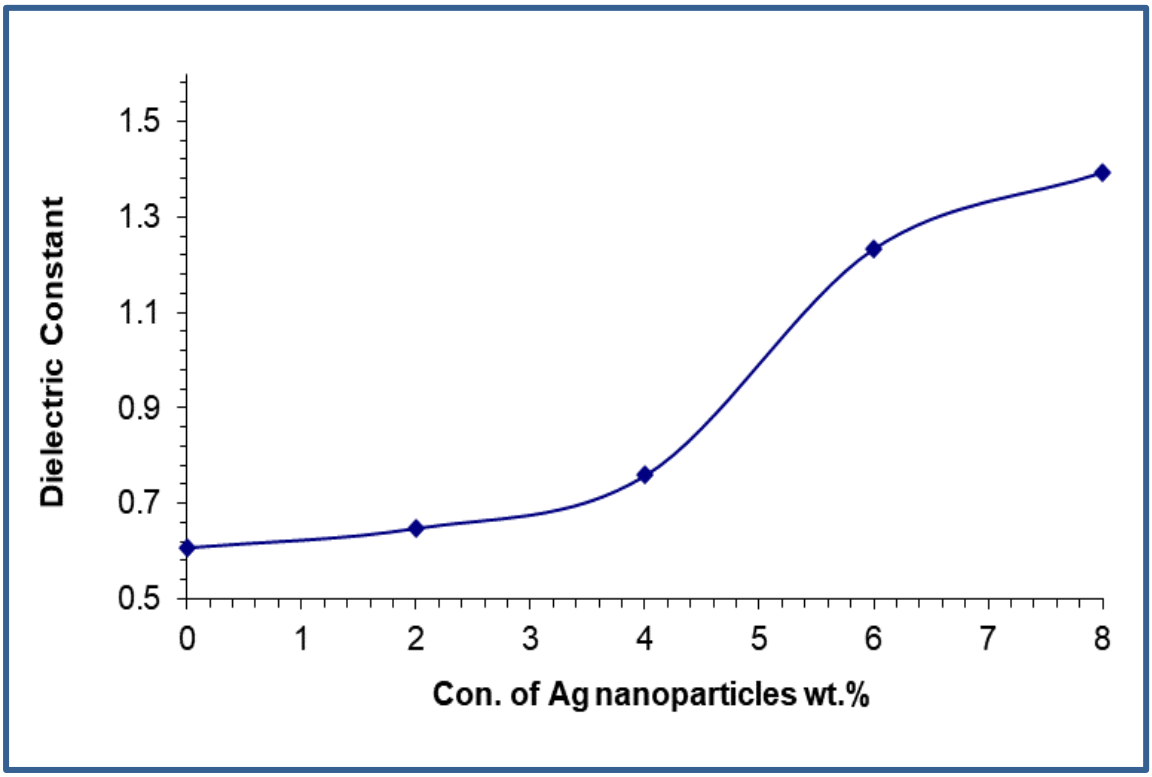

Figure (4.29): Effect of Ag NPs concentration on the Dielectric constant of (PVA/PAA/Ag) Nanocomposite after exposed Ar plasma.

4.4.2 The Dielectric Loss of(PVA/PAA/Ag) Nanocomposites

The dielectric loss (ε″) was calculated from eq. (2.49). The dielectric loss (ε″) of (PVA/PAA/Ag) nanocomposite with the frequency is illustrated in figures. (4.30) and (4.31) after and before irradiation plasma respectively. The graph reveals the reducing of insulator loss values of nanocomposite with an increase in the frequency, this action was attributed to the decrease in the influence of electronic polarization. Insulator loss displayed notable increases with the rise of the loading ratio of Ag NPs as shawm in Figures (4.32) and (4.33) after and before irradiation plasma respectively. The rise in the dielectric loss with the content of the concentration of the Ag NPs can be attributed to the increasing in the electronic charge, which can be raised owing to a rise in the content of the Ag NPs. This behavior is similar with the previous investigation [129]. Also from this figure's, it is noted that the dielectric loss after irradiation have high value compared with dielectric loss before irradiation which attributed to the increased free charge carriers and polarized.

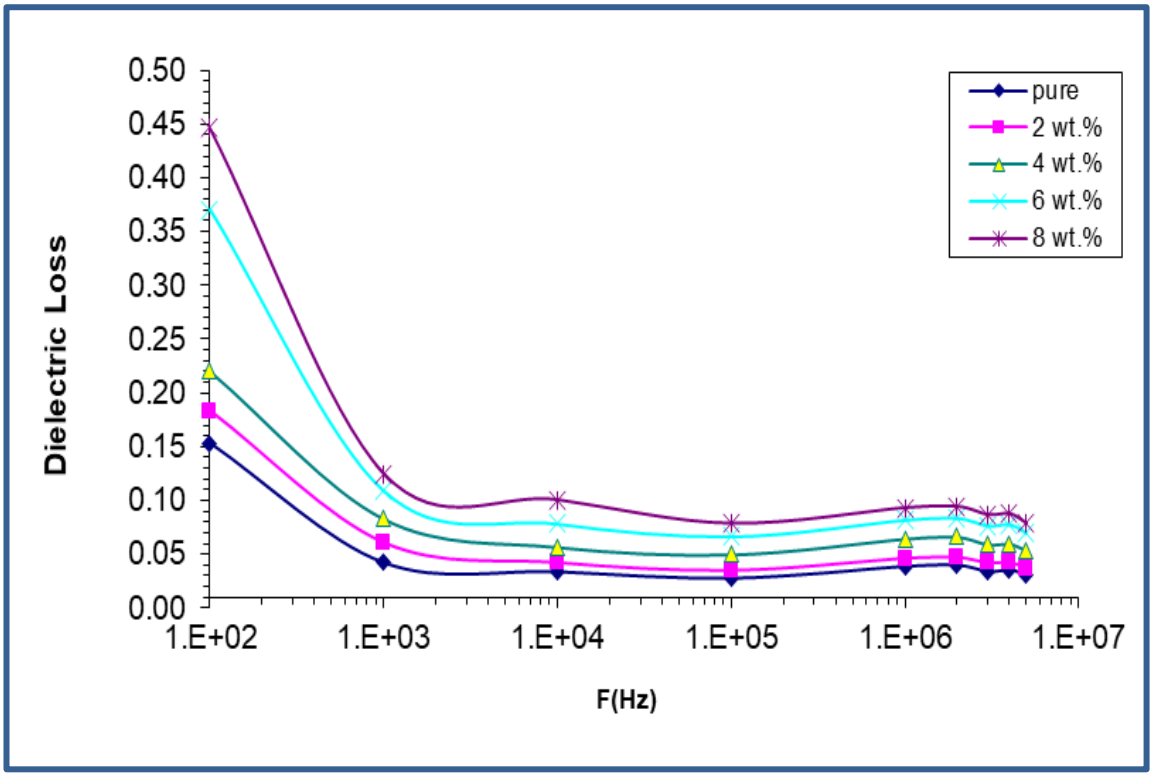

Figure (4.30): Variation of Dielectric loss with Frequencu of (PVA/PAA/Ag) Nanocomposite.

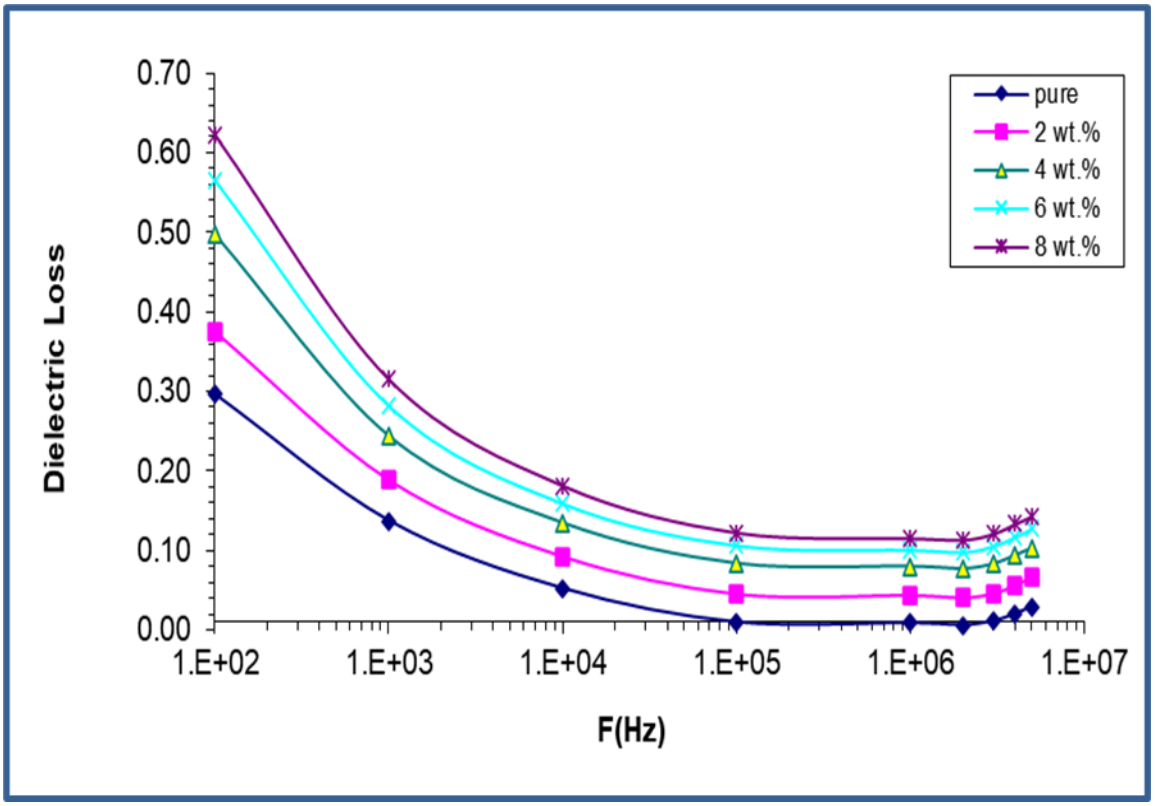

Figure (4.31): Variation of dielectric loss with Frequencu of (PVA/PAA/Ag) Nanocomposite after exposed Ar plasma.

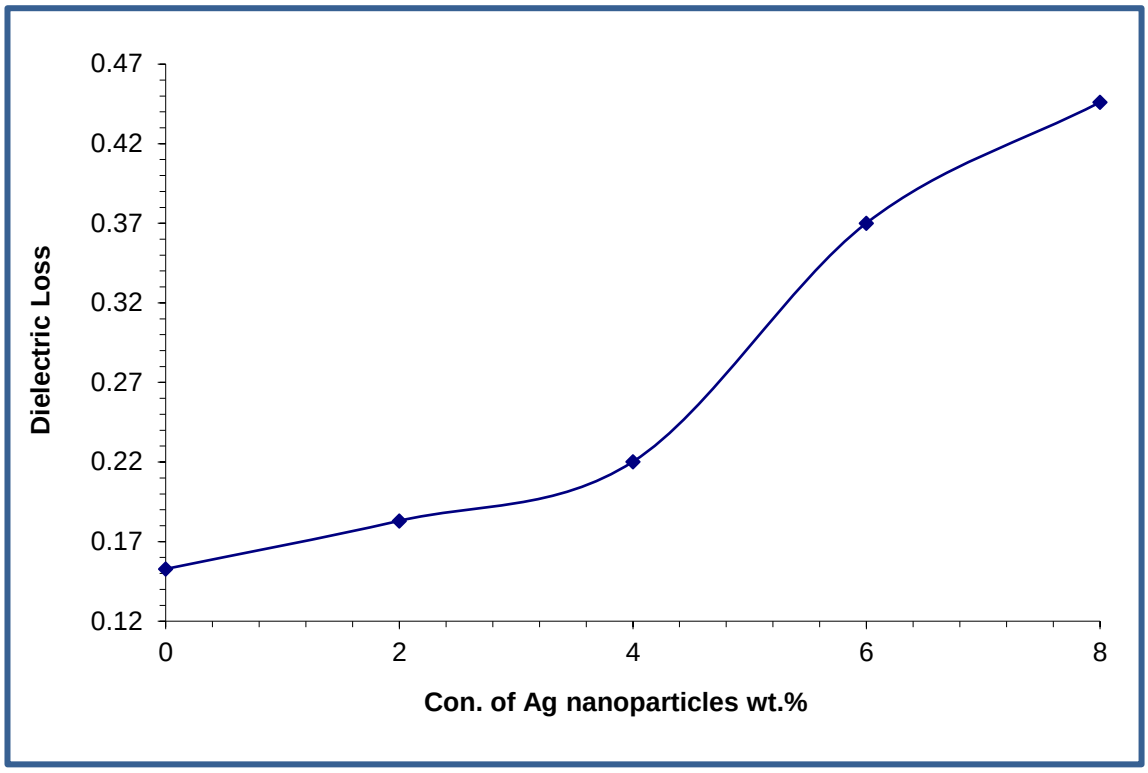

Figure (4.32): Effect of Ag NPs concentration on the dielectric loss of (PVA/PAA/Ag) nanocomposite.

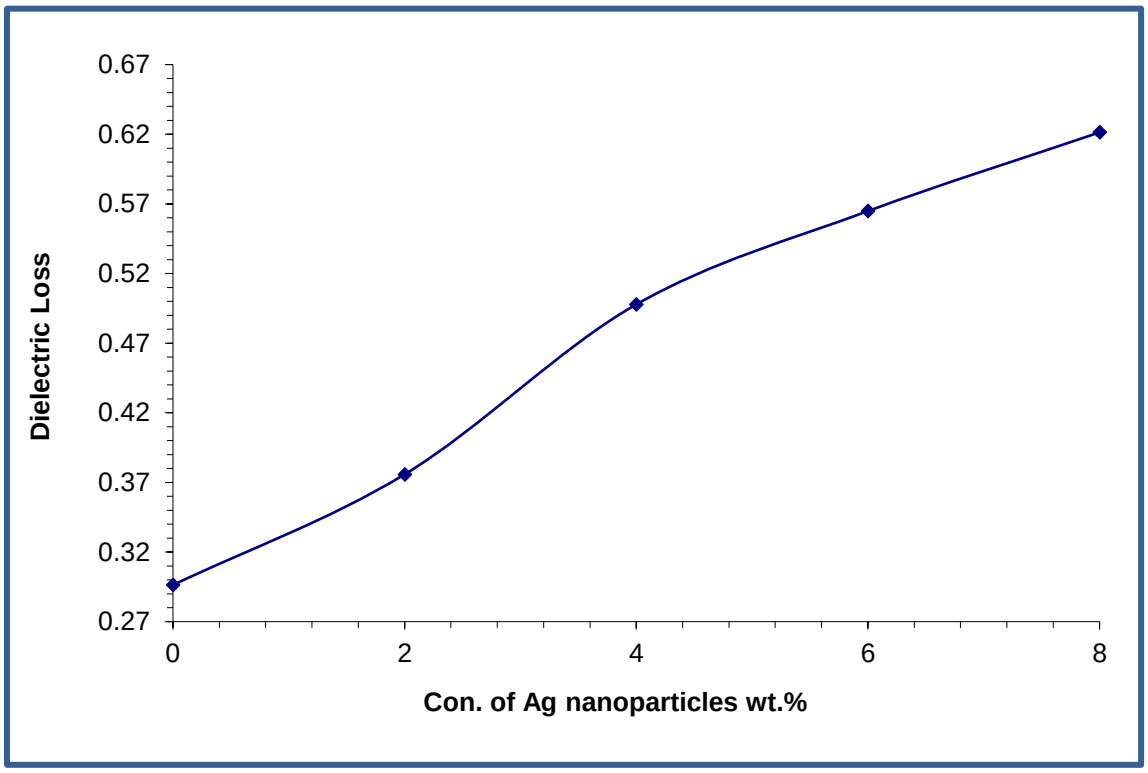

Figure (4.33): Effect of Ag NPs concentration on the dielectric loss of (PVA/PAA/Ag) Nanocomposite after exposed Ar plasma.

4.4.3 The A.C electrical conductivity of (PVA/PAA/Ag) nanocomposites

The A.C conductivity was calculated from eq. (3). Figures (4.34) and (4.35) shows the A.C conductivity for (PVA/PAA/Ag) nanocomposite with frequency after and before irradiation plasma respectively. The graph shows that A.C conductivity performance amplified significantly with the rise in the frequency (f). This is predictable when the charge carrier's number was growing and also due to the excitation of charge carriers to upper statuses in the conduction band. Consequently, the conductivity is increasing when the frequency increased, also the rising ratio of Ag existing significant improving of A.C conductivity in the result of all the nanocomposite in contrast with PVA.PAA are sown in Figures (4.36) and (4.37) after and before irradiation plasma respectively. in similar with the other finding [130]. Also, it is noted that the A.C conductivity after irradiation have high value compared with dielectric loss before irradiation which attributed to the increased free charge carriers and polarized.

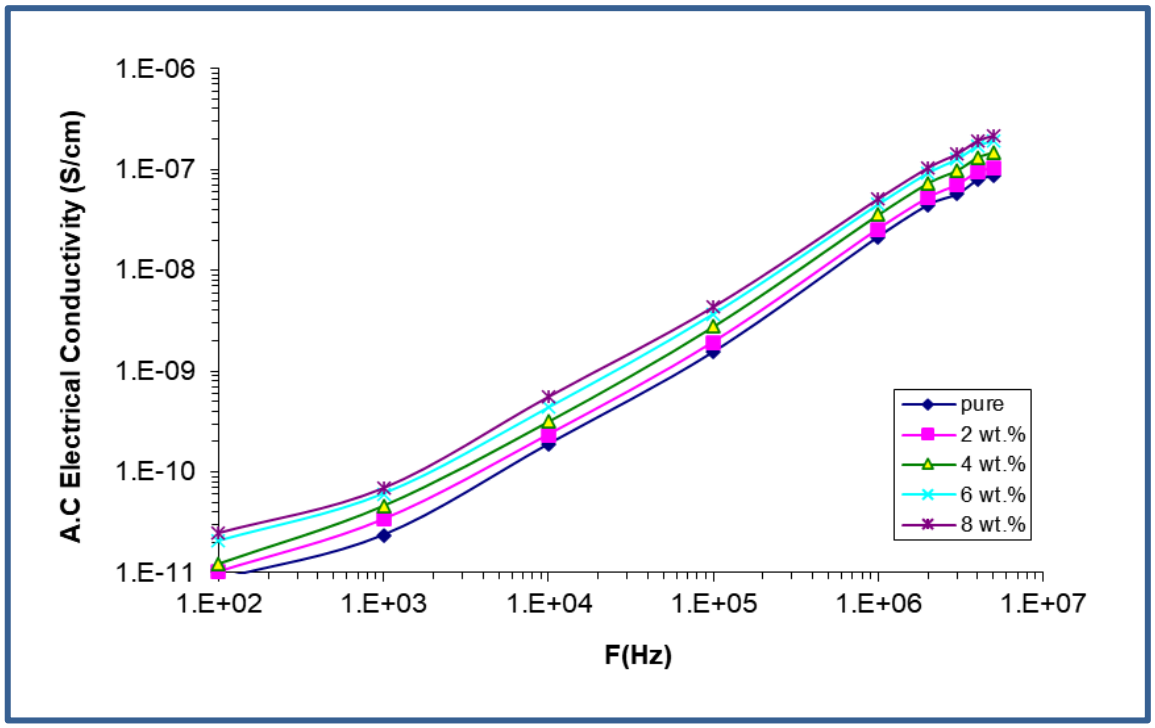

Figure (4.34) Variation of AC electrical conductivity with frequencu of (PVA/PAA/Ag) Nanocomposite.

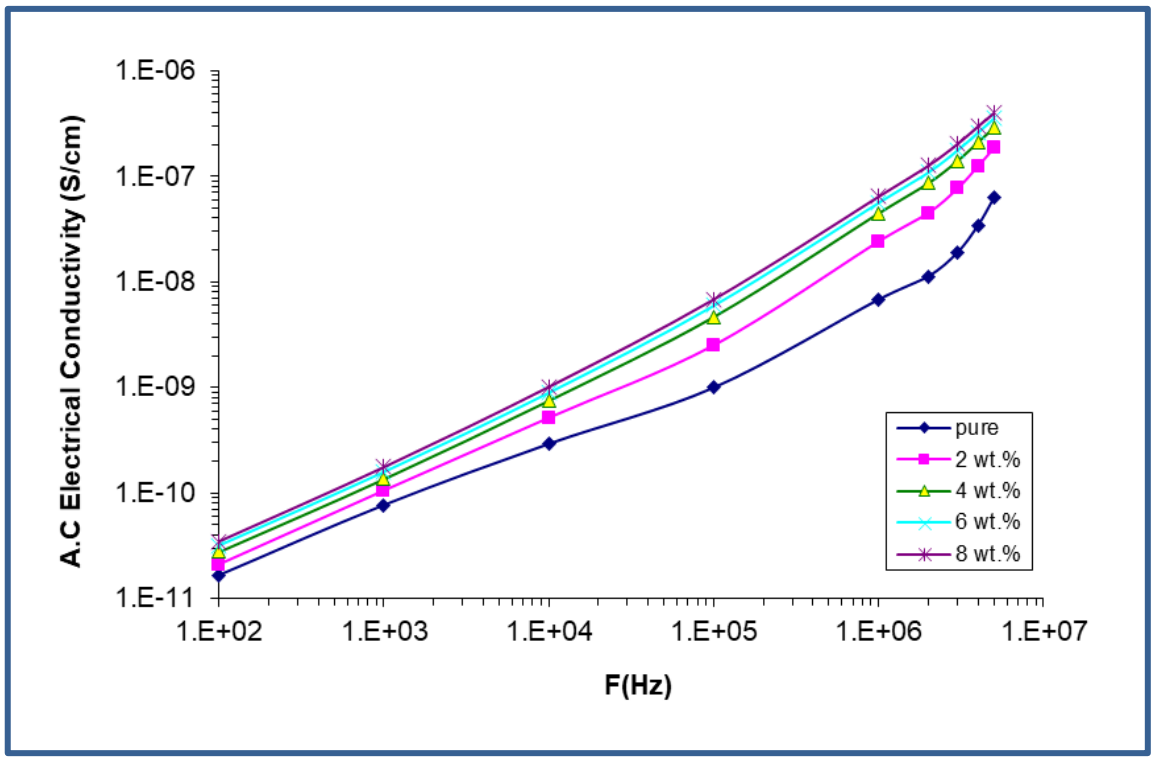

Figure (4.35) Variation of AC electrical conductivity with frequencu of (PVA/PAA/Ag) nanocomposite after exposed Ar plasma.

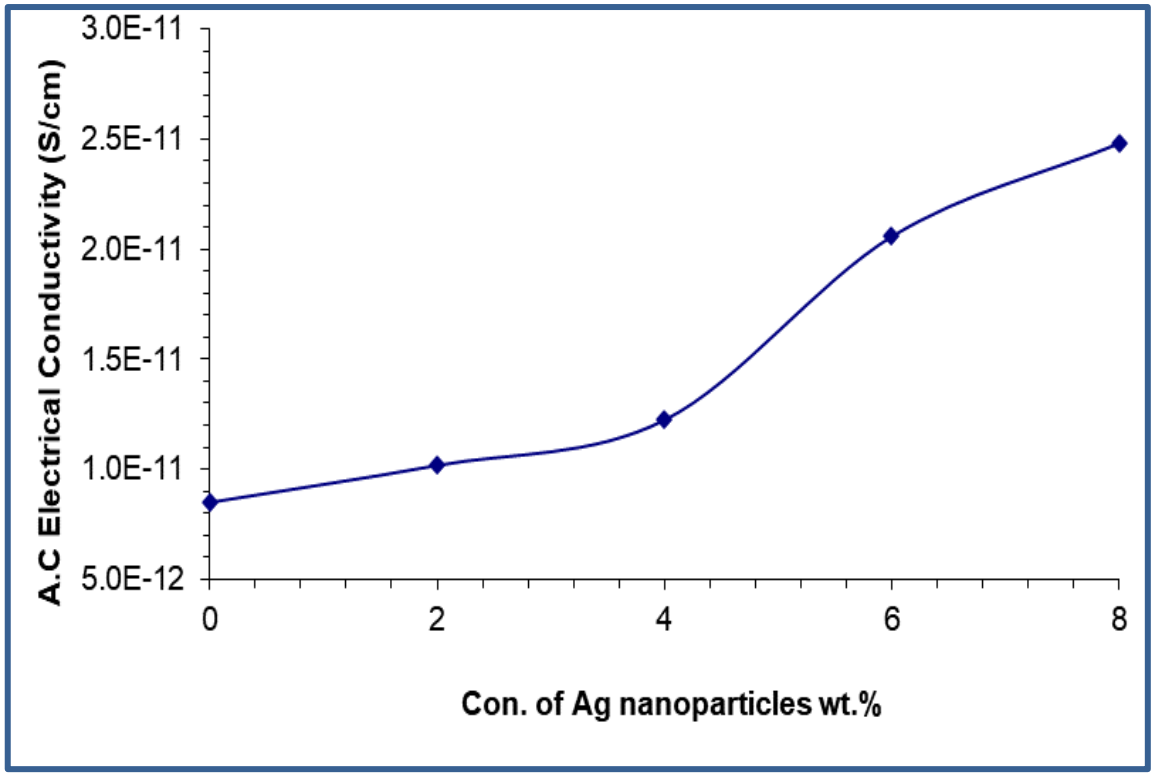

Figure (4.36): Effect of Ag NPs concentration on the AC electrical conductivity of (PVA/PAA/Ag) Nanocomposite.

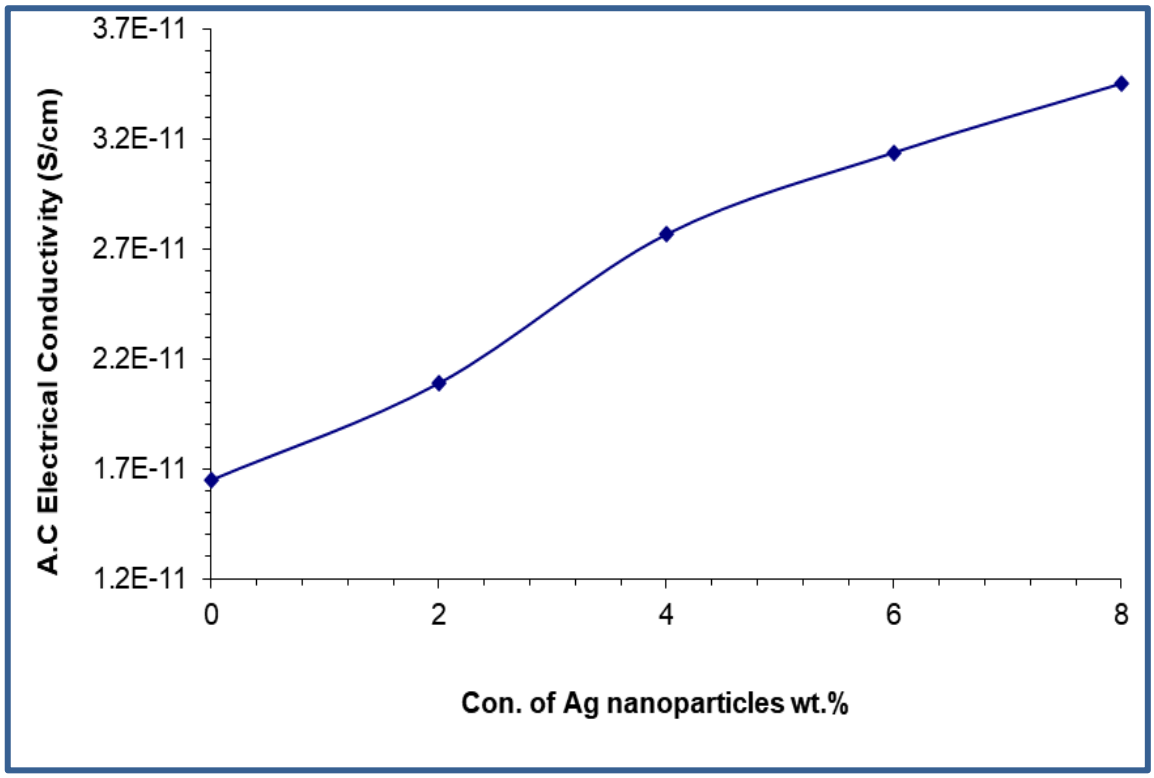

Figure (4.37) Effect of Ag NPs concentration on the AC electrical conductivity of (PVA/PAA/Ag) Nanocomposite after exposed Ar plasma

4.5 Application of (PVA/PAA/Ag) Nanocomposites for Antibacterial Activity.

The antibacterial properties of the (PVA/PAA/Ag) nanocomposites were confirmed in contrast to gram-positive (Staphylococcus aureus) and gram-negative (Escherichia coli) and the obtained data are presented in figures (4.39) and (4.40). As shown in the figures, the inhibition zone rises with increasing the content of Ag NPs. Reactive oxygen species (ROS), which are produced by nanoparticles, are what give nanostructures their bactericidal properties. The electromagnetic interaction between the nanoparticles of nanocomposites and the bacteria will cause the germs to oxidize and die instantly since the nanocomposites contain positive charges while the microbes have negative charges. Singlet oxygen ($_1O^2$) may be the culprit for

destroying the proteins and DNA of bacteria, and ROS, which contains radicals alike super oxide radicals (O^{-2}), hydroxyl radicals (OH), and hydrogen peroxide (H_2O_2), is the primary mechanism causing the antibacterial activity of nanocomposites by the nanoparticles [131].

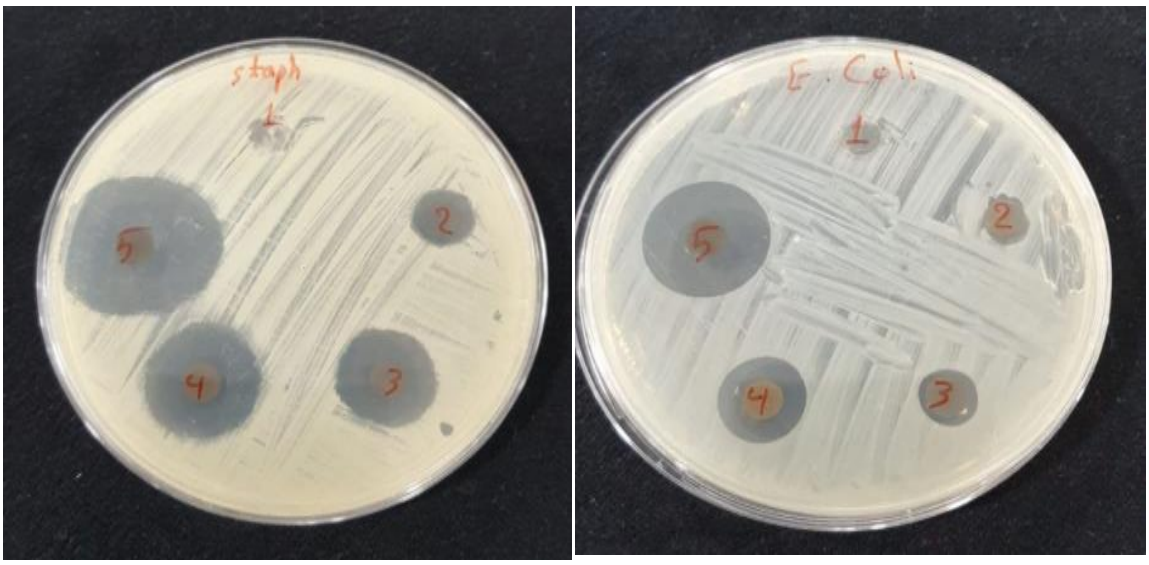

Figure (4.38). Image for inhibition zones of (PVA/PAA/Ag) nanocomposite films on S.aureus and E. coli.

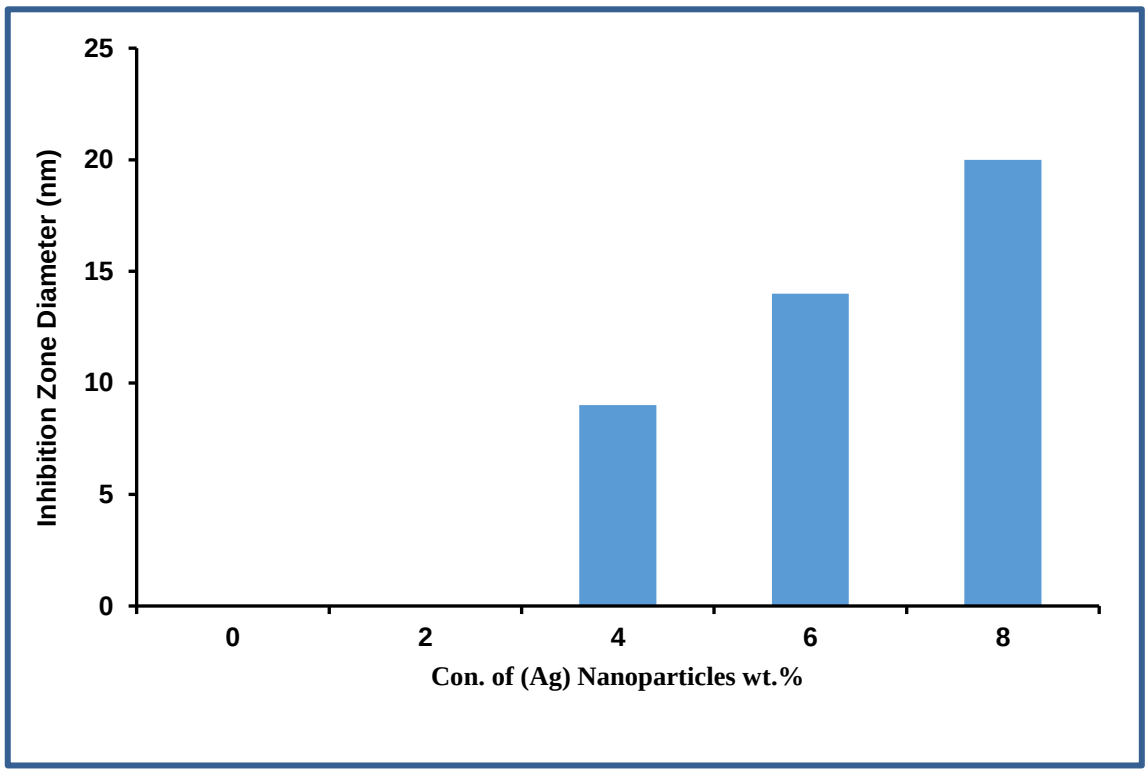

Figure (4.39). Antibacterial effect of (PVA/PAA/Ag) as a function of Ag NPs concentrations on E. coli.

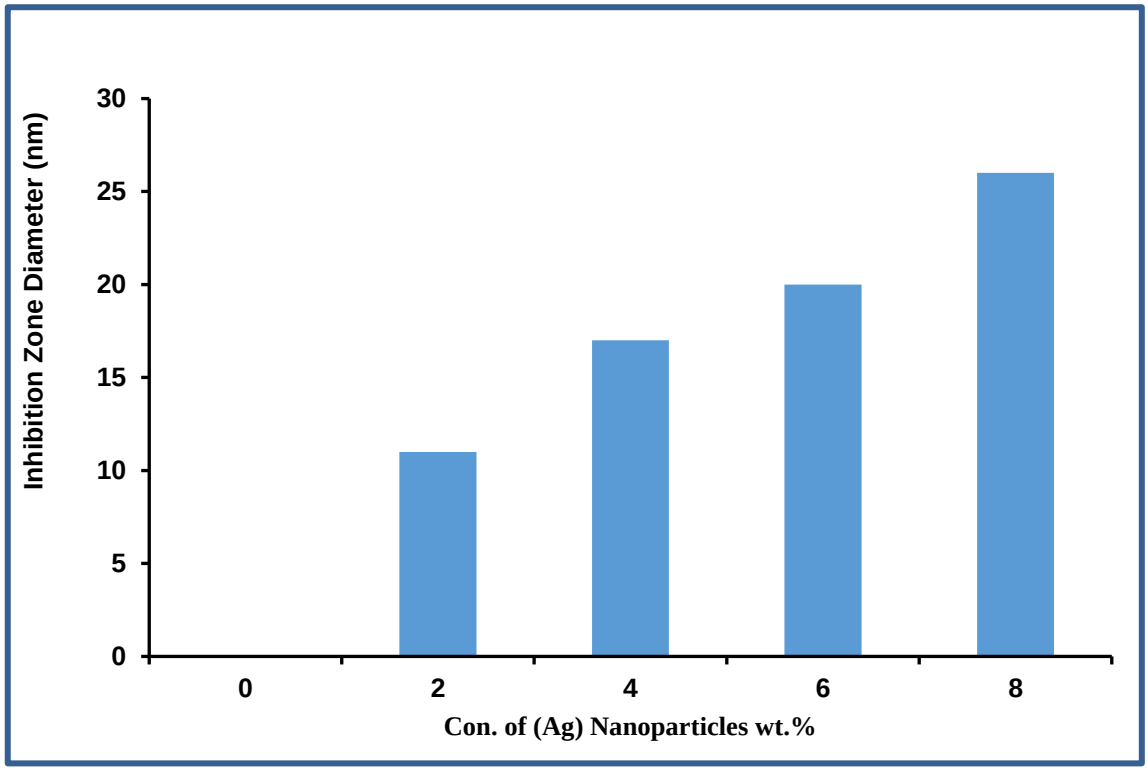

Figure (4.40). Antibacterial effect of (PVA/PAA/Ag) as a function of Ag NPs concentrations on S. aureus.

4.6 Conclusions

From the obtained results and discussions, the following points are concluded:

1- The optical microscope images showed that Ag nanoparticles form a continuous network inside the polymers when the ratio of (8) wt.% before and after exposed Ar plasma. FESEM measurements reveal the surface morphology of the (PVA/PAA/Ag) nanocomposites films, which are homogeneous and coherent with aggregates or chunks scattered at random on the top surface. The variation in the morphology before exposed Ar plasma attributed to the etching procedure promoted by argon plasma species on the (PVA/PAA) surface. FTIR spectra proved that there is no interaction between the polymers and the added nanoparticles.

2- The absorbance, absorption coefficient, refractive index, extinction coefficient, dielectric constant (real, imaginary) and optical conductivity of (PVA/PAA/Ag) nanocomposites before and after exposed Ar plasma increased with the increasing of the concentrations of the Ag nanoparticles. The transmittance and the energy gap for indirect transition (allowed, forbidden) decreased with the increasing of the concentrations of Ag nanoparticles. The optical properties after irradiation plasma have high values compared before irradiation which attributed to the increased free charge carriers and polarized. This give as good indicator these samples could be used as photodetector device.

3- The dielectric constant and dielectric loss for (PVA/PAA/Ag) nanocomposites are increased with the increasing of Ag nanoparticles concentration and decreasing with the increase of frequency of the applied electric field while the A.C electrical conductivity increased with the increasing of nanoparticles concentration and frequency of the applied electric field before and after exposed Ar plasma. The dielectric constant, dielectric loss and A.C electrical conductivity after irradiation have high values compared before irradiation which attributed to the increased free charge carriers and polarized. The advantage of enhancement in electrical properties of (PVA-PAA-Ag) nanocomposite that might be used in electronics device.

4- The inhibition zone diameter increases with the increase in (Ag) nanoparticles concentrations. It is increased to 20 mm for E. coli. at concentration 8% wt. Ag and 26 mm for S. aureus. at concentration 8% wt. Ag.

4.7 Future works

1- Studying the thermal and mechanical properties of (PVA/PAA/Ag) nanocomposites.

2- Studying the effect of gamma radiation on some physical properties of (PVA/PAA/Ag) nanocomposites.

3- Application of (PVA/PAA/Ag) nanocomposites as piezoelectric and gas sensor.

References

Reference

[1] I. Gruin," Polymer materials", PWN, Warsaw, (in Polish), (2003).

[2] B. Bhushan, "Handbook of Nanotechnology", Springer, 3rd edition (2010).

[3] R. P. Feynman, "There is Plenty of Room at the Bottom", Engineering and Science 36, 23, (1960).

[4] G. Marcel, "An introduction to plasma astrophysics and magneto hydro dynamics" Vol. 294. Springer Science & Business Media, 2003.

[5] F.F. Chen, "Plasma Physics and Controlled Fusion" 2nd ed. (Springer, New York, 2006).

[6] R. O. Dendy, "Plasma Physics: An Introductory Course", Cambridge University Press, ISBN (0521484529), (1995).

[7] Y. Eliezer and S. Eliezer, "The Fourth State of Matter: An Introduction to the Physics of Plasma" Bristol: Institute of Physics Publishing, (1989).

[8] T. K. Fowler, "The Fusion Quest, Baltimore, MD: Johns Hopkins" University Press (1997).

[9] Y. Bao, J. Wang, P. Xue, Q. Li, W. Guo, C. Wu, "Lowering the percolation threshold of polymer matrix composite by using raspberry-like carbon black/polystyrene composite particles" Journal of Materials Science, Vol.47, pp. 1289-1295, (2012)

[10] R. Strumpler and J. Glatz-Reichenbach,"Conducting Polymer Composites". Journal of Electroceramics, Vol. 3, No.4, pp.329-346 ,(1999).

[11] R. Ou, S. Gupta, C. A. Parker and R. A. Gerhardt, "Fabrication and Electrical Conductivity of PMMA/CB Composites: Comparison Between an Ordered Carbon Black-Nan wire Segregated Structure and a Randomly Dispersed Carbon Black Structure" Journal of Physical Chemistry B, Vol. 110, No.45, pp. 22362-22370, (2006).

[12] O. Robert, "Polymer Scince and Technology ", Department of Chemical, Engineering University of Benin, Benin city, Nigeria, ISBN 0-8493-8939-9, TP156.P6E24 ,(1996).

[13] J. M. Smith, "Introduction to chemical engineering thermodynamics"., McGraw Hill, 8th edition, (2017)

[14] C. Harper," Handbook of Plastics Elastomers and Composites", Third Edition, McGrawHill Professional Book Group, New York, ch11, (1996).

[15] R. D. Deanin,"The chemistry of plastics" Journal of Chemical Education, Vol. 64, No.1, P.45, (1987).

[16] A. Güneri, "Hand book of composites fabrication", Smithers Rapra Publishing, P. 196, (2001).

[17] E. D. Goddard, and J. V. Gruber, "Principles of polymer science and technology in cosmetics and personal care ", Marcel Dekker, Inc.270 Madison Avenue, New York, Vol. 22, (1999).

[18] A. Balazs, T. Emrick and T. Russel," Nanoparticle polymer composites: where two small worlds meet" Science. Vol. 314, pp. 107-111, (2006).

[19] E. Tang, G. Cheng and M. XL, "Preparation of nano-ZnO/PMMA composite particles via grafting of the co polymer onto the surface of Zinc oxide nano particles powder technol", Vol. 161, pp. 209-214, (2006).

[20] Y. L. Boker, A. He, J. B. Sill, K. Xiang, H.Q. Abetz, C. Li, X. F. Wang, J. Emrick, T. Long, S. Wang, Q. Balas and A. Russell,"Self-directed Self-assembly of Nanoparticle/copolymer Mixtures", Nature, Vol. 434, pp. 55-59, (2005).

[21] M. Zhnag, G. Yu, H. Zeng and Y. Hou, "Two step percolation in polymer blends filled with carbon black", Macromolecules, Vol. 31, pp. 6724-6726, 1998.

[22] P. M. Ajayan, P. Redlich and M. Rühle; "Structure of carbon nanotube based nanocomposites", J. Microsc.-Oxford, Vol. 185, No. 2, pp. 275–282, 1997.

[23] H. J. Gao, B. H. Ji, I. L. Jäger, E. Arzt and P. Fratzl, "Materials become insensitive to flaws at nanoscale: Lessons from Nature", Proc. Nat. Acad., Sci., USA, Vol. 100, No.10, pp. 5997–5600, 2003.

[24] C. Demerlis and D. Schoneker, "Review of the oral toxicity of polyvinyl alcohol (PVA) - PDF Free Download:, Food Chem. Toxicol, Vol. 41, No. 3, pp. 319–326, 2003.

[25] C. Ravindra, M. Sarswati, G. Sukanya, P. Shivalila, Y. Soumya, and K. Deepak, "Tensile and thermal properties of poly (vinyl) pyrrolidone/vanillin incorporated polyvinyl alcohol films", Res. J. Phys. Sci., Vol. 3, No. 8, pp. 1–6, 2015.

[26] k. Choo, Y. C. Ching, C. H. Chuah, S. Julai, and N. S. Liou, "Preparation and characterization of polyvinyl alcohol-chitosan composite films reinforced with cellulose nanofiber", Materials, Vol. 9, No. 8, p.644. 2016, doi:10.3390/ma9080644

[27] I. Sakurada, "Polyvinyl Alcohol Fibers", Taylor & Francis, of International Fiber Science and Technology, Vol. 6, p. 472, 1985.

[28] H. F. Mark, J. I. Kroschwitz, N. M. Bikales, C. G. Overberger and G. Menges, "Encyclopedia of polymer science and engineering", John Wiley & Sons, Chichester, p.841, 1985.

[29] A. Gautam and S. Ram, "Preparation and thermomechanical properties of Ag-PVA nanocomposite films", Mater. Chem. Phys., vol. 119, No. 2, pp. 266–271, 2010, doi:10.1016/j.matchemphys.2009.08.050.

[30] H. Arkaban, M. Barani, M. R. Akbarizadeh, P. S. Chauhan, N. Jadoun, S. D. Soltani and P. Zarrintaj, "Polyacrylic acid nanoplatforms: Antimicrobial,

tissue engineering, and cancer theragnostic applications", Polymers, Vol.14, No.6, p.1259, 2022, doi:10.3390/polym14061259.

[31] Y. Ma, J. Dong, S. Bhattacharjee, S. Wijeratne, M. L. Bruening, G. L. Baker, "Increased protein sorption in poly (acrylic acid)-containing films through incorporation of comb-like polymers and film adsorption at low pH and high ionic strength", Langmuir, Vol. 29, pp. 2946–2954, 2013, doi:10.1021/la305137m.

[32] C. Spagnol, F. H. Rodrigues, A. G. Pereira, A. R. Fajardo, A. F. Rubira, E. C. Muniz, "Superabsorbent hydrogel composite made of cellulose nanofibrils and chitosan-graft-poly (acrylic acid). Carbohydr", Polymers, Vol. (87), pp. 2038–2045, 2012, doi:10.1016/j.carbpol.2011.10.017.

[33] K. Takada, T. Iida, Y. Kawanishi, T. Yasui, A. Yuchi, "An electrochemical actuator based on reversible changes in volume of poly (acrylic acid) gel induced by quinone redox. Sens" Actuators B Chem., Vol.160, pp. 1586–1592, 2011, doi:10.1016/j.snb.2011.09.031.

[34] N. Hisamatsu, T. Iida, T. Yasui, K. Takada, A. Yuchi, "Double-side coated electrochemical actuator based on changes in volume of poly (acrylic acid) gel. Sens." Actuators B Chem., Vol. 203, pp. 289–295, 2014, doi:10.1016/j.snb.2014.06.123.

[35] M. Changez, V. Koul, B. Krishna, A. K. Dinda, V. Choudhary, "Studies on biodegradation and release of gentamicin sulphate from interpenetrating network hydrogels based on poly (acrylic acid) and gelatin: In vitro and in vivo" Biomaterials, Vol. 25, pp.139–146, 2004, doi:10.1016/S0142-9612(03)00466-6.

[36] R. M. Tilaki and S. M. Mahdavi, "Stability, size and optical properties of silver nanoparticles prepared by laser ablation in different carrier media," Appl. Phys. A, Vol. 84, No. 1, pp. 215–219, 2006.

[37] GUHA, Debangshu; RAMACHANDRAN, DUDUKOVIC, "Nanomaterials", A Sojourn. National Centre for Catalysis Research Department of chemistry, 2006.

[38] C. Mandolfino, E. Lertora, C. Gambaro, "Effect of cold plasma treatment on surface roughness and bonding strength of polymeric substrates,"Key engineering materials", Vol. 611, pp. 1484-1493, (2014).

[39] A. M. El Sayed and S. El-Gamal, S., "Synthesis and investigation of the electrical and dielectric properties of (CMC/PVA/Co3O4) nanocomposite films" Journal of Polymer Research, Vol. 22, No.5, pp. 1-12, 2015.

[40] Z. A. Al-Ramadhan, J. Abdulsattar, H. Abdul and K. Hmud," Optical and Morphological Properties of (PVA-PVP-Ag) Nanocomposites", International Journal of Science and Research (IJSR), Vol. 5,No.3 pp. 1828-1836, 2016.

[41] N. A. Awang, M. H. Ahmad, Y. Z. Arief, I. H. Zakaria and N.A. Ahmad, "The effect of plasma-treated boron nitride on partial discharge characteristics of LDPE", International Journal of Electrical and Computer Engineering, Vol. 7, No. 2, p.568, 2017, doi: 10.11591/ijece.v7i2.pp568-575.

[42] A. G. El-Shamy, W. M. Attia and K. M. Abd El Kader, K. M., "Enhancement of the conductivity and dielectric properties of PVA/Ag nanocomposite films using γ irradiation. Materials" Chemistry and Physics, Vol. 191, 2pp.25-229, 2017, doi:10.1016/j.matchemphys.2017.01.026.

[43] H. T. Salloom, A. S. Jasim, A. S. and T. K. Hamad, T. K., "synthesis and optical characterization of Ag/PVA nanocomposites films" Al-Nahrain Journal of Science, Vol. 20, No. 4, pp. 56-63, 2017, doi: 10.22401/JUNS.20.4.10.

[44] A. M. Ismail, M. I. Mohammed and E. G. El-Metwally," Influence of Gamma irradiation on the structural and optical characteristics of Li ion-doped PVA/PVP solid polymer electrolytes", Indian Journal of Physics, Vol.93, No.15, pp.175-183, 2018.

[45] Z. Fan, L. Di, X. Zhang, X. and H. Wang, "A surface dielectric barrier discharge plasma for preparing cotton-fabric-supported silver nanoparticles" Nanomaterials, Vol. 9, No. 7, p 961, 2019, doi:10.3390/nano9070961.

[46] H. S. Rasheed," The effect of Adding (ZrC) Nanoparticles to (PVP-PVA) Blend on their Optical properties for Humidity Sensor Application," Journal of Physics: Conference Series, Vol.1660, 2020, doi:10.1088/1742-6596/1660/1/012058.

[47] W. Wang, Z. Yu, F. K. Alsammarraie, F. Kong, M. Lin and A. Mustapha, A., "Properties and antimicrobial activity of polyvinyl alcohol-modified bacterial nanocellulose packaging films incorporated with silver nanoparticles" Food Hydrocolloids, Vol.100, p.105411, 2020, doi:10.1016/j.foodhyd.2019.105411.

[48] M. R. Atta, Q. A. Alsulami, G. M. Asnag, and A. Rajeh, A., "Enhanced optical, morphological, dielectric, and conductivity properties of gold nanoparticles doped with PVA/CMC blend as an application in organoelectronic devices" Journal of Materials Science: Materials in Electronics, Vol. 32, No. 8, pp. 10443-10457, 2021.

[49] S. J. Zainab and A. H. Majeed, "Structural and Dielectrically Properties of (CMC -PAA-ZrC) Nano Composites for Gamma Shielding Application", Journal of Mechanical Engineering Research and Developments, Vol. 44, No. 8, pp. 371-377, 2021.

[50] T. A. Hameed, F. Mohamed, G. Turky and A. Salama, A. ,"Carboxymethylcellulose/polyvinylpyrrolidone filled with Al-doped ZnO nanoparticles as a promising film for optoelectronic applications" Optical Materials, Vol.134, 1p.13097, 2022.

[51] H. M. Hussein and M. H. Al-Timimi, "Preparation and Study Some Physical Properties of (CMC/PAA: MgO) Nano Composites. Eurasian" Journal of Physics, Chemistry and Mathematics, Vol. 8, pp. 47-55, 2022.

[52] A. Di Gianfrancesco," Materials for Ultra-Supercritical and Advanced Ultra- Supercritical Power Plants", Elsevier Ltd., 978-0- 08-100552- 1, 2017.

[53] S. Ebnesajjad," Surface Treatment of Materials for Adhesive Bonding", Elsevier Inc. ISBN 978-0-323-26435-8, 2014.

[54] G. S. Kino, T. R. Corle" Confocal Scanning Optical Microscopy and Related Imaging Systems", 1st Edition, ISBN: 978012408750, Elsevier, (1996).

[55] D. B. Murphy, "Fundamentals of light microscopy and electronic imaging" John Wiley & Sons, (ISBN: 0-471-25391-X, NLM: QH 211, P. 368, (2002).

[56] Anjam Khursheed, "Scanning electron microscope optics and spectrometers" World scientific publishing Co Pte. Ltd., (2011).

[57] B V. O. Roa, "Laser shockwave sintering of micro and nanoscale powders of yttria-stabilized zirconia", MSc. Thesis, Iowa State University ProQuest Dissertations Publishing, (2010).

[58] Reimer Ludwig, "Scanning electron microscopy: physics of image formation and microanalysis", 2nd, Springer, Vol. 45, (2013).

[59] S. L. Erlandsen, C. Frethem, and Y. Chen, "Field emission scanning electron microscopy (FESEM) entering the 21st century: nanometer resolution and molecular topography of cell structure," J. Histotechnol., Vol. 23, No. 3, pp. 249–259, 2000, doi:10.1179/his.2000.23.3.249

[60] F. T. Infrared and A. Ftir, ―What is FTEM, Aust. Orienteer, W. S. Lau, Infrared characterization for microelectronics. World scientific, Vol. 2013, No. 172, pp. 28–29, 1999.

[61] J. I. Pankove, "Optical processes on semiconductors Dover publication," Inc. New york, 1971.

[62] L. W. Shing, "Infrared characterization for microelectronics" World Scientific Publishing Company, Illustrated edition, P. 172, (1999).

[63] Q. Feng, Zhimin Dang, Na Li and Xiaolong Cao "Studied the preparation and dielectric property of Ag/PVA nano-composite", Materials Sci. and Eng. B, Vol. 99, pp. 325-328, 2003, doi:10.1016/S0921-5107(02)00564-0.

[64] T.O. Owolabi, M.A. Abd Rahman, "Modeling the Optical Properties of a Polyvinyl Alcohol-Based Composite Using a Particle Swarm Optimized Support Vector Regression Algorithm", Polymers, Vol. 13, No. 16, pp. 2697, 2021 doi:10.3390/polym13162697,

[65] R. Khaleel, "Electrical and Optical Properties Modification of Poly (Vinyl Chloride) by Zinc, Copper and Nickel EthylXanthate Chelate Complexes", M. Sc. Thesis, University of Mustansiriah, Collage of Science, 2004.

[66] S. Shekhar, V. Prasad, S. V. Subramanyam, "Structural and electrical properties of composites of polymer-iron carbide nanoparticle embedded in carbon" J. Els., Sci., Vol.18, 2006, doi:10.1016/j.mseb.2006.06.010

[67] O. Stenz," The physics of thin film optical spectra", An Introduction, Winzerlaer Str. 10, 07745 Jena Germany, pp.71-72, 2005.

[68] C. Mwolfe, N. Holouyak and G. B. Stillman, "Physical properties of semiconductor", prentice Hall, New York, 1989.

[69] H. R. A. AL-Dawodi," A study of the structural and optical properties of obliquely deposited (CdS) thin films", M.Sc. Thesis, University Al-Mustansiriyah, College of Science, 2010.

[70] A. G. Nilens, "deep imparity in semiconductors" , Wiley -Interscience pub., 1973.

[71] Q. Li1, Q. Z. Xue, X. L. Gao, Q. B. Zheng, "Temperature dependence of the electrical properties of the carbon nanotube/polymer composites", Express Polym,. Lett.3, Vol.12, pp. 769–777, 2009. doi: 10.3144/expresspolymlett.2009.95

[72] S. S. Chiad, N. F. Habubi, S. F. Oboudi and M. H. Abdul-Allah, "Effect of Thickness on The Optical Parameters of PVA: Ag", Diyala Journal for pure Sciences, vol. 7, no. 3, 2011.

[73] A. Hashim, "Experimental Study of Electrical Properties of (PVA-CoNO3, AgCO3) Composites", American J. of Sci., Res., Vol.68, pp. 56- 61, 2012.

[74] T. R. Dhakal, Mishra, R. Sanjay, Glenn, Zachery, Rai, K. Binod "Synergistic Effect of PVP and PEG on the Behavior of Silver Nanoparticle Polymer Composites", J. of Nanoscience and Nanotechnology, Vol.12, pp. 6389-6396, 2012.

[75] S. M. Hassan," Optical Properties of Prepared Polyaniline and Polymethyl methacrylate blends", International Journal of Application or Innovation in Engineering & Management (IJAIEM) ,Vol. 2,No. 9,pp. 232-235, 2013.

[76] M. Sauer, J. Hofkens and J. Enderlein, "Handbook of Fluorescence Spectroscopy and Imaging, from Single molecules to Ensembles", Wiley-VCH Verlag GmbH & Co. KGaA, Weinheim, Germany, 2010.

[77] M. A. Al-Alousi, "The Effect of Substrate Temperature and The Annealing Time on the Optical Properties of The AgInS2 Thin Films Prepared by chemical spray Pyrolysis Technique", J. of University of Anbar for pure science, vol.4, no.2 2010.

[78] M. Abdelazizand E. M. Abdelrazek, "Effect of Dopant Mixture on Structural, Optical and Electron Spin Resonance Properties of Polyvinyl Alcohol," Physica B, Vol. 390, pp. 1-9, 2007. doi:10.1016/j.physb.2006.07.067.

[79] H. N. Najeeb, G. A. Wahab Ali, A. K. Kodeary, J. Ali, "Doping Effect on Optical Constants of Poly-Vinyl Chloric (PVC)", Academic Research International, Vol.4, no. 3, pp. 53-62, 2013.

[80] M. I. Baker, S. Walsh, Z. Schwartz and B. D. Boyan, "A Review of Polyvinyl Alcohol and it is Uses in Cartilage and Orthopedic Applications", Journal of Biomedical Materials Research: Applied Biomaterials 9999B, vol. 100(5), pp. 1451-1457, 2012. **[81]** M. Meyyappa, Nanotechnology Measurement Handbook, A Guide to Electrical Measurements for Nanoscience Applications, 1st Edition, Keithley Instruments, Inc., USA, 2007.

[82] M. Tyagi and D. Tyagi, "Polymer Nanocomposites and their Applications in Electronics Industry", International Journal of Electronics and Electrical Engineering,Vol. 7, pp. 603-608, 2014.

[83] N. K. Abbas, M. A. Habeeb, and A. J. K. Algidsawi," Influence of Prepared Chloropenta Amine Cobalt (III) Chloride Nanoparticles on The Dielectric Properties of PVA Film", Australian Journal of Basic and Applied Sciences, Vol. 9,pp. 26-34, 2015.

[84] N. A. Azahari, N. Othman and H. Ismail," Biodegradation Studies of Polyvinyl Alcohol/Corn Starch Blend Films in Solid and Solution Media", Journal of Physical Science, Vol. 22, pp.15-31, 2011.

[85] N. B. R. Kumar, V. Crasta, R. F. Bhajantri and B. M. Praveen, "Microstructural and Mechanical Studies of PVA Doped with ZnO and WO3 Composites Films", Journal of Polymers,pp . 7 , 2014, doi:10.1155/2014/846140.

[86] N. C. Jeevan, B. R. N. Babu, and K. Chandrashekara, "Characteristic Analysis of Mechanical Properties on Carbon Fiber Reinforced Plastic", International Journal of Research in Engineering & Advanced Technology (IJREAT),Vol. 3,pp. 305-308, 2015.

[87] N. E. Hill, W. E. Vaughan, A. H. Price, and M. Davis, "Dielectric Properties and Molecular Behavior", Van Nostrand, London, 1969.

[88] N. Saba, M. Tahir and M. Jawaid, “A Review on Potentiality of Nano Filler/Natural Fiber Filled Polymer Hybrid Composites,” Polymers, Vol. 6,pp. 2247-2273, 2014, doi: 10.3390/polym6082247.

[89] S. Wen and D. D. L. Chung, "Electric Polarization in Carbon Fiber-Reinforced Cement", Cement and Concrete Research,Vol. 31, pp.141-147, 2001.

[90] L. Solymar and D. Walsh, "Electrical Properties of Materials, 7th Edition", Oxford University Press, Oxford, New York, 2004.

[91] D. J. Griffith, “Introduction to Electrodynamics 3rd Edition “, Prentice Hall, Inc., New Jersey, USA, 1999.

[92] S. O. Gladkov, “Dielectric Properties of Porous Media,” Springer-Verlag Berlin Heidelberg, New York , USA, 2003.

[93] T. I. Zohdi, “Electromagnetic Properties of Multiphase Dielectrics, A Primer on Modeling, Theory and Computation “, Springer-Verlag Berlin, Heidelberg, Berkeley, USA, 2012, doi: 10.1007/978-3-642-28427-4.

[94] W. Gao and N. M. Sammes, An Introduction to Electronic and Ionic Materials, World Scientific Publishing Co. Pte. Ltd., Singapore, 1999.

[95] A. Chelkowski, "Dielectric physics", 1st edition, pwin-polish sci. Pub. (1980).

[96] O. G. Abdullah, S. A. Hussen, and A. Alani, "Electrical Characterization of Polyvinyl Alcohol Films Doped with Sodium Iodide", Asian Transactions on Science & Technology ,Vol. 1,No. 4, 2011.

[97] L. A. Prystaj, “Effect of Carbon filler Characteristics on the Electrical Properties of Conductive Polymer Composites Possessing Segregated Network Microstructures,” MSc. Thesis, The Academic Faculty, Georgia Institute of Technology, 2008.

[98] H. I. Jafar, N. A. Ali and A. Shawky, "Study of A.C Electrical Properties of Aluminum-Epoxy Composites", Journal of Al-Nahrain University ,Vol.14, pp.77-82, 2011.

[99] T. Seghier and F. Benabed, "Dielectric Properties Determination of High Density Polyethylene (HDPE) by Dielectric Spectroscopy", International Journal of Materials, Mechanics and Manufacturing, vol. 3, no. 2, 2015, doi: 10.7763/IJMMM.2015.V3.179 .

[100] T. Blythe and D. Bloor, Electrical Properties of Polymers, 2nd Edition, Cambridge University Press, UK, 2005 .

[101] R. C. Dorf, The Electrical Engineering Hand Book, CRC Press LLC, 2nd Edition, Piscataway, New Jersey, USA, 2000.

[102] R. S. A. Al-Khafaji, Study the Effect of Iraqi Bentonite Clay addition on the Properties of Porcelain Body Prepared from Local Clays, PhD. Thesis, College of Education/Ibn Al-Haithem, University of Baghdad, 2009.

[103]C. V. S. Reddy, X. Han, Q. Y. Zhu, L. Q. Mai and W. Chen, "Dielectric Spectroscopy Studies on (PVP-PVA) Poly blend Film", Microelectronic Engineering,Vol. 83, pp. 281-285, 2006.

[104] I. Yucedag, A. Kayab, S. Altındalc and I. Uslu," Frequency and Voltage-Dependent Electrical and Dielectric Properties of Al/Co-doped PVA/p-Si Structures at Room Temperature", Chin. Phys, Vol. 23,pp. 047304, 2014, doi: 10.1088/1674-1056/23/4/047304

[105] A. Azam, A. S. Ahmed, M. Oves, M. S. Khan, S. S. Habib and A. Memic, "Antimicrobial activity of metal oxide nanoparticles against gram-positive and gram-negative bacteria: A comparative study", International Journal of Nanomedicine", Vol. 7, pp. 6003-6009, 2012. , doi: 10.2147/IJN.S35347.

[106] Z. Si-Wei, G. Chong-Rui, H. Ying-Zhu, G. Yuan-Ru and P. Qing-Jiang , "The preparation and antibacterial activity of cellulose/ZnO composite: A

review", De Gruyter ,Vol. 16, No.1, pp. 9-20, 2018, doi:10.1515/chem-2018-0006.

[107] N. Tran, A. Mir, D. Mallik, A. Sinha, S. Nayar and TJ. Webster, "Bactericidal effects of iron oxide nanoparticles on staphylococcus aureus", International Journal of Nanomedicine ,Vol. 5, pp. 277-283, 2010.

[108] A. Azam, A. Ahmed, M. Oves, M. Khan and A. Memic, "Size-dependent antimicrobial properties of CuO nanoparticles against gram-positive and -negative bacterial strains", International Journal of Nanomedicine, Vol. 7, pp. 3527-3535, 2012.

[109] KR. Raghupati, RT. Koodali and AC. Manna, "Size-dependent bacterial growth inhibition and mechanism of antibacterial activity of zinc oxide nanoparticles", Langmuir, Vol. 27, pp. 4020-4028, 2011.

[110] M. Singh, S. Singh, S. Prasada and I. Gambhir, "Nanotechnology in medicine and antibacterial effect of silver nanoparticles", Digest Journal of Nanomaterials and Biostructures, Vol. 3, No. 3, PP. 115-122, 2008.

[111] Brooks, J. N., Rognlien, T. D., Ruzic, D. N., & Allain, J. P.. Erosion/redeposition analysis of lithium-based liquid surface divertors. Journal of nuclear materials, vol. 290, pp. 185-190, 2001.

[112] Raut, U., Famá, M., Loeffler, M. J., & Baragiola, R. A. “Cosmic ray compaction of porous interstellar ices”. The Astrophysical Journal, vol. 687(2), pp. 1070, 2008.

[113] R. M. Silverstein,"Infrared spectroscopy" in (Spectrometric Identification of Organic Compounds(8th Edition)), edited by David L. Bryce, (Wiley), 978-0- 470-61637-6,(2015).

[114] N.Rajeswari ,S. Selvasekarapandian , S. Karythikeyan, M. Prabu, G. Hirankumar ,H. Nithya, C. Sanjeeviraja, "Conductivity and dielectric Properties of (PVA-PVP) poly blend film using non-aqueous medium". Journal of Non- Crystalline Solids, vol.357, pp. 3751- 3756, 2011.

[115] M.A. Morsi , A.H. Oraby , A.G.Elshahawy, R.M. Abd El- Hady, "Preparation, structural analysis, morphological investigation and electrical properties of gold nanoparticales filled (PVA-CMC) blend", Journal of Materials Research and Technology, vol.8, No. 6 ,PP. 5996-6010, 2019, doi:10.1016/j.jmrt.2019.09.074

[116] M. A. Habeeb and L. A. Hamza, "Structural, Optical and DC Electrical Properties of (PVA-PVP-Y2O3) Films and Their Application for Humidity Sensor," J. Adv. Phys., vol. 6, no. 1, pp. 1–9, 2017, doi:10.1166/jap.2017.1303.

[117] Camargo, J. S. G. D., Menezes, A. J. D., Cruz, N. C. D., Rangel, E. C., & Delgado-Silva, A. D. O. "Morphological and chemical effects of plasma treatment with oxygen (O 2) and sulfur hexafluoride (SF 6) on cellulose surface". Materials Research, vol. 20, pp. 842-850,218.

[118] O. Abdullah1, D. R. Saber and L. O. Hamasalih, "Complexion Formation in PVA/PEO/CuCl2 Solid Polymer Electrolyte", Universal Journal of Materials Science, vol 3 (1), pp. 1-5 , 2015, doi: 10.13189/ujms.2015.030101.

[119] Abdalameer, N. K. "Effects of cold atmospheric plasma on the optical properties of SnO2 thin film. Advances in Natural and Applied Sciences," vol. 11(9), pp . 357-364,2017.

[120] Jebur, E. K. "Effect of the Dielectric Barrier Discharge Plasma on the Optical Properties of CDS Thin Film", Baghdad Science Journal, vol. 16 (4) ,2019, doi: 10.21123/bsj.2019.16.4(Suppl.).1030.

[121] S.H. Borova, O.M. Shevchuk, N.M. Bukartyk, E.Yu. Nikitishyn and V. Tokarev, "Nanocomposite Films Based on Functional Copolymers with Embedded Carbon Nanotubes", proceedings of the International Conference Nanomaterials: Applications and Properties, Vol. 3, No. 2, 2014,

[122] A. Mohammad, K. Hooshyari, M. Javanbakht, and M. Enhessari, "Fabrication and Characterization of Poly Vinyl Alcohol/ Poly Vinyl Pyrrolidone/MnTiO Nanocomposite Membranes for PEM Fuel Cells", Iranica Journal of Energy & Environment, Vol. 4, No. 2, PP. 86-90, 2013, doi: 10.5829/idosi.ijee.2013.04.02.02

[123] K. Karthikeyan, N. Poornaprakash, N. Selvakumar and Jeyasubrmanian, "Thermal Properties and Morphology of MgO-PVA Nanocomposite Film", Journal of Nanostructured Polymers and Nanocomposites, Vol. 5, No. 4, PP. 83-88, 2009.

[124] N. Elmarzugi1, T. Adali, A. Bentaleb, E. I. Keleb, A. T. Mohamed and A. M. Hamza, " Spectroscopic Characterization of PEG- DNA Biocomplexes by FTIR", Journal of Applied Pharmaceutical Science, vol. 4, no. 8, PP. 6-10 , 2014, doi: 10.7324/JAPS.2014.40802

[125] Mohammed, M. K., Al-Dahash, G., & Al-Nafiey, "Synthesis and characterization of PVA-Graphene-Ag nanocomposite by using laser ablation technique", In Journal of Physics: Conference Series, Vol. 1591, No. 1, pp. 012012, 2020, doi:10.1088/1742-6596/1591/1/012012 .

[126] Abdul kadhim, S. M., Hashim, S., & Rabee, H. "Zinc Oxide and Silver Nanoparticles Adding for Development of Morphological and Optical Properties of Poly (vinyl alcohol)/Poly (vinyl pyrrolidone) Blend Nanocomposites Films" , vol.7, no.2, 2022.

[127] El Sayed, A. M., & El-Gamal, S, "Synthesis and investigation of the electrical and dielectric properties of Co3O4/(CMC+ PVA) nanocomposite films", Journal of Polymer Research, vol, 22(5), pp.1-12, 2015.

[**128]** G. Kandhol, H. Wadhwa, S. Chand, S. Mahendia, and S. Kumar, "Study of dielectric relaxation behavior of composites of Poly (vinyl alchohol) (PVA) and Reduced graphene oxide (RGO)," vol. 160, pp. 384–393, 2019, doi: 10.1016/j.vacuum.2018.11.051

[129] S. Satapathy, P. K. Gupta, K. B. R. Varma, P. Tiwari, and V. Ganeshan, "Study on dielectric behavior of Lithium Tantalate (LT) nano

particle filled poly (vinylidene fluoride)(PVDF) nano composite" arXiv Prepr. arXiv0808.0420, 2008.

[130] B. Rabee, B. Al-Kareem, and B. Al Shafaay, "Effect addition Al2O3 on the (AC, DC) Electrical Properties of Ethylene-Alpha Olefin Copolymer, " Int. J. Sci. Res., vol. 6, pp.2319-7064 ,2017, doi: 10.21275/ART20171429.

[131] Y. T. Prabhu, K. V. Rao, B. S. Kumari, V. S. S. Kumar, and T. Pavani, "Synthesis of Fe 3 O 4 nanoparticles and its antibacterial application," Int. Nano Lett., vol. 5, no. 2, pp. 85–92, 2015.

الخلاصة

تم تحضير المتراكب النانوي (PVA/PAA/Ag) باستخدام طريقة الصب مع نسب وزنية مختلفة من Ag النانوية (0 ,2 ,4 ,6 و 8). wt%. تم فحص الخصائص التركيبية والسطحية والبصرية والكهربائية للمتراكب النانوي (PVA/PAA/Ag). تتضمن الخصائص التركيبية المجهر الضوئي والتحليل الطيفي للأشعة تحت الحمراء (FTIR) وصور المجهر الإلكتروني الماسح (SEM). أظهرت صور المجهر الضوئي توزيع الجسيمات النانوية Ag بشكل شبكة مستمرة داخل البوليمر عند النسبة (8 wt.%) . اظهرت صور (FE-SEM) لسطح الأغشية للمتراكب النانوي (PVA/PAA/Ag) والتي تكون متجانسة ومتماسكة مع الركام أو القطع المنتشرة بشكل عشوائي على السطح العلوي. الاختلاف في سطح الغشاء بعد التعرض لغاز الاركون بلازما هو نتيجة لتطور الانطباع الذي تشجعه أنواع بلازما الأرجون على سطح (PVA / PAA) . اظهر طيف (FTIR) زحف في بعض القمم وزيادة في شدة لقمم اخرى مقارنة مع الغشاء (PVA/PAA) وهذا يشير بانه لايوجد تفاعل بين البوليمر والمواد النانوية المضافة.. أظهرت نتائج الخصائص البصرية للمتراكب النانوي قبل وبعد التعرض للإشعاع بأن الامتصاصية، معامل الامتصاص، معامل الانكسار، معامل الخمود، ثابت العزل الحقيقي والخيالي ،التوصيلية البصرية تزداد مع زيادة تركيز جسيمات النانوية Ag. النفاذية وفجوة الطاقة للانتقال غير مباشر المسموح والممنوع تقل مع زيادة تركيز جسيمات النانوية. انها تقل من ٤,٧٦ الكترون فولت إلى ٢,٩١ الكترون فولت لفجوة الطاقة غير المباشرة المسموحة ب ومن ٤,٢٥ الكترون فولت إلى ١,٦٤ الكترون فولت لفجوة الطاقة غير المباشرة الممنوعة قبل تعريضها لبلازما الأرجون، بينما انخفضت فجوة الطاقة غير المباشرة من ٣,٥٢ الكترون فولت إلى ١,٦٤ الكترون فولت لفجوة الطاقة غير المباشرة المسموح ومن ٢,٩٨ الكترون فولت إلى ٠,١٥ الكترون فولت للممنوعة بعد التعرض لبلازما اركون. اظهرت نتائج الخصائص البصرية بعد التعرض للبلازما لها قيم عالية وهذا يعود الى زيادة حاملات الشحنة الحرة والمستقطبة. هذا يعطي انطباع جيد بانه من الممكن استخدام هذه العينات ككاشف ضوئي. اظهرت نتائج الخصائص العزلية بان ثابت العزلي والفقدان العزلي يزدادان مع زيادة تركيز جسيمات النانوية Ag وتتناقص مع زيادة تردد المجال الكهربائي المسلط بينما التوصيلية الكهربائية المتناوبة (AC) تزداد مع زيادة تركيز جسيمات النانوية Ag و التردد. ثابت العزل، الفقدان العزلي والتوصيلية الكهربائية المتناوبة بعد التشعيع لها قيم عالية مقارنة قبل التشعيع الذي يعزى إلى زيادة حاملات الشحنة الحرة والمستقطبة، ويمكن استخدام هذه الخصائص للأفلام في المكثفات والترانزستور والدوائر الإلكترونية. اختبرت المتراكبات النانوية (PVA/PAA/Ag) كمضادات لبكتريا موجبة غرام (المكورات العنقودية الذهبية) وسالبة غرام

(الشريطية القولونية) و بينت النتائج أن منطقة التثبيط ازدادت بزيادة تراكيز الجسيمات النانوية Ag، انه يزداد الى 20 ملم للبكتريا الشريطية القولونية لتركيز 8 wt.% و 26 ملم للبكتريا للمكورات العنقودية الذهبية عند التركيز 8 wt.%.

جمهورية العراق
وزارة التعليم العالي والبحث العلمي
جامعة بابل / كلية التربية للعلوم الصرفة
قسم الفيزياء

تأثير البلازما الباردة على الخصائص البصرية و الكهربائية لخليط بوليمري مطعم بالنانو فضة

رسالة مقدمة الى
مجلس كلية التربية للعلوم الصرفة – جامعة بابل
وهي جزء من متطلبات نيل درجة ماجستير تربية / الفيزياء

من قبل

زهراء حسون عبيد فرحان

بكالوريوس تربية علوم (الفيزياء)
جامعة بابل ٢٠٠٦

بإشراف

أ. د بهاء حسين صالح ربيع

١٤٤٥ هـ ٢٠٢٣م